Received: 30 October 2025 | Revised: 30 January 2026 | Accepted: 30 January 2026

DOI: 10.1002/epi.70150

Epilepsia®

RESEARCH ARTICLE

Mutation type-specific transcriptomic signatures and readthrough therapy rescue in *SMC1A*-related developmental and epileptic encephalopathy

Maddalena Di Nardo[1] | **Francesca Sardina**[2] | **Maria M. Pallotta**[1] | **Iñigo Marcos-Alcalde**[3] | **Paulino Gómez-Puertas**[3] | **Cinzia Rinaldo**[2] | **Ian D. Krantz**[4,5] | **Antonio Musio**[1]

[1]Institute of Biomedical Technologies, National Research Council, Pisa, Italy

[2]Institute of Molecular Biology and Pathology, National Research Council, Rome, Italy

[3]Molecular Modeling Group, Centro de Biología Molecular Severo Ochoa, Consejo Superior de Investigaciones Científicas - Universidad Autónoma de Madrid, Madrid, Spain

[4]Division of Pediatric Genetics and Genomics, Cohen Children's Medical Center, Northwell Health, Great Neck, New York, USA

[5]Department of Pediatrics, Zucker School of Medicine, Hofstra University, New York, New York, USA

Correspondence
Antonio Musio, Institute of Biomedical Technologies, National Research Council, 56124 Pisa, Italy.
Email: antonio.musio@itb.cnr.it

Present address
Francesca Sardina and Maria M. Pallotta, Institute of Molecular Genetics, National Research Council, Pavia, Italy

Funding information
Ministero dell'Università e della Ricerca, Grant/Award Number: 202227SYBW_LS3_PRIN2022; Italian SMC1A Association; Spanish State Research Agency, Grant/Award Number: PID2021-126625OB-I00/MCIN/AEI/10.13039/501100011033/FEDER,EU

Abstract

Objective: This study was undertaken to investigate the molecular consequences of pathogenic variants in the *SMC1A* gene—particularly those associated with developmental and epileptic encephalopathy (DEE85)—and to evaluate the therapeutic potential of ataluren in restoring SMC1A function and mitigating disease-related transcriptomic and genomic alterations.

Methods: The study analyzed transcriptomic profiles from cell lines derived from individuals with DEE85 and Cornelia de Lange syndrome (CdLS), comparing the effects of different *SMC1A* variants. Particular focus was placed on nonsense variants and their impact on gene expression. Functional assays were conducted to assess the ability of ataluren to restore SMC1A protein expression, correct transcriptional defects, and reduce genomic instability.

Results: Transcriptomic alterations were strongly dependent on variant type, with nonsense variants causing the most profound gene expression changes. DEE85 and CdLS cell lines exhibited distinct transcriptional signatures. Treatment with ataluren led to successful restoration of SMC1A protein levels, partial correction of gene expression abnormalities, and a reduction in genomic instability in cells harboring nonsense variants.

Maddalena Di Nardo and Francesca Sardina contributed equally to this work.

Significance: These findings demonstrate that *SMC1A*-related epileptic encephalopathies are driven by variant-specific molecular mechanisms and highlight the therapeutic promise of ataluren for DEE85. The study supports further development of precision medicine strategies targeting nonsense variants in *SMC1A*, with potential implications for improving diagnosis, treatment, and quality of life in affected individuals.

KEYWORDS

ataluren, Cornelia de Lange syndrome, developmental and epileptic encephalopathy (DEE85), SMC1A, transcriptomic profiles

1 | INTRODUCTION

The cohesin complex is a multisubunit protein complex of four main subunits: the SMC1A and SMC3 adenosine triphosphatases (ATPases), the kleisin RAD21, and either SA1 or SA2 (STAG1 or STAG2), which link the SMC heterodimer to the DNA and regulatory factors.[1] One of the primary functions of cohesin is to hold sister chromatids together from S phase until their separation during anaphase, a process essential for accurate chromosome segregation.[2] It interacts with DNA by encircling chromatin fibers and is loaded onto chromatin by the NIPBL-MAU2 complex. Although cohesin loading is genome-wide, its stable chromatin binding and retention are highly regulated and often restricted to specific genomic locations, notably at sites co-occupied by the architectural protein CTCF.[3] Cohesin participates in the establishment and maintenance of topologically associating domains (TADs) and chromatin loops, which bring distal regulatory elements such as enhancers into close spatial proximity with their target promoters.[4,5] These structures help define regulatory neighborhoods and insulate genes from inappropriate enhancer activity. CTCF serves as a boundary element, and together with cohesin, forms loop anchors in a process known as loop extrusion, in which cohesin extrudes loops of chromatin until it encounters convergently oriented CTCF sites.[6,7]

The cohesin complex is also a crucial guardian of genome stability, performing several interconnected functions that ensure the faithful transmission of genetic material, the repair of damaged DNA, and the preservation of chromosomal architecture. Cohesin is actively recruited to sites of DNA damage in a process dependent on the SMC-loading factor NIPBL, independently of its canonical role in cohesion.[8,9] Cells deficient in cohesin subunits or its regulators show hypersensitivity to genotoxic stress such as ionizing radiation, mitomycin C, and replication inhibitors, underscoring cohesin's protective role during genotoxic challenges.[10] Perturbation of cohesin function—by mutation or depletion—leads to widespread gene expression changes that often precede alterations in chromatin accessibility or TAD architecture and genome instability. Such effects are observed in both developmental diagnoses and cancer.[10–12]

Key points

- Mutation-specific impact: nonsense variants in *SMC1A* lead to the most severe transcriptomic disruptions and genomic instability, distinguishing DEE85 from CdLS at the molecular level.
- Therapeutic potential of ataluren: treatment with ataluren restores SMC1A protein expression and partially corrects gene expression defects in cells with nonsense variants, supporting its use in precision therapies for DEE85.
- Stratified clinical relevance: comparative transcriptomic analysis reveals distinct molecular signatures between epileptic and developmental phenotypes, highlighting the need for variant-informed diagnostic and therapeutic strategies.

Germline variants in *SMC1A* have been identified as one of the genetic causes of Cornelia de Lange syndrome (CdLS), a multisystem developmental diagnosis characterized by growth delay, intellectual disability (ID), limb differences, and distinctive facial features. Although pathogenic variants in *NIPBL* account for the majority of CdLS cases, *SMC1A* variants, missense or small in-frame deletion, represent a significant subset, often associated with a milder or atypical phenotype.[13–15] Recently, de novo variants in *SMC1A* have been reported in individuals with developmental and epileptic encephalopathy (DEE85), typically characterized by early onset seizures, global developmental delay, ID, and drug-resistant epilepsy. Unlike the milder CdLS phenotypes associated

with in-frame or missense mutations, the epileptic phenotypes are frequently linked to loss-of-function variants such as nonsense, frameshift, or splice-site mutations.[16–23] This condition significantly impacts patients' quality of life; however, because no dedicated studies have yet been conducted, there is an urgent need to investigate these patients, who often have limited therapeutic options. Understanding the molecular and clinical features of their condition could lead to earlier diagnosis, better seizure control, and ultimately the development of targeted therapies.

Ataluren is a small-molecule drug designed to promote ribosomal readthrough of premature termination codons, which are responsible for approximately 12% of all inherited disease-causing mutations.[24] By enabling the translation machinery to bypass nonsense mutations, ataluren can restore the production of full-length, functional proteins. Clinically, ataluren has shown promise in treating Duchenne muscular dystrophy (DMD) caused by nonsense mutations in the dystrophin gene. It was approved by the European Medicines Agency for ambulatory patients aged 2 years and older.[25,26] Beyond DMD, ataluren has been investigated in cystic fibrosis, aniridia, and other rare genetic disorders where nonsense mutations disrupt essential protein function.[27]

This study highlights how transcriptomic alterations caused by pathogenic *SMC1A* variants are strongly dependent on mutation type, with nonsense mutations inducing the most extensive and profound changes in gene expression. Comparative analysis between DEE85 and CdLS cell lines confirms the presence of distinct transcriptional signatures, underscoring the complexity of the molecular mechanisms underlying these clinical phenotypes. Furthermore, treatment with ataluren successfully restored SMC1A protein expression, partially corrected gene expression defects, and reduced genomic instability in cells carrying nonsense mutations. These findings support the therapeutic potential of ataluren for DEE85 and pave the way for precision medicine approaches targeting *SMC1A*-related epileptic encephalopathies.

2 | MATERIALS AND METHODS

2.1 | Cell lines

Lymphocytes from 11 unrelated DEE85 girls characterized by ID and drug-resistant epilepsy (epileptic [EP] cells) were immortalized by Epstein–Barr virus. All patients harbored variants (deletion, frameshift, nonsense, and missense) in the *SMC1A* gene. In addition, three CdLS (carrying missense variants in the *SMC1A* gene) and three healthy and normal control cell lines were used in this study (Table S1). Lymphoblastoid cell lines (LCLs) were grown in RPMI 1640 medium supplemented with 10% fetal bovine serum, 100 U/mL penicillin, .1 mg/mL streptomycin, and 1% L-glutamine. This study was conducted according to the principles expressed in the Declaration of Helsinki. Informed consent was obtained from the families, according to the procedures established by the National Research Council Ethical Clearance (199894/2023).

2.2 | Structural modeling of SMC1A

The structural model of the homodimer of human proteins SMC1A (UniprotKB id: Q14683) and SMC3 (UniprotKB id: Q9UQE7) was generated from the following structures present in the Protein Data Bank: 7OGT (crystal structure of the folded elbow of the yeast SMC1 protein), 7DG5 (crystal structure of mouse Smc1-Smc3 hinge domain), and 8POA (human Cohesin ATPase module).[28,29] Four partial models were extracted from this model for molecular dynamics simulations: a head model, containing amino acids 2–169 and 1061–1227 of SMC1A, amino acids 1–162 and 1029–1215 of SMC3, as well as two ATP molecules and two Mg^{++} atoms; a hinge model, containing amino acids 479–679 of SMC1A and amino acids 468–687 of SMC3; a coiled-coil model, containing amino acids 226–308, 444–487, 668–710, and 849–890 of SMC1A and amino acids 264–311, 450–495, 676–723, and 905–957 of SMC3, around amino acid Arg693; and a second coiled-coil model, containing amino acids 205–249 and 908–1022 of SMC1A and amino acids 204–251 and 918–991 of SMC3, around amino acid Tyr983. The structures of the wild-type domains were modeled by combining residue positions obtained using Phyre 2[30] and SwissModel.[31] The structures of the SMC1A Gly32Glu, Arg96Cys, Arg496His, Arg693Gly, and Tyr983Cys variants were modeled using the models of the wild-type domains as templates.

2.2.1 | Molecular dynamics simulation of wild-type and variant proteins

The nine structural models, four corresponding to the partial models of the wild-type complex and five corresponding to each of the variants, were subjected to 200 ns of unrestrained molecular dynamics (MD) simulation using the Amber18 package (https://ambermd.org; University of California, San Francisco), essentially as previously described.[32] Briefly, after solvation, initial wild-type and variant model structures were subjected to 10 000 cycles of energy minimization, followed by a

1-ns restrained equilibration phase in which the temperature was smoothly raised to 297 K, after which the restraints were gradually removed over 10 ns. Each system was then subjected to a 200-ns free MD production phase. Trajectories were analyzed using cpptraj[33] and VMD.[34] Plots were generated using PyMOL (https://pymol.org).

2.3 | DNA synthesis and quantitative real-time polymerase chain reaction

Total RNA was isolated from LCLs using the RNeasy Mini Kit (Qiagen), and cDNA was synthesized with SuperScript II Reverse Transcriptase and oligo(dT) primers (Invitrogen). Quantitative polymerase chain reaction (PCR) reactions were performed in duplicate using QuantiTect SYBR Green PCR Master Mix (Qiagen) on a Rotor-Gene 3000 system (Corbett). Gene expression levels were normalized to hypoxanthine phosphoribosyltransferase. As no significant differences were observed among control cell lines, their data were pooled. Primer sequences used for mRNA analysis are listed in Table S2. Statistical differences in gene expression among EP, CdLS, and control cell lines were assessed using Student *t*-test.

2.4 | Ataluren treatment

Cells were treated with .5, 1.5, or 3 μg/mL ataluren for 24 h. After treatment, either total protein was extracted for Western blot analysis or mRNA was isolated to assess gene expression profiles.

2.5 | Statistical analysis

Differences in the number of chromosomal aberrations were assessed using Student *t*-test. Statistical significance was defined as a $p < .05$.

3 | RESULTS

3.1 | Mutation-type specific transcriptomic alterations in *SMC1A*-related epilepsy

Genome-wide transcriptional profiling was performed on 11 LCLs derived from DEE85 girls, all carrying pathogenic variants in the *SMC1A* gene (EP1–EP14). For comparison, we included three LCLs from individuals with clinically diagnosed CdLS harboring *SMC1A* variants (CdL363, CdL565, CdL060), and three control LCLs (LCL1, LCL3, LCL4). Among the EP cell lines, one carried a deletion encompassing *SMC1A*, two had nonsense variants, three had missense variants, and five carried frameshift variants (Table S1). Most variants mapped to the protein's coiled-coil regions, with two positioned in the N-head domain and one near the hinge region (Figure S1). *SMC1A* variants did not affect transcription (data not shown). To assess whether the protein is produced, we performed immunoblot analysis of SMC1A across all cell lines. In all cases, SMC1A levels were comparable to control cells, except in EP1 and EP2 cells carrying nonsense variants (Figure S2). Differential gene expression analysis (DGEA) comparing EP cell lines to controls identified 449 differentially expressed genes (DEGs; 284 were upregulated and 165 downregulated; Figure S3A, Table S3). Gene Ontology (GO) enrichment analysis showed involvement in angiogenesis, transcriptional regulation, cell adhesion and migration, signal transduction, and neuronal migration (Figure 1A). To assess variant-specific effects, we performed separate DGEA comparisons for each subgroup. EP cell lines with frameshift variants showed 411 DEGs (251 upregulated and 160 downregulated) enriched mainly in pathways involved in transcriptional regulation (Figure 1B, Figure S3B, Table S4). Missense variants affected 296 genes (133 upregulated and 163 downregulated), with pathways linked to transcriptional control, angiogenesis, signal transduction, and cell migration (Figure 1C, Figure S3C, Table S5). Nonsense variants caused the most extensive changes, with 1429 misregulated genes (656 upregulated and 773 downregulated). Beyond transcriptional dysregulation, this group showed enrichment in chromatin remodeling, apoptosis, cell adhesion, cell proliferation, and intracellular signaling (Figure 1D, Figure S3D, Table S6). A comparative analysis revealed that 105 genes were shared between nonsense and frameshift groups (Figure 2A), with 99 showing concordant expression trend, albeit with variable intensity, and six genes (*ABHD6, AGMAT, GATA4*, *ATP11C, CYP1B1*, and *SERPINB10*) reversing direction (Figure 2B). Differential expression was validated by quantitative real-time PCR (Figure S4). Only 15 genes (*CD99L2*, *CHD3*, *CTNNA2*, *DERL3*, *FAAH*, *FAM78A*, *GNB4*, *HMGN5*, *NFATC2*, *POU4F1*, *PRKCH*, *PTK2*, *SLC26A11*, *TUBB2B*, and *TYMP*) were common to all three mutation types—frameshift, nonsense, and missense (Figure 2C)—indicating limited overlap and mutation-specific transcriptional signatures. These findings suggest that although nonsense and frameshift mutations may share some downstream effects, nonsense variants exert broader and more disruptive impacts on

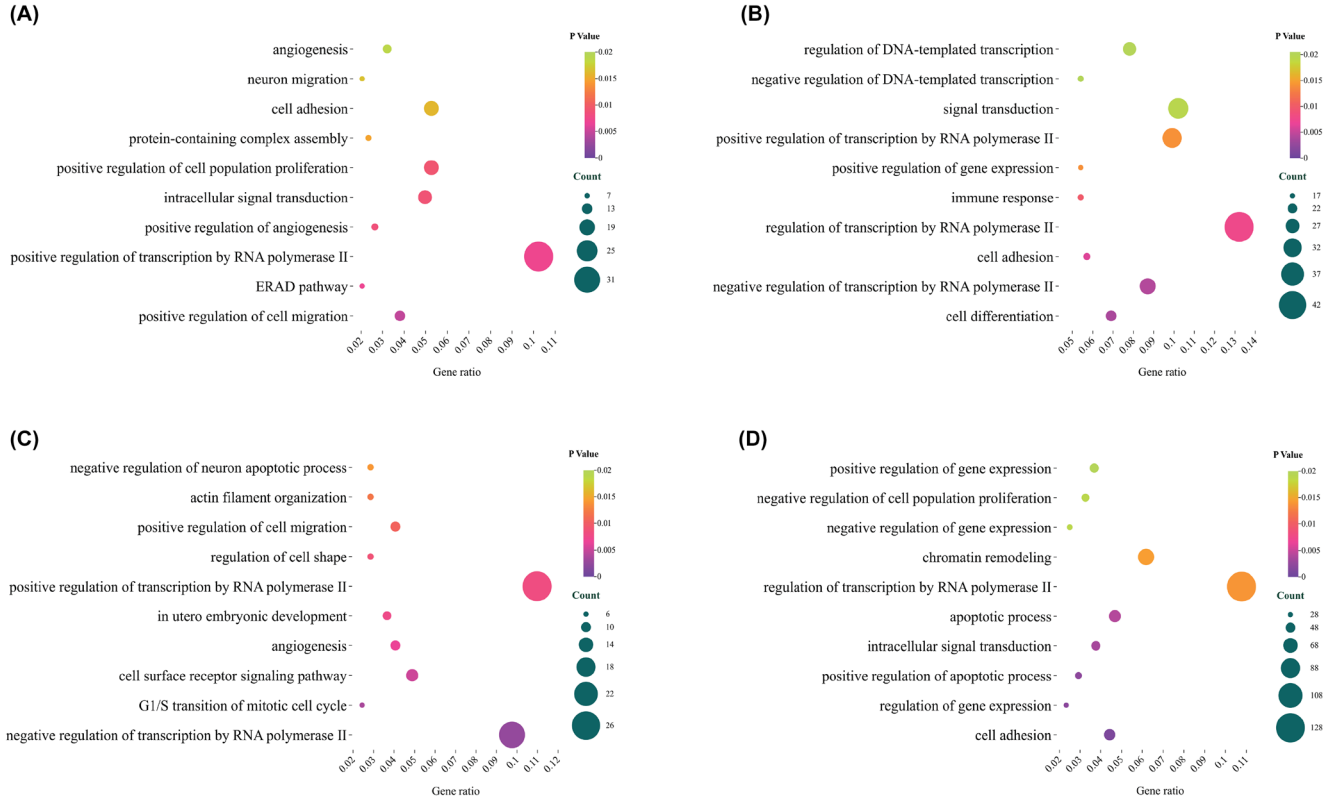

FIGURE 1 Transcriptomic profiling reveals distinct metabolic pathway alterations in epileptic (EP) cells. Metabolic pathway enrichment analysis was performed using EnrichR on differentially expressed genes (DEGs) from EP cells compared to controls. Bubble plots illustrate the enriched pathways across Gene Ontology categories for the following: (A) all EP cells, (B) EP cells carrying frameshift variants, (C) EP cells harboring missense variants, and (D) EP cells carrying nonsense variants. Each plot highlights deregulated pathways specific to the genetic subgroup, reflecting both shared and unique transcriptomic signatures. Dot size corresponds to the number of DEGs associated with each pathway, and color intensity indicates statistical significance (*p*-value). These analyses underscore the impact of variant type on cellular metabolism and provide insights into genotype-specific molecular mechanisms. ERAD, endoplasmic reticulum-associated degradation.

gene regulation. Taken together, altered gene expression appears to be a hallmark of DEE85, with nonsense variants producing the most severe transcriptional dysregulation.

3.2 | Transcriptomic comparison of CdLS and DEE85 reveals mutation-specific signatures

Given the known clinical differences between CdLS and DEE85 caused by *SMC1A* variants,[35] we directly compared the transcriptomic profiles of CdLS-derived LCLs to DEE85 samples to gain insights into the molecular mechanisms underlying these phenotypic divergences. Principal component analysis further underscored these differences. EP nonsense samples formed a distinct cluster separate from CdLS, indicating a clear divergence in gene expression programs. In contrast, EP frameshift and missense samples exhibited greater dispersion, consistent with higher transcriptional heterogeneity (Figure 3A). This analysis identified 587 DEGs (374 were downregulated and 213 upregulated), associated with transcription, translation, DNA replication, and mRNA processing (Figure 3B,C, Table S7). To isolate DEE85-specific expression patterns, we excluded genes shared with CdLS and controls, yielding 382 uniquely dysregulated genes (Figure 3D). GO analysis of this set revealed enrichment not only in transcriptional regulation but also in chromatin remodeling, angiogenesis, intracellular signaling transduction, and neuronal migration (Figure 3E). Finally, transcriptomic comparison between EP and CdLS cell lines, both carrying missense variants in *SMC1A*, identified 480 DEGs (220 downregulated, 260 upregulated), pointing to altered biological processes including calcium-mediated signaling, RNA processing, chromatin looping, and DNA repair (Figure 3F,G, Table S8).

These observations support that although both disorders involve *SMC1A* variants, their molecular

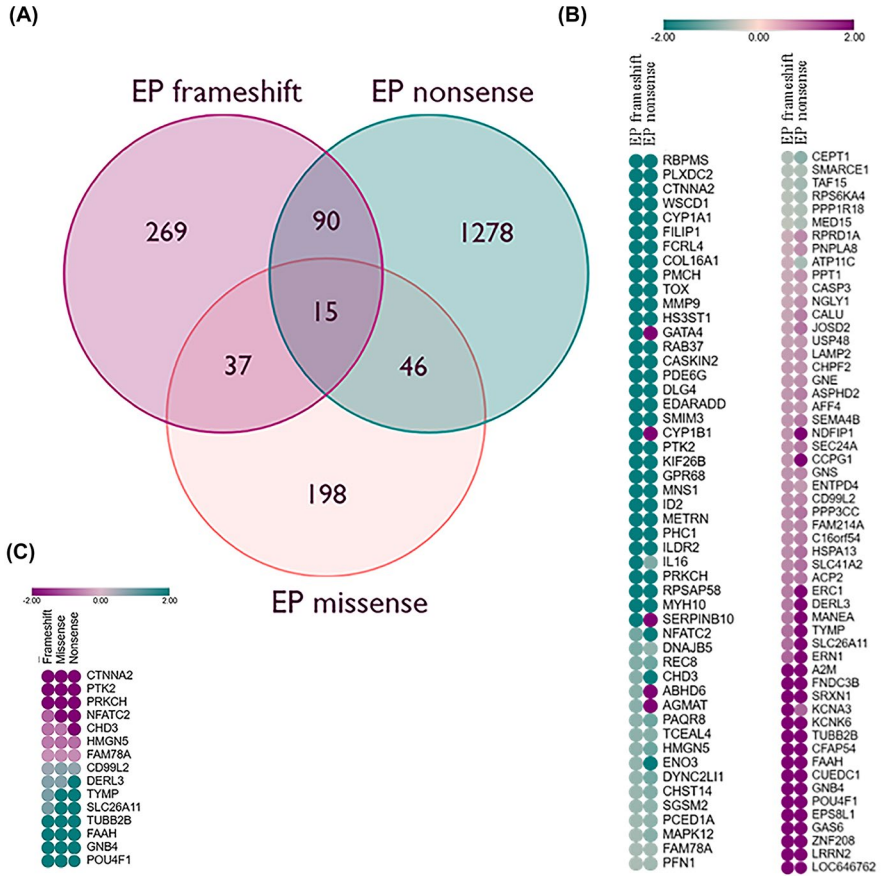

FIGURE 2 Comparative transcriptomic analysis across *SMC1A* variant groups. (A) Venn diagram illustrating the overlap of differentially expressed genes (DEGs) between nonsense and frameshift groups, revealing 105 shared genes. (B) Heatmap showing that 99 of these genes exhibit a concordant expression trend across both groups, albeit with varying magnitude, whereas six genes (*ABHD6*, *AGMAT*, *GATA4*, *ATP11C*, *CYP1B1*, and *SERPINB10*) display opposite regulation. (C) Only 15 DEGs are shared among frameshift, nonsense, and missense groups, highlighting limited transcriptomic overlap and supporting the presence of mutation-specific expression signatures. EP, epileptic cells.

consequences differ substantially depending on variant type. Nonsense variants appear to exert more severe effects on cohesin function and downstream gene expression.

3.3 | Comparative molecular dynamics of wild-type and mutant SMC1A protein structures

Given that missense variants in the *SMC1A* gene have traditionally been associated with CdLS but have more recently also been identified in cases of DEE85, structural modeling of SMC1A represents a critical tool for elucidating the molecular mechanisms by which specific variants may alter protein conformation and disrupt cohesin function. Therefore, to analyze the potential impact of variants on the SMC1A/SMC3 complex structure, partial models were generated for each domain corresponding to areas surrounding the variants (Figure 4A). Among the five variants studied, only two, Gly32Glu and Arg693Gly, exhibited significant deviations from the wild-type protein behavior. Figure 4B shows the result of the molecular dynamics simulation of the Gly32Glu variant. In the wild-type protein, the Gly32 residue is located near the positively charged Lys38 amino acid, which closely contacts the phosphate groups of the ATP molecule in the ATPase active site of SMC1A (Figure 4B, left). Substituting Gly32 with Glu, a negatively charged amino acid, distorts the interaction between Lys38 and ATP (Figure 4B, center). Figure 4B (right) shows the distance between the nitrogen atom of the amino group of Lys38 and the phosphorus atom of the gamma phosphate group of the ATP molecule in the 200-ns trajectories of the wild-type protein (gray line) and the Gly32Glu variant (black line). In the wild-type protein, this distance remains constant at approximately .4 nm, maintaining close contact between the γ phosphate group and the amino group. In contrast, the Gly32Glu variant exhibits a much greater and highly variable distance, indicating local instability that will likely affect the affinity for ATP and/or the ATPase activity of the head domain. Figure 4C shows the possible effect of the Arg693Gly variant on the coiled-coil domain of the SMC1A/SMC3 dimer. In the wild-type protein, the positively charged amino acid Arg693 of SMC1A interacts with the negatively charged amino acid Glu476 of SMC3. This interaction stabilizes the position of the coiled coil of both molecules locally (Figure 4C, left). The change from arginine to glycine causes the loss of this interaction, resulting in the separation of the two proteins and local disorganization of the structure (Figure 4C, center). Figure 4C (right) shows the measurement of the distance between the α carbons of the amino acids Arg693 (or Gly693) of SMC1A and Glu479 of

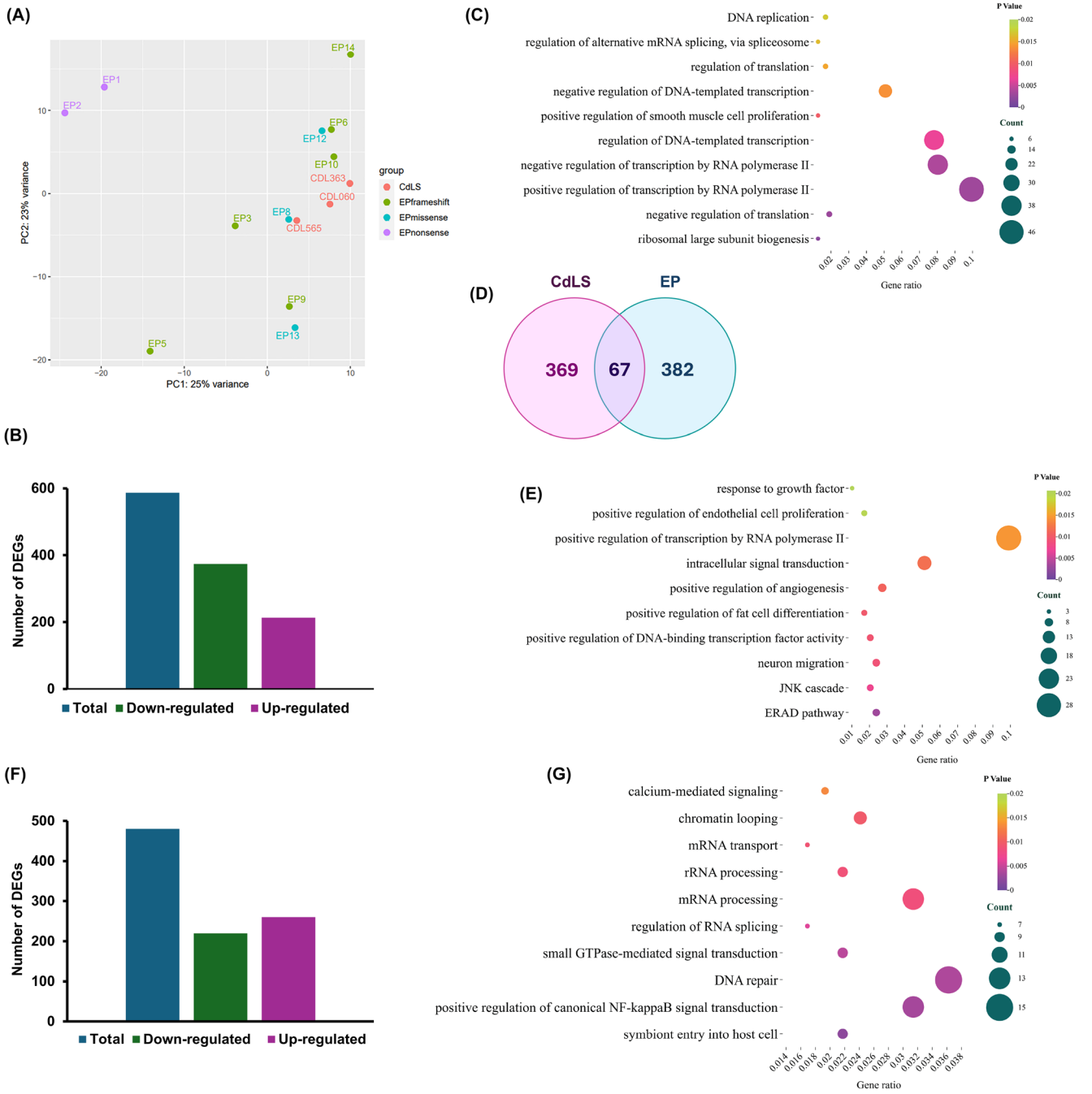

FIGURE 3 Transcriptomic divergence between Cornelia de Lange syndrome (CdLS) and developmental and epileptic encephalopathy (DEE85) highlights variant-specific molecular signatures. (A) Principal component analysis (PCA) highlights distinct clustering of epileptic (EP) nonsense samples, clearly separated from CdLS, whereas EP frameshift and missense samples show greater dispersion, consistent with increased transcriptional heterogeneity. (B) Differential expression analysis identified 587 differentially expressed genes (DEGs) between DEE85 and CdLS (374 downregulated, 213 upregulated). (C) Bubble plot illustrates the pathways across Gene Ontology (GO)-enriched categories enriched in pathways related to transcription, translation, DNA replication, and mRNA processing. (D) To define DEE85-specific signatures, genes shared with CdLS and controls were excluded, yielding 382 uniquely dysregulated genes. (E) GO enrichment analysis of this DEE85-specific gene set revealed significant involvement in transcriptional regulation, chromatin remodeling, angiogenesis, intracellular signaling, and neuronal migration. (F) A focused comparison between EP and CdLS samples carrying *SMC1A* missense variants identified 480 DEGs (220 downregulated, 260 upregulated). (G) Bubble plot showing that these DEGs are implicated in biological processes such as calcium-mediated signaling, RNA processing, chromatin looping, and DNA repair. Dot size corresponds to the number of DEGs associated with each pathway, and color intensity indicates statistical significance (*p*-value). ERAD, endoplasmic reticulum-associated degradation; GTPase, guanosine triphosphatase.

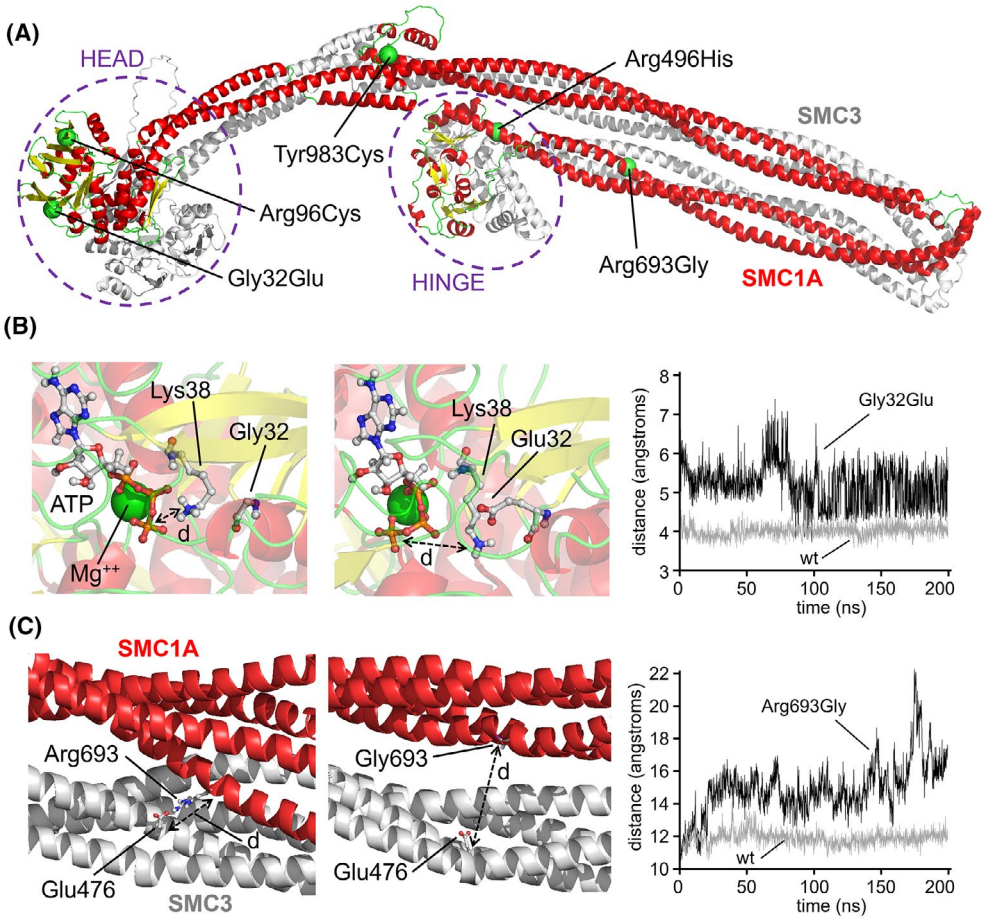

FIGURE 4 Effect of the Gly32Glu and Arg693Gly variants in the three-dimensional structure of the SMC1A/SMC3 dimer. (A) Three-dimensional model of the SMC1A/SMC3 dimer. The SMC1A protein is colored according to its secondary structure elements. The SMC3 protein is shown in gray. The positions of the HEAD and HINGE domains are shown, as well as the positions of the alpha carbons of the amino acids corresponding to the Gly32Glu, Arg96Cys, Arg496His, Arg693Gly, and Tyr983Cys variants of SMC1A (green spheres). (B) Glu32Gly variant. The positions of the amino acids Gly32 (or Glu32) and Lys38, the adenosine triphosphate (ATP) molecule, and the Mg^{2+} atom of the active center of SMC1A are shown after 200 ns of molecular dynamics simulation of the head domain model of the wild-type (wt) protein (left) or the Gly32Glu variant (center). Right: Plot showing the evolution of the distance "d" (in angstroms) between the nitrogen atom of the amino group of Lys38 and the phosphorus atom of the gamma phosphate group of the ATP molecule during the 200-ns simulation. Gray line: Wild-type protein; black line: Gly32Glu variant. (C) Arg693Gly variant. The partial model of the coiled-coil domain of SMC1A/SMC3 in the vicinity of amino acid Arg693 (or Gly693) of SMC1A is shown after 200 ns of molecular dynamics simulation of the wild-type protein (left) and the Arg693Gly variant (center). Right: Plot showing the evolution of the distance "d" (in angstroms) between the alpha carbons of Arg693 (or Gly693) of SMC1A and Glu479 of SMC3 during the 200-ns molecular dynamics simulation. Gray line: Wild-type protein; black line: Arg693Gly variant. Drawings were generated using PyMOL.

SMC3 along the 200-ns molecular dynamics simulation. The gray line shows that this distance remains constant at approximately 1.2 nm in the wild-type protein, whereas the black line shows that it increases to values greater than 2.0 nm in the Arg693Gly variant, indicating the local separation of the coiled-coil domains of both proteins. This local disorganization and possible defect in the dimer's correct structure may explain the variant's effect on the SMC1A/SMC3 ring's functionality. The remaining three variants—Arg96Cys, Arg496His, and Tyr983Cys—did not show substantial structural deviations from the wild-type protein. Specifically, the Arg96Cys variant is located in a β-sheet of the head domain, distant from the ATPase centers and surrounded by polar residues (Thr53, Ser103, Tyr105). Substitution with Cys, a similarly polar but smaller residue, preserved the local structure throughout the simulation. The Tyr983Cys variant is located in a flexible loop of the coiled-coil region, surrounded by polar residues (Gln224, Tyr229, Glu232). The substitution did not induce notable changes in the local environment. Finally, the Arg496His variant maps in an α-helix of the hinge domain and oriented toward the solvent. Replacement with His, another positively charged residue, did not alter the structural behavior during the simulation.

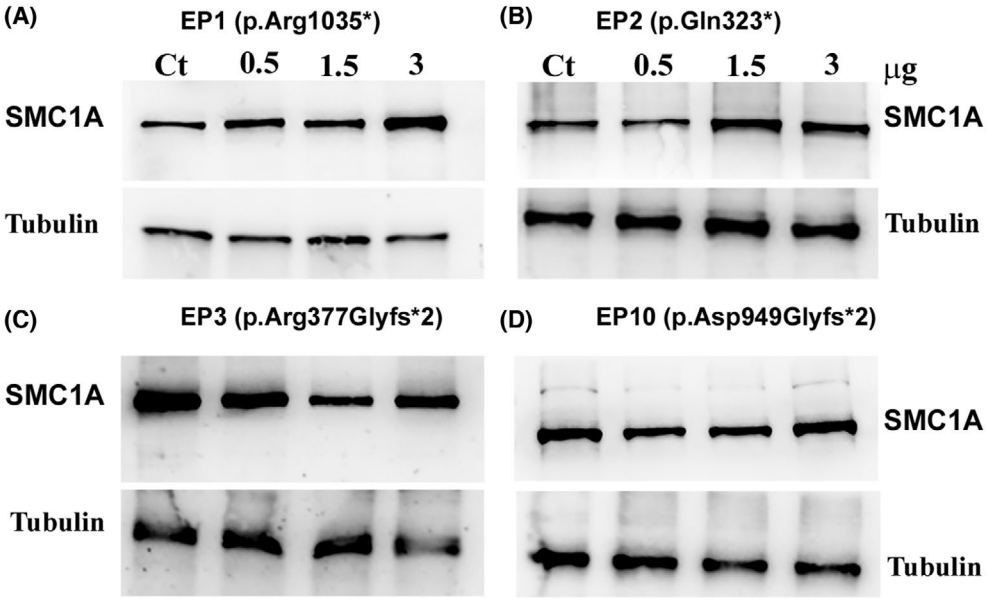

FIGURE 5 Ataluren restores SMC1A protein expression in lymphoblastoid cell lines (LCLs) carrying nonsense variants but not frameshift mutations. (A) Western blot analysis of SMC1A protein levels in EP1 LCLs (c.3103C>T, p.Arg1035*) following 24-h treatment with increasing concentrations of ataluren (.5, 1.5, and 3 μg/mL). A dose-dependent increase in SMC1A expression is observed. (B) Similar analysis in EP2 LCLs (c.901C>T, p.Gln323*) confirms ataluren-induced restoration of SMC1A protein levels. (C) EP3 LCLs carrying a frameshift variant (c.1063delC) show no detectable change in SMC1A expression upon ataluren treatment, indicating lack of responsiveness. (D) Consistent with this, EP10 LCLs harboring the c.2842_2845dup frameshift variant also fail to respond to ataluren, supporting the specificity of its mechanism of action for nonsense-mediated translational readthrough. The images shown are representative of two independent experiments.

3.4 | Ataluren reverses transcriptional and genomic defects in cells with *SMC1A* nonsense variants

Despite advances in understanding the molecular basis of DEE85, no effective therapies currently exist. Ataluren (PTC124), a translational readthrough-inducing drug, has shown promise in rescuing gene expression in disorders caused by nonsense mutations, including DMD, Shwachman–Diamond syndrome, and cystic fibrosis, both in vitro and in vivo.[26,36–40] Moreover, it has undergone clinical trials in patients with DMD and cystic fibrosis, supporting its relevance for disorders caused by premature stop codons.[25,41,42]

To evaluate whether ataluren could restore SMC1A protein expression, LCLs from two patients carrying nonsense variants in *SMC1A* (EP1: c.3103C>T, p.Arg1035* and EP2: c.901C>T, p.Gln323*) were treated with increasing doses of ataluren (.5, 1.5, and 3 μg/mL) for 24 h. The dosing rationale was based on clinical pharmacokinetic data. In phase II/III trials in patients with DMD and cystic fibrosis, oral administration of ataluren (4–40 mg/kg) resulted in plasma concentrations typically ranging from 2 to 30 μg/mL.[27] In addition, in myoblasts from *mdx* mice, Western blotting revealed a dose-dependent restoration of full-length dystrophin following ataluren treatment (.6–3 μg/mL).[43] Accordingly, we selected in vitro concentrations of .5, 1.5, and 3 μg/mL, which fall within or slightly below the clinically observed range, thereby ensuring physiological relevance while minimizing potential cytotoxicity in cell culture. Western blot analysis demonstrated the increase of SMC1A protein in both cell lines (Figure 5A,B, Figure S5). In contrast, EP3 and EP10 cells carrying a frameshift variant, c.1063delC and c.2842_2845dup respectively, showed no response, confirming the specificity of ataluren for nonsense alleles (Figure 5C,D).

To determine whether newly synthesized SMC1A is incorporated into the cohesin complex, we performed coimmunoprecipitation of SMC3 with SMC1A. These experiments confirmed the physical association between SMC1A and SMC3, whereas no signal was observed in control Western blotting with IgG-coated beads (Figure S6). Given the role of *SMC1A* in cohesin-mediated gene regulation and genome stability, we first investigated the transcriptional impact of ataluren. Transcriptomic profiling of treated EP1 cells revealed a dose-dependent response, with 1786, 2792, and 4920 DEGs identified at .5, 1.5, and 3 μg/mL, respectively (Figure 6A). When aggregating data across doses and comparing treated versus untreated cells, we detected 2064 DEGs (1113 downregulated and 951 upregulated; Figure 6B, Table S9), enriched in key biological processes including nervous system development, cell

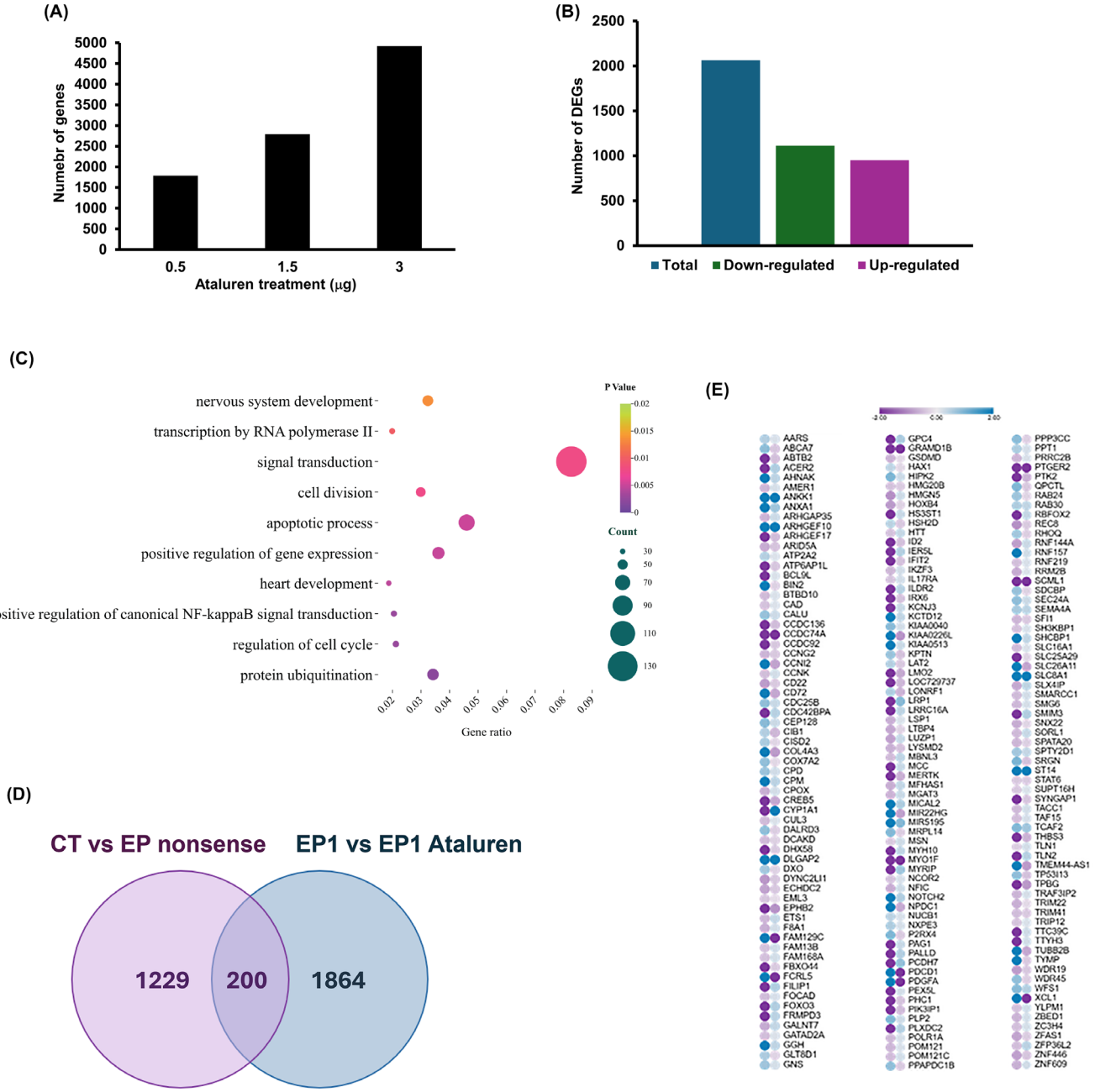

FIGURE 6 Transcriptomic response to ataluren in EP1 cells carrying a nonsense variant in *SMC1A*. (A) Transcriptomic profiling of EP1 lymphoblastoid cells treated with increasing concentrations of ataluren (.5, 1.5, and 3 μg/mL for 24 h) revealed a dose-dependent effect, with 1786, 2792, and 4920 differentially expressed genes (DEGs), respectively. (B) Aggregated analysis across all doses identified 2064 DEGs (1113 downregulated and 951 upregulated) when comparing treated versus untreated cells. (C) Gene Ontology enrichment analysis of these DEGs highlighted significant involvement in biological processes such as nervous system development, cell cycle progression, transcriptional regulation, and apoptosis. Dot size reflects the number of DEGs associated with each pathway; color intensity indicates statistical significance (*p*-value). (D) Venn diagram showing a core set of 200 genes consistently affected across all treatment concentrations. (E) Heatmap illustrating that 116 of these genes (58%) exhibit a reversal in expression direction following treatment, suggesting a robust and specific transcriptional reprogramming induced by ataluren. CT, control cells; EP, epileptic cells.

cycle and division, transcriptional regulation, and apoptosis (Figure 6C). Notably, 200 genes were consistently affected across all concentrations, with 116 (58%) showing a reversal in expression direction following treatment (Figure 6D,E).

A comparable pattern emerged in EP2 cells, where ataluren modulated the expression of 1152 and 1938 genes at 1.5 and 3 μg/mL, respectively (Figure S7A). Upon pooling the treatment data, we identified 1347 DEGs (703 downregulated, 644 upregulated; Figure S7B

and Table S10), again enriched in pathways related to cell proliferation, signal transduction, and cell adhesion (Figure S7C). Consistently, 161 genes were altered across doses, with 44.7% reverting toward control expression levels (Figure S7D,E). Finally, we also assessed spontaneous chromosomal instability. Of 100 metaphases, 24 (EP1) and 21 (EP2) exhibited both gaps and breaks (Figure S8A–C), whereas only 2–3 gaps per 100 metaphases were observed in control cells. These differences were statistically significant ($p < .05$). After ataluren treatment, aberration levels dropped to near control levels (Figure S8A).

In summary, ataluren effectively rescues SMC1A expression in nonsense mutant cells, restores normal gene expression, and reduces genomic instability, supporting its potential as a targeted therapy for DEE85.

4 | DISCUSSION

This study provides novel insights into the molecular consequences of *SMC1A* variants in patients affected by DEE85, a severe neurodevelopmental diagnosis characterized by early onset, severe ID, and drug-resistant epilepsy. By performing genome-wide transcriptomic profiling in LCLs carrying different types of *SMC1A* variants—nonsense, frameshift, and missense—we demonstrate that each variant type is associated with a distinct transcriptional signature. Notably, nonsense variants exerted the most profound effects on global gene expression, with more than 1429 DEGs, compared to 411 and 296 DEGs in frameshift and missense variants, respectively. This aligns with clinical observations that patients with nonsense variants often present with more severe neurodevelopmental phenotypes. In contrast, missense and frameshift variants produced more moderate and heterogeneous effects, suggesting partial retention of cohesin activity. The comparative analysis between variant subgroups revealed minimal overlap in dysregulated genes, with only 15 genes shared across all three mutation types. This limited convergence underscores the complexity of *SMC1A*-related pathogenesis and suggests that each mutation class may perturb distinct regulatory networks. Interestingly, nonsense and frameshift variants shared a subset of misregulated genes, with most showing concordant expression trends, whereas a few reversed direction, highlighting nuanced differences in downstream effects. The data revealed that dysregulated genes in DEE85 are involved in crucial biological processes including transcriptional regulation, chromatin remodeling, signal transduction, and neuronal migration, pathways directly relevant to brain development and function. These findings reflect the severity of the associated phenotype and suggest that the functional impact of *SMC1A* variants is highly variant type-dependent and transcriptomic profiling could serve as a valuable tool for stratifying patients and predicting clinical outcomes.

Germline pathogenic variants in the *SMC1A* gene are associated with both CdLS and DEE85. CdLS is generally linked to missense variants or small in-frame deletions that produce milder clinical manifestations, whereas DEE85 is predominantly caused by loss-of-function variants in *SMC1A*.[13,14,35,44,45] Comparison with CdLS cell lines revealed further transcriptomic divergence, despite their shared genetic origin. CdLS samples exhibited a more restrained transcriptional profile, consistent with the milder clinical phenotype typically associated with missense or in-frame *SMC1A* variants.[13,14,35] In contrast, DEE85 samples—particularly those with nonsense variants—displayed extensive dysregulation in genes involved in transcription, translation, DNA replication, and mRNA processing. Principal component analysis confirmed the separation of DEE85 nonsense samples from CdLS, supporting the hypothesis that loss-of-function variants in *SMC1A* disrupt cohesin's regulatory functions more severely, leading to broader transcriptomic instability and more aggressive neurological manifestations.

Although computational simulations are not yet sufficient to independently predict pathogenicity, they offer valuable molecular-scale insights into the impact of missense variants. To elucidate the molecular basis underlying phenotypic differences, we therefore performed structural modeling and molecular dynamics simulations of selected *SMC1A* missense variants. The simulations revealed that only Gly32Glu and Arg693Gly variants significantly affect the structural integrity of the SMC1A/SMC3 complex, potentially impairing cohesin function. Of note, the Gly32Glu variant likely disrupts ATP binding and hydrolysis in the head domain, which could compromise the ATPase-driven activity essential for cohesin loading and release, and the Arg693Gly variant destabilizes the coiled-coil interface between SMC1A and SMC3, possibly affecting the mechanical stability and proper assembly of the cohesin ring.

For Arg96Cys, Arg496His, and Tyr983Cys, the absence of observable structural changes does not exclude pathogenic effects. Molecular dynamics simulations do not capture folding-related perturbations, and these variants may induce misfolding or subtle conformational shifts during protein maturation. In particular, Arg496His, located in the hinge domain and exposed to the solvent, may influence interactions with other cohesin components or DNA. Although structurally stable in simulation, its position suggests potential functional relevance. Supporting this hypothesis, experimental evidence indicates that the Arg496His change impairs DNA repair mechanisms and elevates oxidative stress levels, both of which contribute to genomic instability.[46,47]

Although significant progress has been made in elucidating the molecular mechanisms underlying DEE85, there are still no effective treatments available. Ataluren, a drug that promotes translational readthrough, has demonstrated potential in restoring full-length protein in diseases caused by nonsense variants—such as DMD—in both in vitro and in vivo studies.[26] Ataluren treatment of EP1 and EP2 LCLs, both harboring nonsense *SMC1A* variants, resulted in the re-expression of full-length SMC1A protein, which was incorporated into the cohesin complex. In contrast, no effect was observed in cells carrying a frameshift variant, confirming the variant-specific mechanism of action. This observation further supports the notion that ataluren can counteract the molecular defects caused by nonsense variants. Clinical trials have shown that ataluren can slow disease progression in certain DMD patients and improve some aspects of lung function in cystic fibrosis, although its efficacy varies depending on the mutation and individual patient factors.[25,41,42,48,49] Strikingly, ataluren also reversed the expression of up to 58% of the previously dysregulated genes in these lines and significantly reduced the number of spontaneous chromosomal aberrations, restoring genomic stability to near control levels. These findings strongly suggest that restoration of SMC1A protein can rescue both transcriptional and genomic integrity, highlighting the central role of cohesin dysfunction in DEE85 pathology.

5 | CONCLUSIONS

Taken together, these results indicate that DEE85 is primarily a transcriptional disorder driven by cohesin dysfunction, and that nonsense *SMC1A* variants have the most deleterious effect on the cellular transcriptome. The success of ataluren in restoring SMC1A protein and reversing molecular defects provides compelling preclinical evidence for its potential as a targeted therapy for a subset of DEE85 patients. In conclusion, this work emphasizes the importance of variant-type stratification in both mechanistic and therapeutic studies of *SMC1A*-related disorders. It also identifies ataluren as a promising candidate for personalized intervention in DEE85 patients carrying nonsense variants, opening new avenues for precision medicine in developmental epilepsies.

AUTHOR CONTRIBUTIONS

Maddalena Di Nardo: Investigation; data curation. **Francesca Sardina**: Investigation; data curation. **Maria M. Pallotta:** Investigation; data curation. **Iñigo Marcos-Alcalde**: Investigation; data curation. **Paulino Gómez-Puertas**: Conceptualization (supporting); investigation; data curation; writing—review and editing. **Ian D. Krantz**: Conceptualization (supporting); investigation; data curation; writing—review and editing; funding acquisition. **Cinzia Rinaldo**: Conceptualization (supporting); investigation; data curation; writing—review and editing. **Antonio Musio**: Conceptualization (lead); investigation; data curation; formal analysis; writing—original draft preparation; writing—review and editing; funding acquisition.

ACKNOWLEDGMENTS

The computational support of the Centro de Computación Científica CCC-UAM is gratefully recognized. We extend our deepest gratitude to the patients affected by *SMC1A*-related epilepsy and their families for their invaluable participation in this study. We also sincerely thank the SMC1A Foundation for their continued collaboration and support, with special appreciation to Mr. Daniele Ciampa, European delegate of the Foundation, for his dedicated engagement. Open access publishing facilitated by Consiglio Nazionale delle Ricerche, as part of the Wiley - CRUI-CARE agreement.

FUNDING INFORMATION

This work was supported by the project 202227SYBW_LS3_PRIN2022, by a donation from the Italian SMC1A Association to A.M., and by Spanish Government grant PID2021-126625OB-I00 (MCIN/AEI/10.13039/501100011033/FEDER,EU.2022) to P.G.-P.

CONFLICT OF INTEREST STATEMENT

None of the authors has any conflict of interest to disclose. We confirm that we have read the Journal's position on issues involved in ethical publication and affirm that this report is consistent with those guidelines.

DATA AVAILABILITY STATEMENT

The relevant data supporting the findings of this study are available in this article and its Supporting Information files. All NGS raw files have been deposited into NCBI Sequence Read Archive under accession number PRJNA1370816.

ORCID

Maddalena Di Nardo https://orcid.org/0000-0002-1481-2101
Francesca Sardina https://orcid.org/0000-0001-6474-2079
Maria M. Pallotta https://orcid.org/0000-0001-7731-8621
Iñigo Marcos-Alcalde https://orcid.org/0000-0002-0674-6423
Paulino Gómez-Puertas https://orcid.org/0000-0003-3131-729X

Cinzia Rinaldo https://orcid.org/0000-0001-6124-762X
Ian D. Krantz https://orcid.org/0000-0003-2442-1128
Antonio Musio https://orcid.org/0000-0001-7701-6543

REFERENCES

1. Yatskevich S, Rhodes J, Nasmyth K. Organization of chromosomal DNA by SMC complexes. Annu Rev Genet. 2019;53:445–82.
2. Losada A. Cohesin in cancer: chromosome segregation and beyond. Nat Rev Cancer. 2014;14:389–93.
3. Merkenschlager M, Nora EP. CTCF and Cohesin in genome folding and transcriptional gene regulation. Annu Rev Genomics Hum Genet. 2016;17:17–43.
4. Rao SS, Huntley MH, Durand NC, Stamenova EK, Bochkov ID, Robinson JT, et al. A 3D map of the human genome at kilobase resolution reveals principles of chromatin looping. Cell. 2014;159:1665–80.
5. Schwarzer W, Abdennur N, Goloborodko A, Pekowska A, Fudenberg G, Loe-Mie Y, et al. Two independent modes of chromatin organization revealed by cohesin removal. Nature. 2017;551:51–6.
6. Davidson IF, Bauer B, Goetz D, Tang W, Wutz G, Peters JM. DNA loop extrusion by human cohesin. Science. 2019;366:1338–45.
7. Fudenberg G, Imakaev M, Lu C, Goloborodko A, Abdennur N, Mirny LA. Formation of chromosomal domains by loop extrusion. Cell Rep. 2016;15:2038–49.
8. Strom L, Karlsson C, Lindroos HB, Wedahl S, Katou Y, Shirahige K, et al. Postreplicative formation of cohesion is required for repair and induced by a single DNA break. Science. 2007;317:242–5.
9. Heidinger-Pauli JM, Unal E, Guacci V, Koshland D. The kleisin subunit of cohesin dictates damage-induced cohesion. Mol Cell. 2008;31:47–56.
10. Di Nardo M, Musio A. Cohesin – bridging the gap among gene transcription, genome stability, and human diseases. FEBS Lett. 2025;599:190–208.
11. Di Nardo M, Pallotta MM, Musio A. The multifaceted roles of cohesin in cancer. J Exp Clin Cancer Res. 2022;41:96.
12. Di Nardo M, Astigiano S, Baldari S, Pallotta MM, Porta G, Pigozzi S, et al. The synergism of SMC1A cohesin gene silencing and bevacizumab against colorectal cancer. J Exp Clin Cancer Res. 2024;43:49.
13. Musio A, Selicorni A, Focarelli ML, Gervasini C, Milani D, Russo S, et al. X-linked Cornelia de Lange syndrome owing to SMC1L1 mutations. Nat Genet. 2006;38:528–30.
14. Deardorff MA, Kaur M, Yaeger D, Rampuria A, Korolev S, Pie J, et al. Mutations in cohesin complex members SMC3 and SMC1A cause a mild variant of cornelia de Lange syndrome with predominant mental retardation. Am J Hum Genet. 2007;80:485–94.
15. Kline AD, Moss JF, Selicorni A, Bisgaard AM, Deardorff MA, Gillett PM, et al. Diagnosis and management of Cornelia de Lange syndrome: first international consensus statement. Nat Rev Genet. 2018;19:649–66.
16. Symonds JD, Joss S, Metcalfe KA, Somarathi S, Cruden J, Devlin AM, et al. Heterozygous truncation mutations of the SMC1A gene cause a severe early onset epilepsy with cluster seizures in females: detailed phenotyping of 10 new cases. Epilepsia. 2017;58:565–75.
17. Goldstein JH, Tim-Aroon T, Shieh J, Merrill M, Deeb KK, Zhang S, et al. Novel SMC1A frameshift mutations in children with developmental delay and epilepsy. Eur J Med Genet. 2015;58:562–8.
18. Lebrun N, Lebon S, Jeannet PY, Jacquemont S, Billuart P, Bienvenu T. Early-onset encephalopathy with epilepsy associated with a novel splice site mutation in SMC1A. Am J Med Genet A. 2015;167A:3076–81.
19. Jansen S, Kleefstra T, Willemsen MH, de Vries P, Pfundt R, Hehir-Kwa JY, et al. De novo loss-of-function mutations in X-linked SMC1A cause severe ID and therapy-resistant epilepsy in females: expanding the phenotypic spectrum. Clin Genet. 2016;90:413–9.
20. Baranano KW, Kimball A, Fong SL, Egense AS, Hudon C, Kline AD. Further characterization of SMC1A loss of function epilepsy distinct from Cornelia de Lange syndrome. J Child Neurol. 2022;37:390–6.
21. Elwan M, Fowkes R, Lewis-Smith D, Winder A, Baker MR, Thomas RH. Late-onset cluster seizures and intellectual disability associated with a novel truncation variant in SMC1A. Epilepsy Behav Rep. 2022;19:100556.
22. Yang Y, Chen L, Wang Z, Ding Y, Liu Y. A de novo frameshift variant in SMC1A causes non-classic Cornelia de Lange syndrome with epilepsy: a case report and literature review. Mol Genet Genomic Med. 2025;13:e70058.
23. Amllal N, Lyahyai J, Afif L, Kriouile Y, Sefiani A, Elalaoui SC. Highlighting the different facets of SMC1A truncating variants: two patients with novel SMC1A pathogenic variants. Epileptic Disord. 2025;27:114–6.
24. Mort M, Ivanov D, Cooper DN, Chuzhanova NA. A meta-analysis of nonsense mutations causing human genetic disease. Hum Mutat. 2008;29:1037–47.
25. Bello L, Riguzzi P, Albamonte E, Astrea G, Battini R, Barp A, et al. Opinion of the Italian Association of Myology on ataluren for the treatment of nonsense mutation Duchenne muscular dystrophy. Drugs R D. 2025;25:99–106.
26. Welch EM, Barton ER, Zhuo J, Tomizawa Y, Friesen WJ, Trifillis P, et al. PTC124 targets genetic disorders caused by nonsense mutations. Nature. 2007;447:87–91.
27. Michorowska S. Ataluren-promising therapeutic premature termination codon readthrough frontrunner. Pharmaceuticals (Basel). 2021;14:785.
28. Petela NJ, Gonzalez Llamazares A, Dixon S, Hu B, Lee BG, Metson J, et al. Folding of cohesin's coiled coil is important for Scc2/4-induced association with chromosomes. Elife. 2021;10:e67268.
29. Vitoria Gomes M, Landwerlin P, Diebold-Durand ML, Shaik TB, Durand A, Troesch E, et al. The cohesin ATPase cycle is mediated by specific conformational dynamics and interface plasticity of SMC1A and SMC3 ATPase domains. Cell Rep. 2024;43:114656.
30. Kelley LA, Mezulis S, Yates CM, Wass MN, Sternberg MJ. The Phyre2 web portal for protein modeling, prediction and analysis. Nat Protoc. 2015;10:845–58.
31. Waterhouse A, Bertoni M, Bienert S, Studer G, Tauriello G, Gumienny R, et al. SWISS-MODEL: homology modelling of protein structures and complexes. Nucleic Acids Res. 2018;46:W296–W303.

32. Ros-Pardo D, Gomez-Puertas P, Marcos-Alcalde I. STAG2: computational analysis of missense variants involved in disease. Int J Mol Sci. 2024;25:1280.
33. Roe DR, Cheatham TE 3rd. PTRAJ and CPPTRAJ: software for processing and analysis of molecular dynamics trajectory data. J Chem Theory Comput. 2013;9:3084–95.
34. Humphrey W, Dalke A, Schulten K. VMD: visual molecular dynamics. J Mol Graph. 1996;14:33–8, 27–38.
35. Musio A. The multiple facets of the SMC1A gene. Gene. 2020;743:144612.
36. Goldmann T, Overlack N, Wolfrum U, Nagel-Wolfrum K. PTC124-mediated translational readthrough of a nonsense mutation causing usher syndrome type 1C. Hum Gene Ther. 2011;22:537–47.
37. Li M, Andersson-Lendahl M, Sejersen T, Arner A. Muscle dysfunction and structural defects of dystrophin-null sapje mutant zebrafish larvae are rescued by ataluren treatment. FASEB J. 2014;28:1593–9.
38. Liu X, Zhang Y, Zhang B, Gao H, Qiu C. Nonsense suppression induced readthrough of a novel PAX6 mutation in patient-derived cells of congenital aniridia. Mol Genet Genomic Med. 2020;8:e1198.
39. Cipolli M, Boni C, Penzo M, Villa I, Bolamperti S, Baldisseri E, et al. Ataluren improves myelopoiesis and neutrophil chemotaxis by restoring ribosome biogenesis and reducing p53 levels in Shwachman-diamond syndrome cells. Br J Haematol. 2024;204:292–305.
40. Bezzerri V, Pegoraro A, Hristodor AM, Crane GM, Meneghelli I, Brignole C, et al. Ataluren improves hematopoietic and pancreatic disorders in Shwachman-diamond syndrome patients: a compassionate program case-series. Nat Commun. 2025;16:8189.
41. Campbell C, Barohn RJ, Bertini E, Chabrol B, Comi GP, Darras BT, et al. Meta-analyses of ataluren randomized controlled trials in nonsense mutation Duchenne muscular dystrophy. J Comp Eff Res. 2020;9:973–84.
42. Mercuri E, Osorio AN, Muntoni F, Buccella F, Desguerre I, Kirschner J, et al. Safety and effectiveness of ataluren in patients with nonsense mutation DMD in the STRIDE registry compared with the CINRG Duchenne natural history study (2015–2022): 2022 interim analysis. J Neurol. 2023;270:3896–913.
43. Kayali R, Ku JM, Khitrov G, Jung ME, Prikhodko O, Bertoni C. Read-through compound 13 restores dystrophin expression and improves muscle function in the mdx mouse model for Duchenne muscular dystrophy. Hum Mol Genet. 2012;21:4007–20.
44. Huisman S, Mulder PA, Redeker E, Bader I, Bisgaard AM, Brooks A, et al. Phenotypes and genotypes in individuals with SMC1A variants. Am J Med Genet A. 2017;173:2108–25.
45. Gibellato E, Cianci P, Mariani M, Parma B, Huisman S, Smigiel R, et al. SMC1A epilepsy syndrome: clinical data from a large international cohort. Am J Med Genet A. 2024;194:e63577.
46. Revenkova E, Focarelli ML, Susani L, Paulis M, Bassi MT, Mannini L, et al. Cornelia de Lange syndrome mutations in SMC1A or SMC3 affect binding to DNA. Hum Mol Genet. 2009;18:418–27.
47. Gimigliano A, Mannini L, Bianchi L, Puglia M, Deardorff MA, Menga S, et al. Proteomic profile identifies dysregulated pathways in Cornelia de Lange syndrome cells with distinct mutations in SMC1A and SMC3 genes. J Proteome Res. 2012;11:6111–23.
48. Kerem E, Konstan MW, De Boeck K, Accurso FJ, Sermet-Gaudelus I, Wilschanski M, et al. Ataluren for the treatment of nonsense-mutation cystic fibrosis: a randomised, double-blind, placebo-controlled phase 3 trial. Lancet Respir Med. 2014;2:539–47.
49. Konstan MW, VanDevanter DR, Rowe SM, Wilschanski M, Kerem E, Sermet-Gaudelus I, et al. Efficacy and safety of ataluren in patients with nonsense-mutation cystic fibrosis not receiving chronic inhaled aminoglycosides: the international, randomized, double-blind, placebo-controlled Ataluren confirmatory trial in cystic fibrosis (ACT CF). J Cyst Fibros. 2020;19:595–601.

SUPPORTING INFORMATION

Additional supporting information can be found online in the Supporting Information section at the end of this article.

How to cite this article: Di Nardo M, Sardina F, Pallotta MM, Marcos-Alcalde I, Gómez-Puertas P, Rinaldo C, et al. Mutation type-specific transcriptomic signatures and readthrough therapy rescue in *SMC1A*-related developmental and epileptic encephalopathy. Epilepsia. 2026;00:1–14. https://doi.org/10.1002/epi.70150

1 SUPPLEMENTARY MATERIAL AND METHODS

1.1 Library preparation and RNA sequencing

Samples were processed for RNA-seq analyses as previously described [1]. Briefly, library preparation was performed using the Universal Plus mRNA-Seq kit (Tecan Genomics, Redwood City, CA), following the manufacturer's protocol. RNA samples were quantified and assessed for quality using the Agilent 2100 Bioanalyzer RNA assay (Agilent Technologies, Santa Clara, CA). Final libraries were evaluated using the Qubit 3.0 Fluorometer (Invitrogen, Carlsbad, CA) and the Agilent Bioanalyzer DNA assay. Sequencing libraries were then processed and sequenced in paired-end 150 bp mode on the NovaSeq 6000 platform (Illumina, San Diego, CA).

1.2 RNA-Seq analysis

Raw sequencing data were processed using Illumina BCL Convert v3.9.31, which performed base calling, demultiplexing, and adapter masking. During demultiplexing, adapter sequences were masked by converting them to *N* characters, with corresponding base quality scores overwritten to 2 to facilitate downstream trimming using standard quality filtering tools. Subsequent trimming of low-quality bases and residual adapter sequences was carried out using ERNE software [2]. Cleaned reads were then aligned to the *Homo sapiens* reference genome (hg38) using STAR with default parameters. STAR, a splice-aware aligner optimized for RNA-Seq data, enabled accurate mapping and identification of exon-exon junctions [3]. Transcript assembly and quantification were performed with StringTie, allowing reconstruction of full-length transcripts and estimation of expression levels for multiple spliced isoforms at each gene locus [4]. For quality control, the RSeqQC5 package was employed to assess read strand specificity and gene body coverage, ensuring the integrity and reliability of the RNA-Seq dataset [5].

1.2.1 Pair-wise differential expression analysis

Differential expression analysis was conducted using DESeq2, which applies a Generalized Linear Model (GLM) to estimate expression levels for each gene and transcript. The method incorporates shrinkage estimation for both dispersion and fold change values, enhancing the stability and

interpretability of the results. This approach allows for a more quantitative assessment, emphasizing the magnitude of differential expression rather than its mere presence. Normalization of count data was performed using the median-of-ratios method, and statistical significance was evaluated through the Wald test [6, 7].

1.2.2 Pathway analysis and function

Differentially expressed genes (DEGs)were functionally analysed for associated biological processes using the Database for Annotation, Visualization, and Integrated Discovery (DAVID), version 2025_1 (https://david.ncifcrf.gov). For each annotated term, enrichment was assessed by calculating the corresponding *p*-value, and terms with $p < 0.05$ were considered significantly enriched.

1.3 Western blotting

Western blotting was performed as described previously [1]. Briefly, whole-cell protein extracts cells were prepared using a lysis buffer containing 25 µM Tris-HCl (pH 8.0), 55 µM NaCl, 1 µM EDTA, and a protease inhibitor cocktail (Sigma-Aldrich). Protein concentrations were determined using the Bradford Protein Assay (Thermo Scientific). Equal amounts of protein (20 µg per lane) were separated by SDS-PAGE and transferred to nitrocellulose membranes (Amersham). Membranes were incubated with a primary anti-SMC1A antibody (Fortis Life Sciences), followed by a peroxidase-conjugated secondary antibody (Sigma). Detection was performed using a chemiluminescence system (Amersham), and signals were visualized with a Chemidoc imaging system (Bio-Rad). An anti-tubulin antibody (Merck) was used as a loading control. The ImageJ software was used to carry out semiquantitative image analysis of immunoblotting data, expressed by percent of ataluren treatments (0.5, 1.5 and 3 µg/ml)/control ratio.

1.4 Spontaneous genomic instability assay

Spontaneous genomic instability in cell lines carrying nonsense *SMC1A* variants was assessed using standard cytogenetic protocols. Briefly, colcemid was added to cell cultures for 90 minutes to arrest cells in metaphase, followed by hypotonic treatment with 0.075 M KCl for 20 minutes at 37°C.

Cells were then fixed with multiple changes of Carnoy's fixative (methanol:acetic acid, 3:1). Fixed cells were dropped onto clean, moist microscope slides. For each patient sample, 100 metaphases were analysed. Chromosomal aberrations, including gaps and breaks, were visualized by Giemsa staining and scored by direct microscopic examination.

SUPPLEMENTARY REFERENCES

1. Di Nardo M, Astigiano S, Baldari S, Pallotta MM, Porta G, Pigozzi S, et al. The synergism of SMC1A cohesin gene silencing and bevacizumab against colorectal cancer J Exp Clin Cancer Res. 2024 Feb 16;43:49.
2. Del Fabbro C, Scalabrin S, Morgante M, Giorgi FM. An extensive evaluation of read trimming effects on Illumina NGS data analysis PLoS One. 2013;8:e85024.
3. Dobin A, Davis CA, Schlesinger F, Drenkow J, Zaleski C, Jha S, et al. STAR: ultrafast universal RNA-seq aligner Bioinformatics. 2013 Jan 1;29:15-21.
4. Pertea M, Pertea GM, Antonescu CM, Chang TC, Mendell JT, Salzberg SL. StringTie enables improved reconstruction of a transcriptome from RNA-seq reads Nat Biotechnol. 2015 Mar;33:290-295.
5. Wang L, Wang S, Li W. RSeQC: quality control of RNA-seq experiments Bioinformatics. 2012 Aug 15;28:2184-2185.
6. Love MI, Huber W, Anders S. Moderated estimation of fold change and dispersion for RNA-seq data with DESeq2 Genome Biol. 2014;15:550.
7. Anders S, Huber W. Differential expression analysis for sequence count data Genome Biol. 2010;11:R106.

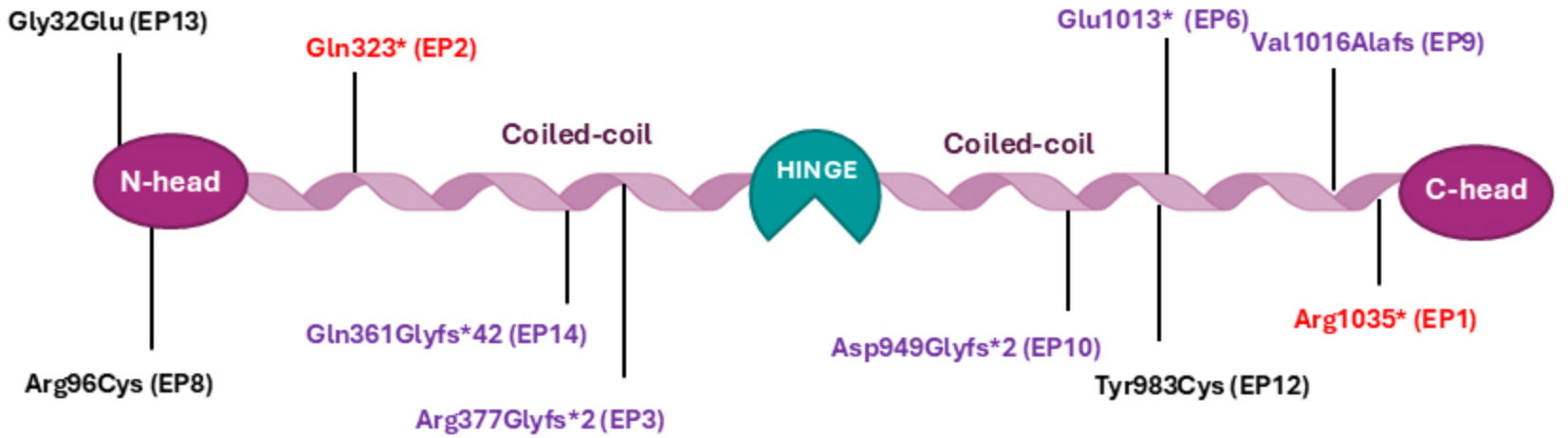
Gly32Glu (EP13)
Gln323* (EP2)
Glu1013* (EP6)
Val1016Alafs (EP9)
Coiled-coil
Coiled-coil
N-head
HINGE
C-head
Gln361Glyfs*42 (EP14)
Arg1035* (EP1)
Asp949Glyfs*2 (EP10)
Arg96Cys (EP8)
Tyr983Cys (EP12)
Arg377Glyfs*2 (EP3)
Nonsense variant
Frameshift variant
Missense variant

Fig. S1

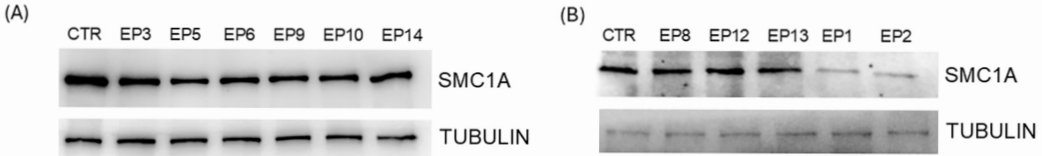
(A)
CTR
EP3
EP5
EP6
EP9
EP10
EP14
SMC1A
TUBULIN
(B)
CTR
EP8
EP12
EP13
EP1
EP2
SMC1A
TUBULIN

Fig. S2

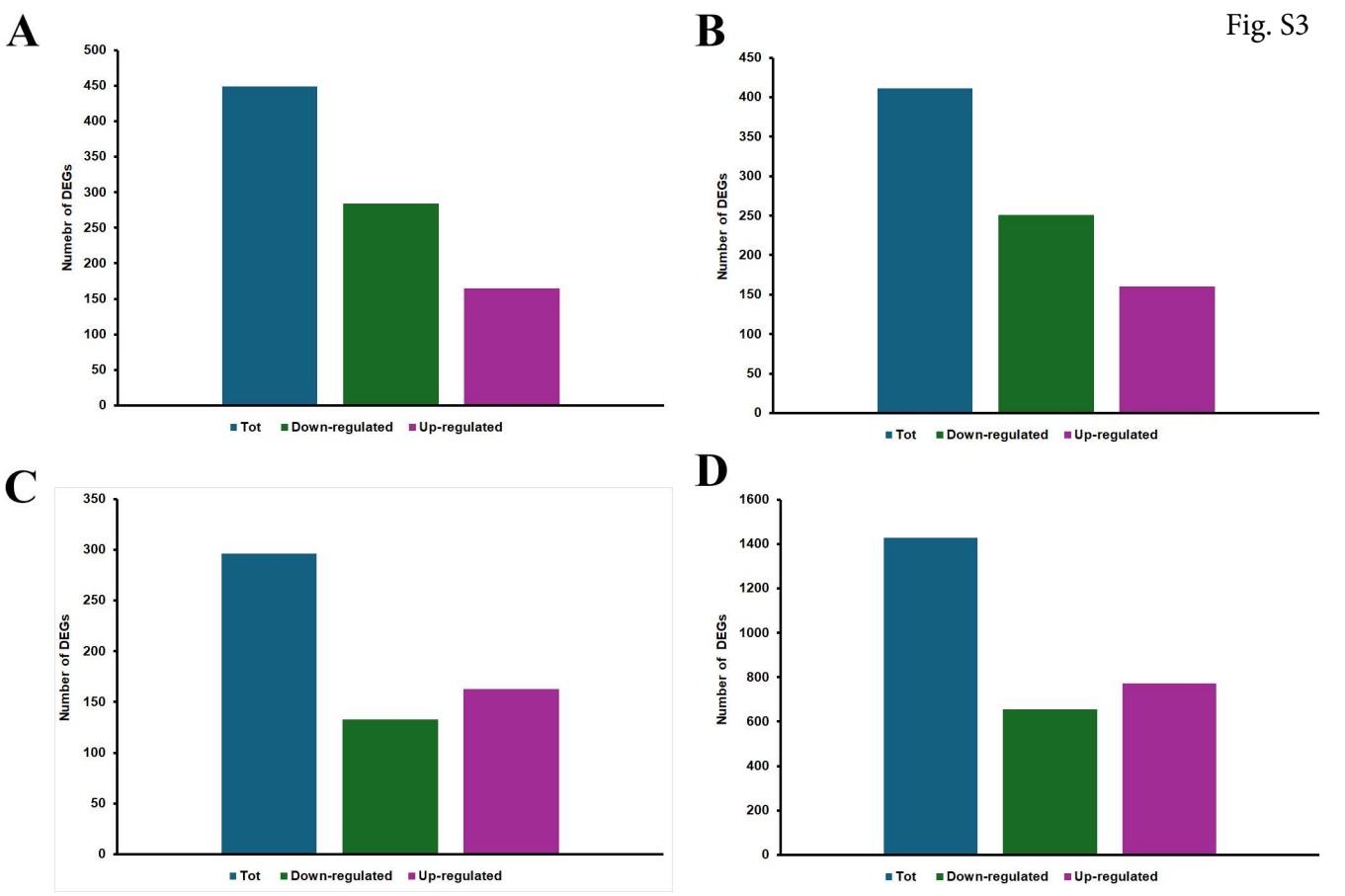
A
Numebr of DEGs
500
450
400
350
300
250
200
150
100
50
0
Tot
Down-regulated
Up-regulated
B
Number of DEGs
450
400
350
300
250
200
150
100
50
0
Tot
Down-regulated
Up-regulated
C
Number of DEGs
350
300
250
200
150
100
50
0
Tot
Down-regulated
Up-regulated
D
Number of DEGs
1600
1400
1200
1000
800
600
400
200
0
Tot
Down-regulated
Up-regulated

Fig. S4

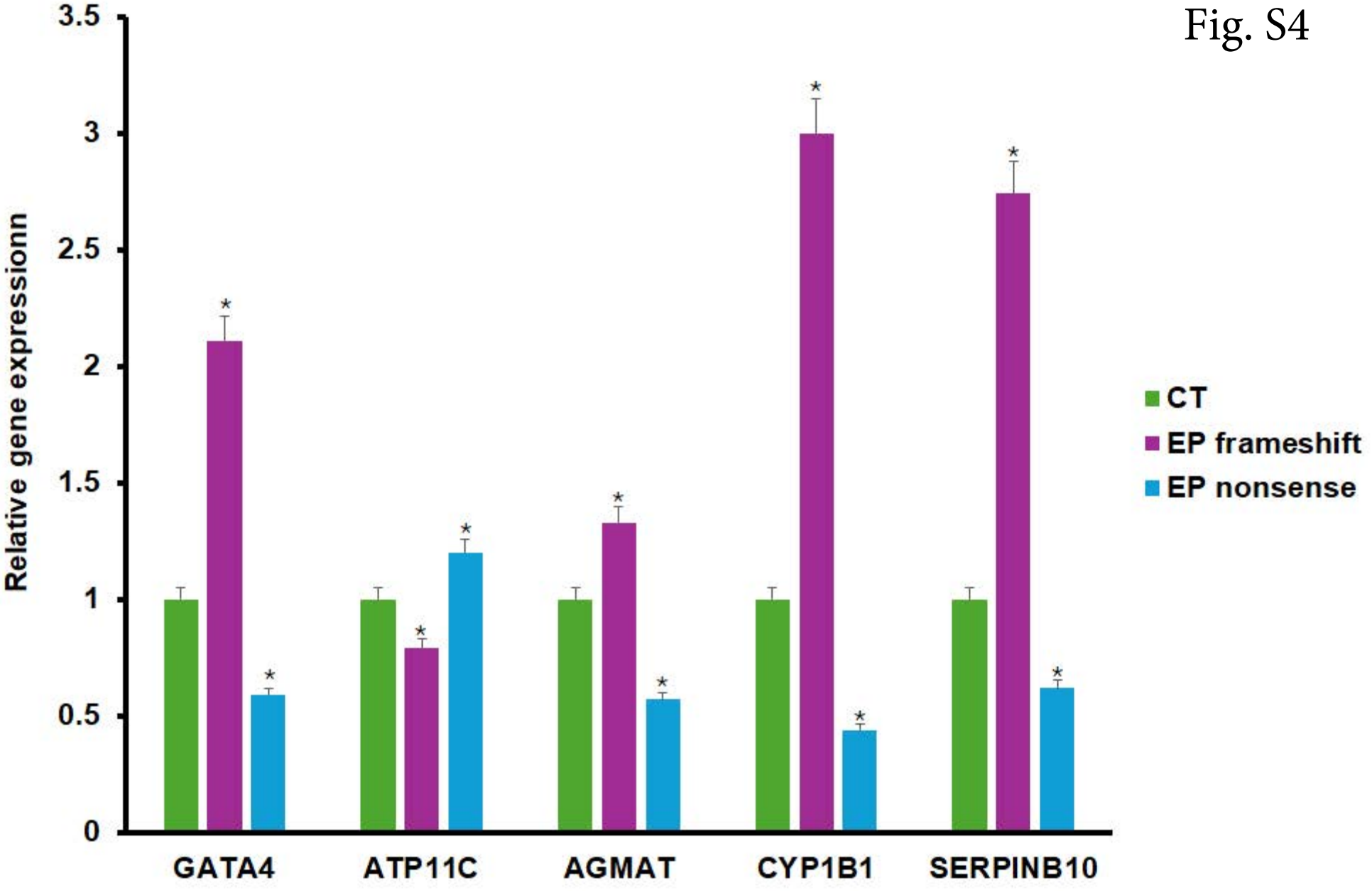
Relative gene expressionn
3.5
3
2.5
2
1.5
1
0.5
0
GATA4
ATP11C
AGMAT
CYP1B1
SERPINB10
CT
EP frameshift
EP nonsense

Fig. S5

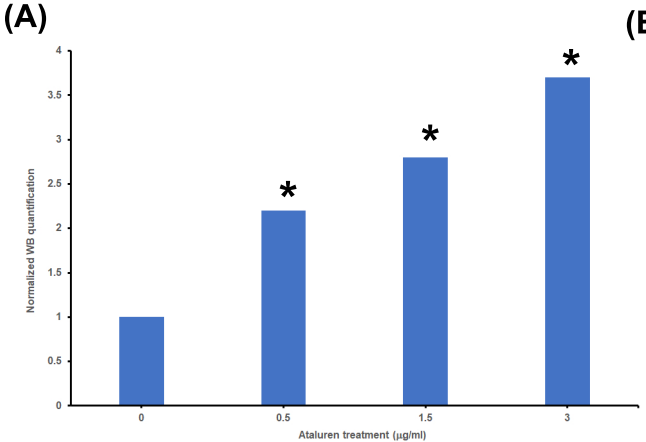
(A)
Normalized WB quantification
4
3.5
3
2.5
2
1.5
1
0.5
0
*
*
*
0
0.5
1.5
3
Ataluren treatment (μg/ml)

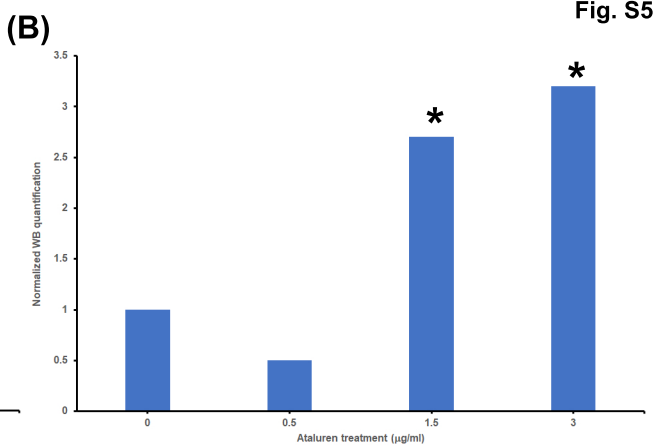
(B)
Normalized WB quantification
3.5
3
2.5
2
1.5
1
0.5
0
*
*
0
0.5
1.5
3
Ataluren treatment (μg/ml)

(A)

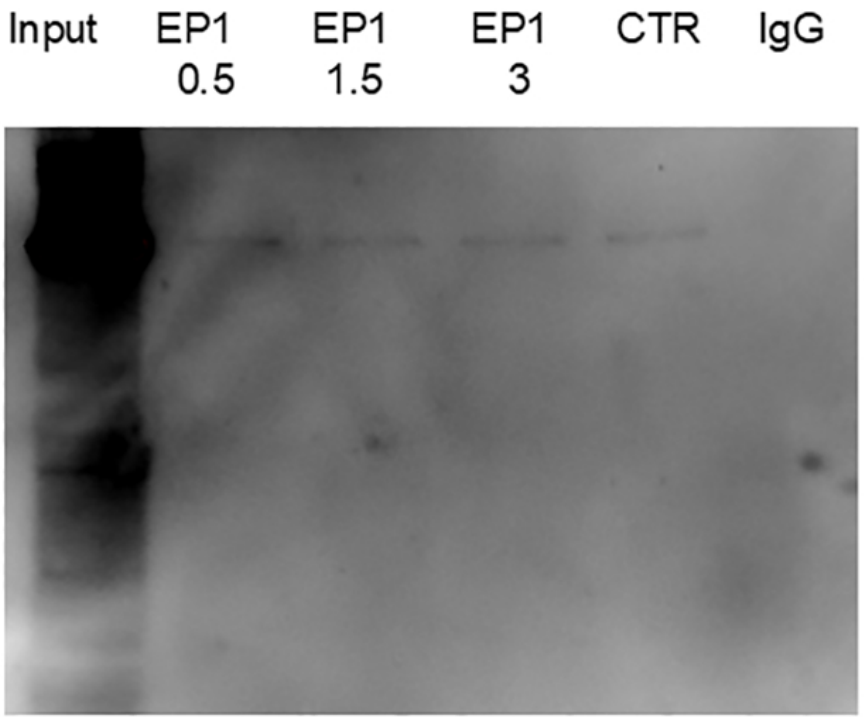

(B)

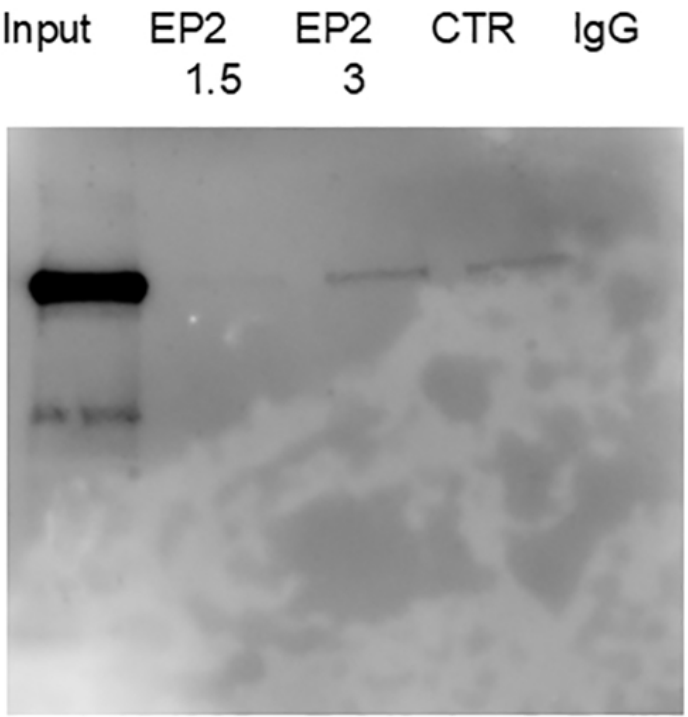

Fig. S6

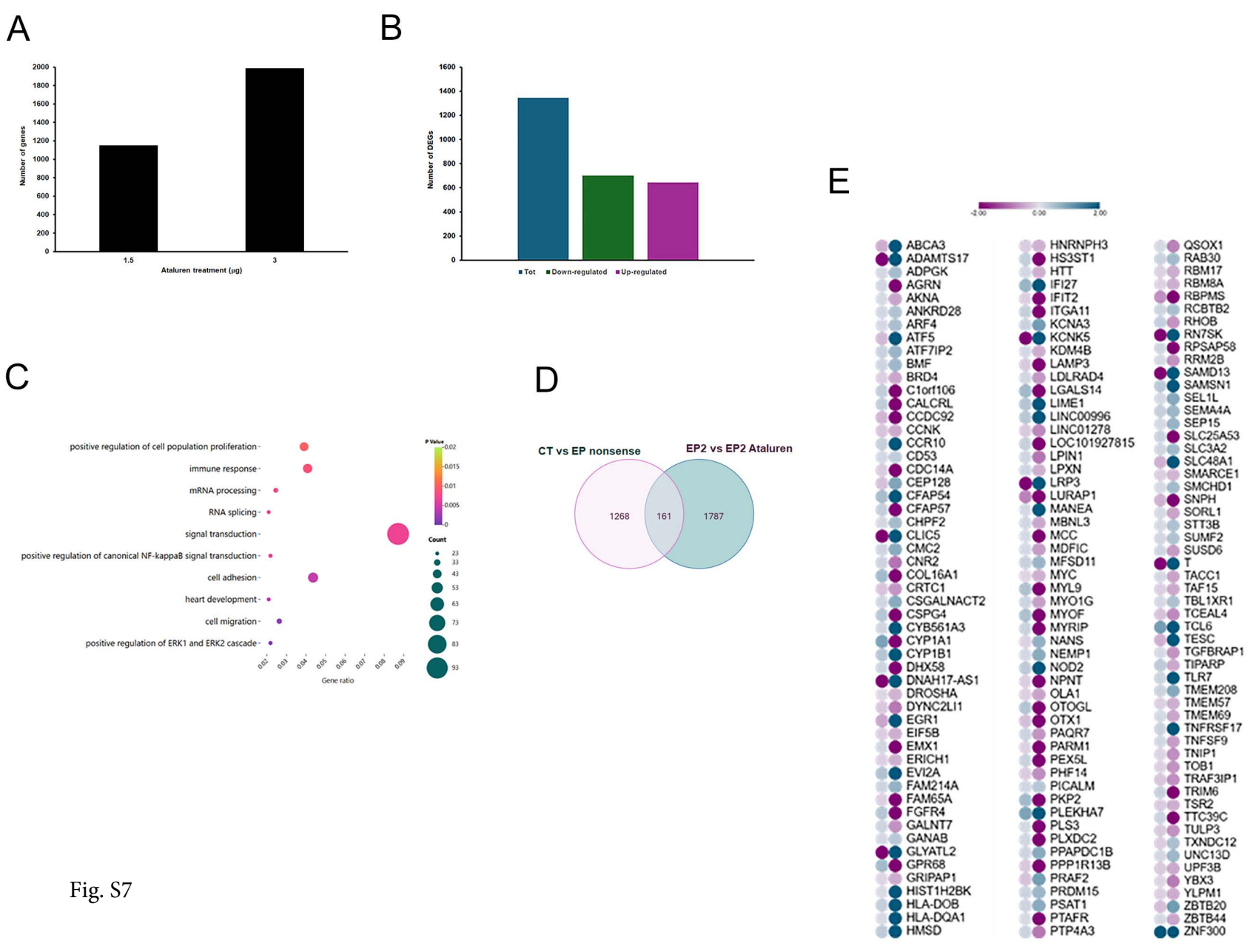
A
Number of genes
2000
1800
1600
1400
1200
1000
800
600
400
200
0
1.5
3
Ataluren treatment (μg)
B
Number of DEGs
1600
1400
1200
1000
800
600
400
200
0
Tot
Down-regulated
Up-regulated
C
positive regulation of cell population proliferation
immune response
mRNA processing
RNA splicing
signal transduction
positive regulation of canonical NF-kappaB signal transduction
cell adhesion
heart development
cell migration
positive regulation of ERK1 and ERK2 cascade
Gene ratio
P Value
0.02
0.015
0.01
0.005
0
Count
23
33
43
53
63
73
83
93
D
CT vs EP nonsense
EP2 vs EP2 Ataluren
1268
161
1787
E
-2.00
0.00
2.00
ABCA3
ADAMTS17
ADPGK
AGRN
AKNA
ANKRD28
ARF4
ATF5
ATF7IP2
BMF
BRD4
C1orf106
CALCRL
CCDC92
CCNK
CCR10
CD53
CDC14A
CEP128
CFAP54
CFAP57
CHPF2
CLIC5
CMC2
CNR2
COL16A1
CRTC1
CSGALNACT2
CSPG4
CYB561A3
CYP1A1
CYP1B1
DHX58
DNAH17-AS1
DROSHA
DYNC2LI1
EGR1
EIF5B
EMX1
ERICH1
EVI2A
FAM214A
FAM65A
FGFR4
GALNT7
GANAB
GLYATL2
GPR68
GRIPAP1
HIST1H2BK
HLA-DOB
HLA-DQA1
HMSD
HNRNPH3
HS3ST1
HTT
IFI27
IFIT2
ITGA11
KCNA3
KCNK5
KDM4B
LAMP3
LDLRAD4
LGALS14
LIME1
LINC00996
LINC01278
LOC101927815
LPIN1
LPXN
LRP3
LURAP1
MANEA
MBNL3
MCC
MDFIC
MFSD11
MYC
MYL9
MYO1G
MYOF
MYRIP
NANS
NEMP1
NOD2
NPNT
OLA1
OTOGL
OTX1
PAQR7
PARM1
PEX5L
PHF14
PICALM
PKP2
PLEKHA7
PLS3
PLXDC2
PPAPDC1B
PPP1R13B
PRAF2
PRDM15
PSAT1
PTAFR
PTP4A3
QSOX1
RAB30
RBM17
RBM8A
RBPMS
RCBTB2
RHOB
RN7SK
RPSAP58
RRM2B
SAMD13
SAMSN1
SEL1L
SEMA4A
SEP15
SLC25A53
SLC3A2
SLC48A1
SMARCE1
SMCHD1
SNPH
SORL1
STT3B
SUMF2
SUSD6
T
TACC1
TAF15
TBL1XR1
TCEAL4
TCL6
TESC
TGFBRAP1
TIPARP
TLR7
TMEM208
TMEM57
TMEM69
TNFRSF17
TNFSF9
TNIP1
TOB1
TRAF3IP1
TRIM6
TSR2
TTC39C
TULP3
TXNDC12
UNC13D
UPF3B
YBX3
YLPM1
ZBTB20
ZBTB44
ZNF300

Fig. S7

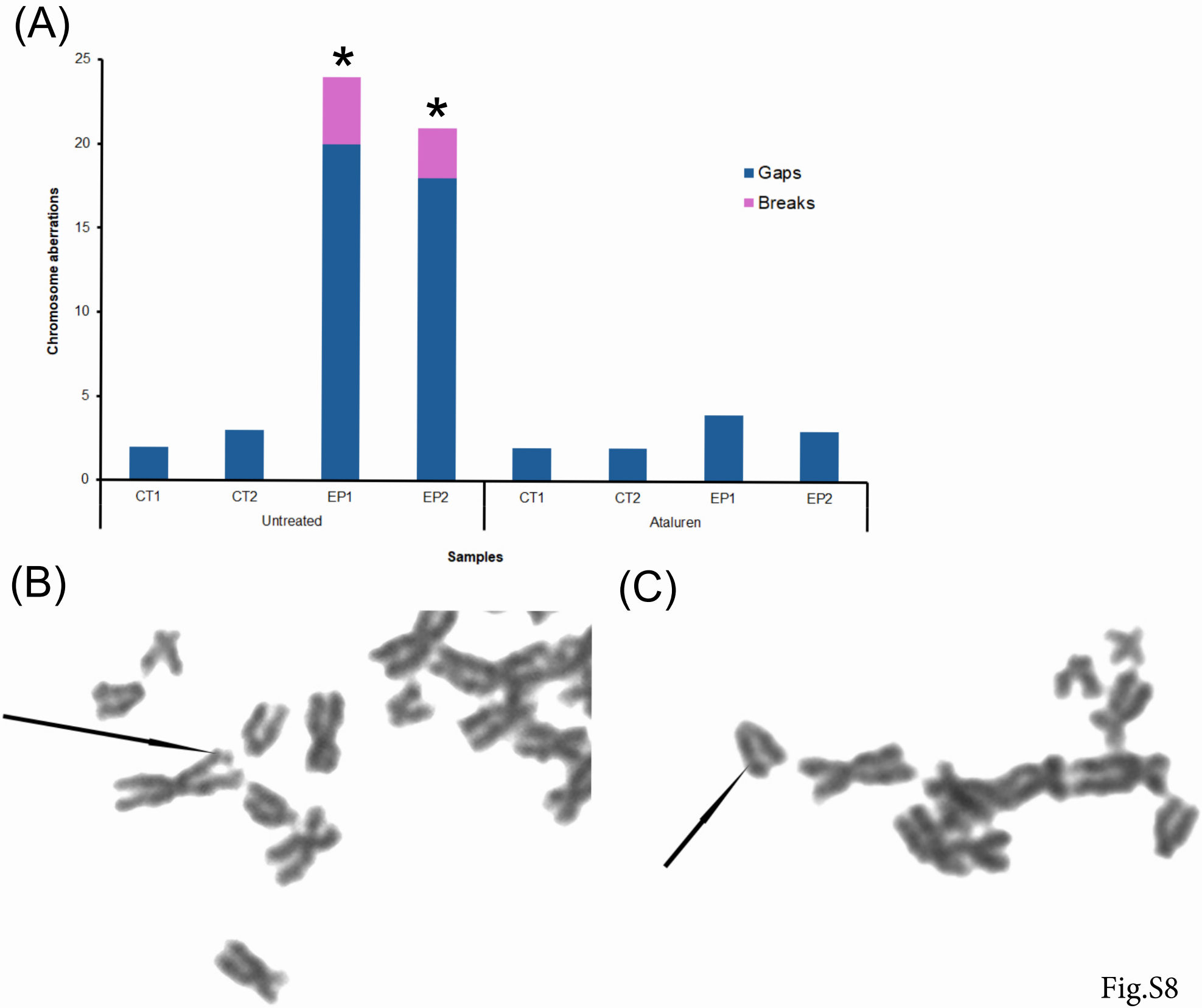
(A)
25
20
15
10
5
0
Chromosome aberrations
*
*
Gaps
Breaks
CT1
CT2
EP1
EP2
CT1
CT2
EP1
EP2
Untreated
Ataluren
Samples
(B)
(C)

Fig.S8

SUPPLEMENTARY FIGURE LEGENDS

Supplementary Figure 1. Localization of amino acid changes identified in DEE85 patients carrying variants in the *SMC1A* gene. The protein length is not in scale.

Supplementary Figure 2. (A) Protein blotting revealed that SMC1A levels in EP cells with frameshift variants (EP3, EP5, EP6, EP9, EP10, and EP14) were comparable to controls. (B) Cells carrying missense variants (EP8, EP12, EP13) showed the same pattern, while EP1 and EP2, harbouring nonsense variants, displayed decreased SMC1A protein levels.

Supplementary Figure 3. (A) Differential gene expression analysis (DGEA) comparing EP cell lines to controls identified 449 DEGs (284 were upregulated and 165 downregulated). (B) EP cell lines with frameshift variants showed 411 DEGs (251 upregulated and 160 downregulated). (C) Missense variants affected 296 genes (133 upregulated and 163 downregulated). (D) Nonsense variants caused the most extensive changes, with 1,429 misregulated genes (656 upregulated and 773 downregulated).

Supplementary Figure 4. RNA-seq data validation through quantitative-PCR.

Supplementary Figure 5. ImageJ software was employed for semiquantitative analysis of immunoblotting data. (A) Ataluren restored SMC1A protein expression in EP1 LCLs carrying the c.901C>T, p.Arg1035 nonsense variant. (B) A similar analysis in EP2 LCLs, harbouring the c.901C>T, p.Gln323* nonsense variant, confirmed ataluren-induced restoration of SMC1A protein levels, with the exception of treatment at 0.5 μg/ml.

Supplementary Figure 6. (A) Newly synthesized SMC1A coimmunoprecipitated with SMC3 in EP1 and (B) EP2 cell lines carrying nonsense variants. No signal was detected in the IPs using IgG-coated beads.

Supplementary Figure 7. Transcriptomic response to ataluren in EP2 cells carrying a nonsense variant in *SMC1A*. (A) Transcriptomic profiling of EP2 lymphoblastoid cells treated with increasing concentrations of ataluren (1.5, and 3 μg/ml for 24 hours) revealed a dose-dependent effect, with 1,152 and 1,938 DEGs, respectively. (B) Upon pooling the treatment data, we identified 1,347

DEGs (703 downregulated, 644 upregulated). (C) GO enrichment analysis of these DEGs highlighted significant involvement in biological processes such again enriched in pathways related to cell proliferation, signal transduction, cell adhesion. (D) Consistently, 161 genes were altered across doses, with 44.7% reverting toward control expression levels.

Supplementary Figure 8. (A) Karyotypic analysis of 100 Giemsa-stained metaphase spreads showed that EP1 and EP2 cells displayed markedly elevated chromosomal aberration frequencies (24 and 21 per 100 metaphases, respectively) compared with controls (2–3/100). Following ataluren treatment, aberration levels decreased to values comparable to controls. Representative partial metaphases illustrating chromosomal abnormalities are shown in (B) a break and (C) a gap in EP1 cells. Aberrations are indicated by arrows.

Supplementary Table 1. EP, CdLS and control cell lines used for the transcriptome analysis.

Sample	SMC1A variant	Amino acid change	Type
EP1	c.3103C>T	p.Arg1035*	Nonsense
EP2	c.901C>T	p.Gln323*	Nonsense
EP3	c.1063delC	p.Arg377Glyfs*2	Frameshift
EP5	19.5 Kb deletion		Frameshift
EP6	c.1609delG	p.Glu1013*	Frameshift
EP8	c.286C>T	p.Arg96Cys	Missense
EP9	c.3046_3048delGTGindG	p.Val1016Alafs	Frameshift
EP10	c.2842_2845dup	p.Asp949Glyfs*2	Frameshift
EP12	c.2948A>G	Tyr983Cys	Missense
EP13	c.95C>A	Gly32Glu	Missense
EP14	c.1078_1079delAG	Gln361Glyfs*42	Frameshift
CdL363	c.2077C>G	Arg693Gly	Missense
CdL565	c.2046_2048delAGA	Glu683del	Deletion
CdL060	c.1487G>A	Arg496His	Missense
LCL1			Control
LCL3			Control
LCL4			Control

Supplementary Table 2. Primer used for RNA-seq data validation.

GENE	PRIMER FORWARD	PRIMER REVERSE
GATA4	CAGCAAGTGAGAAGCGAGAC	GATGGCACTGGCTGAACTT
ATP11C	TGGAAGAACTGCGTGTCCT	GCAGCAGCATCATCATCTTC
AGMAT	TCACCTTCGTGGTCATCGAC	GCAGCAGAAGGTGCAGAAAC
CYP1B1	CCTGGAGACCTTCGGCAAC	GGTGATGAAGGCGTTGTTGG
SERPINB10	GGACCTCAGCCTGACTACCA	CAGGATGAAGTCCAGGGCAT
ABHD6	TGCTGGTCATCTTCGGCTAC	GGATGACGATGACGAGGAAG
HPRT	AGCCAGACTTTGTTGGATTTG	TACTAAGCAGATGGCCACAGA

Supplementary Table 3. Differentially expressed genes (up- and downregulated) in EP cell lines compared to controls.

Down-regulated

Gene	log2FoldChange
PNMAL1	-8,20827E+14
GSTM1	-7,66371E+14
RPRM	-5,93135E+14
FRAS1	-5,68833E+14
SEMA3A	-5,41414E+14
ASB9	-5,25452E+14
PITX2	-5,185E+14
TRIM31	-5,10712E+14
MIR646HG	-4,96669E+14
LOC101926935	-4,94256E+14
UGT2A3	-4,8869E+14
LINC01087	-4,82924E+14
WSCD1	-4,77784E+14
BMP3	-4,77487E+14
RBPMS	-4,76671E+14
RNF217	-4,72396E+14
PLS3	-4,71219E+14
FOXG1	-4,68042E+14
ITGA2	-4,36085E+14
FAM71D	-4,35572E+14
CLDN11	-4,2429E+14
LINC01426	-4,19238E+14
OR4C6	-4,18478E+14
TCF7L1	-4,12116E+14
CCDC149	-4,02013E+14
NOL4	-3,98752E+14
HOGA1	-3,95391E+14
MMP23A	-3,83062E+14
FAM86B1	-3,72323E+14
DNAH14	-3,68768E+14
KCNJ2	-3,68443E+14
ANXA3	-3,6745E+14
FLJ46906	-3,5871E+14
RP1L1	-3,56662E+14
HIC1	-3,53786E+14
SOWAHC	-3,52624E+14
LINC01320	-3,49907E+14
USP32P1	-3,49847E+14
SEMA5A	-3,47181E+14
ST7-OT4	-3,44031E+14
C14orf132	-3,4084E+14
NR2F2	-3,37902E+14

IL1B	-3,3724E+14
PRKCH	-3,20962E+14
PTPRG	-3,18772E+14
LOC102724301	-3,16755E+14
SPEF2	-3,09783E+14
GPM6A	-3,07364E+14
CASC10	-3,07233E+14
TNIP3	-3,058E+14
CREB3L3	-3,04867E+14
PCDHGB4	-3,03269E+14
LOC100130298	-3,0144E+14
TEKT4P2	-2,99621E+14
AMOTL1	-2,97156E+14
LINC01252	-2,91069E+14
BANK1	-2,88131E+14
CYP1A1	-2,78283E+14
MYRF	-2,71008E+14
ROBO3	-2,65134E+14
NAP1L2	-2,61833E+14
TOX	-2,58625E+14
RGS6	-2,55021E+14
ADGRA3	-2,54345E+14
PMCH	-2,53014E+14
MAN1C1	-2,49914E+14
LGR4	-2,45858E+14
OGDHL	-2,44852E+14
FAM198B	-2,44225E+14
GABRB2	-2,41138E+14
PLXNA2	-2,37974E+14
DPP4	-2,35894E+14
FCRL4	-2,34298E+14
ITGA5	-2,33453E+14
FCGRT	-2,29157E+14
COL16A1	-2,2841E+14
ANKRD18A	-2,27494E+14
ROBO1	-2,2461E+14
F5	-2,21425E+14
ACKR3	-2,20762E+14
HLA-DRB6	-2,19721E+14
NPIPA5	-2,17215E+14
CCL17	-2,17102E+14
PARD3	-2,11667E+14
MYH10	-2,11612E+14
SIGLEC14	-2,09967E+14
LOC729737	-2,05041E+14
HS3ST1	-2,00454E+14
STAM-AS1	-1,98999E+14

RAB37	-1,98566E+14
ARHGEF17	-1,94247E+14
CSRNP3	-1,91191E+14
ARRB1	-1,9084E+14
UST	-1,90104E+14
EDARADD	-1,83084E+14
HLA-G	-1,79918E+14
DISP2	-1,77461E+14
TNFRSF19	-1,76789E+14
CR1	-1,76746E+14
RILPL1	-1,73847E+14
CFP	-1,71432E+14
UBQLNL	-1,69688E+14
PCGF2	-1,64906E+14
TNFSF12	-1,62912E+14
NCALD	-1,61265E+14
GIMAP6	-1,60845E+14
LOC554206	-1,58673E+14
ARHGAP24	-1,57518E+14
CASKIN2	-1,56479E+14
DLG4	-1,54236E+14
TMEM229B	-1,53871E+14
ZBTB47	-1,52845E+14
C1orf106	-1,50916E+14
AMZ1	-1,5039E+14
NHSL1	-1,47954E+14
ANKRD34A	-1,45973E+14
PTK2	-1,41729E+14
MS4A14	-1,40071E+14
MGAT4A	-1,38696E+14
MPEG1	-1,35357E+14
ID2	-1,35285E+14
ZNF362	-1,31528E+14
NUDT13	-1,31345E+14
SMIM3	-1,30358E+14
GPR68	-1,29935E+14
CCDC122	-1,27383E+14
EMID1	-1,26106E+14
KCND2	-1,2598E+14
LRP6	-1,23211E+14
TRO	-1,22209E+14
MBOAT2	-1,21753E+14
ACY1	-1,21709E+14
CLIC6	-1,17583E+14
CDK5R1	-1,17067E+14
MNS1	-1,1651E+14
TMEM132A	-1,15355E+14

KIF26B	-1,11587E+14
RIMKLB	-1,07126E+14
NFATC2	-1,05016E+14
SLC45A3	-1,04539E+14
IL2RB	-1,02074E+14
EOMES	-5,27506E+13
KCNJ12	-5,08884E+13
FCRL3	-2,76882E+13
SYNGR1	-2,59966E+13
SORBS2	-2,16873E+13
BHLHE22	-1,76857E+13
TUBA8	-1,59371E+13
WWTR1	-1,55832E+13
LIN7A	-1,51832E+13
LRRIQ3	-1,47034E+13
SEPN1	-1,43195E+13
H1F0	-1,38507E+13
NEURL2	-1,16383E+13
METRN	-1,14342E+13
PHC1	-1,07823E+13
NRARP	-1,02328E+13
DNASE1L3	-1,48911E+12
C1QTNF9B-AS1	-0,985454224
THBS3	-0,977874366
SNHG25	-0,960205606
ZGLP1	-0,939135092
TTC39C	-0,926096682
IL16	-0,921235249
FAM86B3P	-0,919168895
PIK3R6	-0,909975263
TMEM136	-0,905680193
LMO7	-0,901516508
LRP5	-0,894688134
MCPH1-AS1	-0,891687392
RNF144A	-0,88431173
P2RY11	-0,85299404
NT5E	-0,846372078
CBLB	-0,833118839
ETS2	-0,828824273
KTN1-AS1	-0,789375954
CDPF1	-0,785252515
PHLDB3	-0,778528068
RRN3P1	-0,778491349
GSAP	-0,775964618
CTSC	-0,769565071
HMGN5	-0,76221232
FAM86DP	-0,742537069

LZTS2	-0,741160553
AHR	-0,731280741
DHRS4L2	-0,72720644
GRAMD3	-0,725952668
SPINT1	-0,719161926
CYTH3	-0,718206286
DNAJB5	-0,713712846
EID2B	-0,697360344
ENG	-0,672921847
PAAF1	-0,659604108
ENO3	-0,658241902
TSEN54	-0,65186642
TESPA1	-0,646300072
TMEM198B	-0,645561989
CBLN3	-0,635158782
SNX29	-0,629907255
RBM26-AS1	-0,615843983
TSPYL2	-0,610224537
TCEAL4	-0,608368853
TCEAL1	-0,605725123
IKZF2	-0,600613951
ZNF579	-0,594709596
CCDC28B	-0,594633516
PSMD5-AS1	-0,590040786
CHST14	-0,58996655
FBF1	-0,588083112
TFPT	-0,544113221
RAI1	-0,534427906
PCED1A	-0,52647624
SGSM2	-0,524915201
SIK2	-0,520957833
INAFM2	-0,510703922
AGAP3	-0,495296481
HEATR6	-0,495207119
DHFRL1	-0,492836059
PABPN1	-0,489830648
IFT81	-0,479398202
TPCN1	-0,47478551
MAPK12	-0,466215099
ZNF512B	-0,466064391
FAM78A	-0,452300942
SVIP	-0,447001319
ACP6	-0,445471604
SMG6	-0,43959945
ZNF496	-0,43651371
CHKA	-0,434868706
DAPP1	-0,434618158

CDC42EP3	-0,432809206
BRD3	-0,4302674
CEPT1	-0,427983259
LRRC20	-0,427673435
ZNF74	-0,427340412
FBXL19	-0,426918644
SSBP4	-0,42017247
COPRS	-0,418211158
ALKBH4	-0,417943487
MSANTD2	-0,410055636
TMEM110	-0,405645454
ZSWIM4	-0,404179178
CCDC125	-0,389049574
ZMYM3	-0,38605345
HDGFRP2	-0,384484635
MBOAT7	-0,383439707
ZNF234	-0,376489949
MAPK7	-0,376013396
RPIA	-0,374716402
SCFD2	-0,357612432
TBC1D22B	-0,355402311
DCAKD	-0,355095059
CALM3	-0,355023603
EML3	-0,344819967
SUSD6	-0,339704113
BIVM	-0,333750078
ERCC2	-0,331373126
CSK	-0,324539999
TAF15	-0,319962724
GATAD2A	-0,298804748
STX4	-0,295477994
TRIP6	-0,287009852
HNRNPA2B1	-0,285270834
CCDC71	-0,283311392
RPS6KA4	-0,280735375
ANP32A	-0,279886617
C11orf73	-0,278587248
CARM1	-0,27638242
UCK2	-0,270240571
CDC34	-0,262468567
PBX2	-0,259764428
UCKL1	-0,258735147
INTS9	-0,254838514
HNRNPH3	-0,252344322
CTNNBL1	-0,250302252
AKT1	-0,235450318
TRIM11	-0,22910094

PDCD7	-0,206054491
NACC1	-0,205113516
CACTIN	-0,198329218
FAM192A	-0,182825964
NAA60	-0,179087885
FIP1L1	-0,174927809
ATXN2L	-0,167708907

Up-regulated

Gene	log2FoldChange
CAPZA1	0,167452553
RAB5A	0,192710041
SEC22A	0,227184502
BRF2	0,238598264
ITFG2	0,248152999
ERO1A	0,257068851
TM9SF3	0,258506768
RABGEF1	0,258980243
SELT	0,268865392
SCFD1	0,270459721
CHMP2B	0,280320332
TMED4	0,288449622
RANBP9	0,290505753
GATC	0,294139612
ZNF562	0,309298348
ATG4A	0,311540617
CASC4	0,316829517
SDE2	0,326418219
ATF2	0,328938753
MAGT1	0,329052132
PPT1	0,329157896
TTC37	0,329999584
PNPLA8	0,335605042
TM2D3	0,3414044
RETSAT	0,341611108
EMC3	0,342661237
GZF1	0,344743941
ZNF136	0,358248327
CINP	0,360494998
ADPGK	0,361570073
GSKIP	0,361748462
USP48	0,364003615
NGLY1	0,364877872
ITFG1	0,367310608
SLC35A5	0,375642186
TVP23B	0,380929974

CD46	0,383746215
RAP1B	0,387287851
DTWD1	0,388045326
GBA	0,392247219
TAPT1	0,405607504
CDKN1B	0,426240648
ENTPD4	0,443655426
SEC24D	0,445483947
BTN3A1	0,448997726
SARAF	0,464832742
GNE	0,466781706
CHPF2	0,467195274
LAMP2	0,46961364
MAP4K3	0,47055624
ZNF709	0,473793226
RHBDD1	0,476462149
P2RY10	0,478648502
JOSD2	0,489875628
ZNF527	0,49313342
MYO5A	0,497522595
LMAN1	0,499844727
LONRF1	0,507851885
POLE4	0,511491277
ASPHD2	0,521598702
ZXDB	0,522668142
CLIP4	0,53427951
KCTD7	0,54401132
C16orf54	0,551610009
GNS	0,556083411
RELL1	0,56134346
PPP3CC	0,563315472
C10orf32	0,565162272
C15orf57	0,565246639
JAK2	0,580831218
OSTM1	0,584493014
HERPUD1	0,586969845
ZNF383	0,593804135
ZNF506	0,594064275
ELL2	0,601188411
HSPA13	0,626719929
HELB	0,626944932
UBE2J1	0,639279746
ICAM2	0,645374304
CCPG1	0,652301013
SLC41A2	0,6575883
PAM	0,667039117
RNF24	0,670392742

SRGN	0,676592286
ANXA2	0,680979839
WNT10A	0,687132146
ZNF784	0,702580297
TXNDC11	0,733226502
FRRS1	0,734485108
ACP2	0,736044439
PDK1	0,742863075
PDE4DIP	0,744638134
RNF122	0,746093621
DNLZ	0,785079585
MANEA	0,79211581
HECA	0,811469881
APOL6	0,831228556
MIR22HG	0,836387592
PQLC3	0,844442345
C15orf65	0,873848592
TSTD1	0,890080574
CPEB3	0,915550811
ACRC	0,935705487
XBP1	0,945013407
MAN1A1	0,946047149
TTC22	0,956468831
RNF103	0,966736689
PIM2	0,980442728
TUBB2B	1,30946E+13
CHST6	1,52716E+13
ACOXL	1,63318E+13
FHDC1	1,76623E+13
NUGGC	1,82082E+13
TYMP	1,01783E+14
PPP1R32	1,05366E+14
FNDC3B	1,074E+14
SLC26A11	1,07688E+14
TICAM2	1,08901E+14
SNX16	1,12274E+14
ANGPTL2	1,18012E+14
ANP32A-IT1	1,21275E+14
C12orf74	1,2164E+14
GNB4	1,26617E+14
BCAS1	1,34577E+14
AGAP2-AS1	1,38337E+14
LOC101927686	1,46109E+14
TTC39A	1,46274E+14
LOC100507195	1,51257E+14
FAAH	1,55226E+14
SSC4D	1,55317E+14

LOXL2	1,56941E+14
EDN1	1,60079E+14
MIAT	1,63557E+14
PFN2	1,6419E+14
LMTK3	1,71736E+14
NEUROG2	1,73238E+14
M1AP	1,74231E+14
EPS8L1	1,74988E+14
FAM66B	1,81452E+14
PVRL4	1,81613E+14
DENND2C	1,84492E+14
POU4F1	1,94835E+14
F2R	2,01601E+14
PTPRO	2,11842E+14
LOC103908605	2,12072E+14
ADAM21	2,2514E+14
TRPV3	2,2784E+14
MUC20	2,34698E+14
NRN1	2,36213E+14
LOC102546229	2,46023E+14
EMP2	2,54E+14
XXYLT1-AS1	2,74534E+14
JSRP1	2,75519E+14
WNK4	2,78956E+14
MYO18B	2,799E+14
LRRN2	2,94599E+14
A2M	3,04141E+14
TMPRSS3	3,12831E+14
PRKD1	3,22302E+14
LOC646762	3,46586E+14
USP44	3,68748E+14
RGPD1	3,85216E+14
LDLRAD2	4,48837E+14
OVCH1-AS1	5,14766E+14
PROSER2-AS1	6,66255E+14

Supplementary Table 4. Differentially expressed genes (up- and downregulated) in EP cell lines carrying frameshift variants compared to controls.

Down-regulated

Gene	log2FoldChange
PNMAL1	-8,13026E+14
TDRD12	-5,93242E+14
TMEM176A	-5,6568E+14
LINC01087	-5,56304E+14
CD7	-5,50249E+14
MIR646HG	-5,42462E+14
LOC101926935	-5,41395E+14
RBPMS	-5,40574E+14
MKRN3	-5,10486E+14
AOC1	-5,08035E+14
PLXDC2	-4,98768E+14
BMP3	-4,92426E+14
CTNNA2	-4,90331E+14
WSCD1	-4,76387E+14
FAM71D	-4,65683E+14
KCNJ15	-4,47387E+14
OR4C6	-4,43893E+14
LINC01426	-4,30409E+14
GLIPR1L2	-4,29524E+14
DNAH14	-4,28324E+14
HCK	-4,19139E+14
IL1B	-3,98484E+14
C14orf132	-3,75539E+14
HIC1	-3,68464E+14
SNCG	-3,66472E+14
NR2F2	-3,6382E+14
C2orf91	-3,6174E+14
SOWAHC	-3,55905E+14
HMX3	-3,55657E+14
NOXA1	-3,49006E+14
SPEF2	-3,44947E+14
CREB3L3	-3,3534E+14
ANXA3	-3,3493E+14
GPM6A	-3,29485E+14
CYP1A1	-3,11335E+14
NSG1	-3,11244E+14
ADGRE4P	-3,10358E+14
AFAP1L1	-3,00454E+14
SOBP	-2,9508E+14
FCRL3	-2,90836E+14

FILIP1	-2,89086E+14
EMILIN1	-2,80664E+14
ROBO1	-2,73288E+14
FCRL4	-2,73143E+14
CCL17	-2,70573E+14
FBN2	-2,68981E+14
DPP4	-2,66676E+14
GPR82	-2,65285E+14
COL16A1	-2,59969E+14
NAP1L2	-2,59784E+14
TEKT4P2	-2,56724E+14
HLA-DRB6	-2,55334E+14
PMCH	-2,53144E+14
SYCP2	-2,52283E+14
PGLYRP4	-2,47335E+14
TOX	-2,44696E+14
TULP2	-2,43507E+14
MMP9	-2,3569E+14
PLXNA2	-2,33748E+14
SORBS2	-2,27456E+14
HS3ST1	-2,24173E+14
GATA4	-2,21829E+14
FAM129B	-2,19585E+14
GRPR	-2,18785E+14
MAN1C1	-2,12416E+14
MAL	-2,09058E+14
UST	-2,07766E+14
CLEC4A	-2,05511E+14
TUBA8	-2,05199E+14
HLA-G	-2,01688E+14
KRT7	-2,00855E+14
OTP	-2,00472E+14
MYO7B	-1,96382E+14
RAB37	-1,94885E+14
NCALD	-1,91416E+14
NFATC4	-1,90353E+14
DNASE1L3	-1,87245E+14
CASKIN2	-1,81813E+14
LOC100507600	-1,80249E+14
GUCY1A3	-1,73926E+14
ACKR3	-1,72902E+14
GEM	-1,7243E+14
RAB38	-1,7074E+14
CMTM3	-1,70214E+14
AMZ1	-1,65149E+14
HOOK1	-1,64103E+14
LINC01094	-1,63915E+14

PDE6G	-1,63791E+14
DLG4	-1,59891E+14
LRRIQ3	-1,59528E+14
GRIN2D	-1,57473E+14
GIMAP6	-1,56424E+14
FRMD4A	-1,5498E+14
CETP	-1,53291E+14
IL9R	-1,49417E+14
EDARADD	-1,48434E+14
CCDC122	-1,45743E+14
ZNF362	-1,43905E+14
SMIM3	-1,43654E+14
ADAMTS12	-1,42819E+14
CCDC74B	-1,41299E+14
CDK5R1	-1,40381E+14
CYP1B1	-1,36007E+14
ANO5	-1,34877E+14
TNFSF4	-1,3046E+14
MGAT4A	-1,30085E+14
PTK2	-1,29267E+14
EMID1	-1,28902E+14
KIF26B	-1,28724E+14
MBOAT2	-1,26436E+14
GPR68	-1,2405E+14
NRARP	-1,24026E+14
LOC728175	-1,23893E+14
RIMKLB	-1,22963E+14
CLIC6	-1,22451E+14
MNS1	-1,20919E+14
H1F0	-1,20717E+14
ZGLP1	-1,12186E+14
CNR1	-1,11508E+14
ID2	-1,09568E+14
BHLHE40	-1,074E+14
METRN	-1,04469E+14
PHC1	-1,04364E+14
ILDR2	-1,04008E+14
IL16	-1,00841E+14
LTA	-1,00806E+14
A4GALT	-1,00798E+14
ANKRD20A12P	-4,30303E+13
ST7-OT4	-3,73117E+13
IL17RE	-3,43917E+13
PRKCH	-3,26926E+13
GIPC3	-3,14606E+13
CDH17	-2,92089E+13
FCGRT	-2,88471E+13

RPSAP58	-2,22295E+13
DAPK2	-2,02859E+13
LOC554206	-1,82683E+13
FES	-1,80261E+13
MYH10	-1,70983E+13
SMO	-1,62077E+13
SERPINB10	-1,39906E+13
TMEM132A	-1,1933E+13
KCND2	-1,05619E+13
LOC100130298	-3,26355E+12
PIK3R6	-0,97731706
TK2	-0,974380693
DBN1	-0,970460133
PLA2G4C	-0,95804104
GSAP	-0,935247362
NFATC2	-0,921688759
STAG3	-0,91918832
CRACR2B	-0,912071053
LACC1	-0,89794391
ETS2	-0,870620006
CDPF1	-0,866129954
RRN3P1	-0,863049472
SGK223	-0,846261608
TNF	-0,840522422
DNAJB5	-0,833465923
NR2F6	-0,829751157
LMO7	-0,825888171
HES1	-0,822182204
PAAF1	-0,817397845
IFNGR1	-0,814399316
EXD3	-0,811107101
GRAMD3	-0,796856545
TIMP1	-0,795848346
IL2RB	-0,788950828
REC8	-0,7850489
EID2B	-0,776958909
TCEAL3	-0,771233509
RASSF2	-0,767291178
ALDH2	-0,762934624
LY6G5B	-0,756317762
CBLB	-0,747752913
CHD3	-0,743536851
RGS10	-0,741653226
CYTH3	-0,735824403
ABHD6	-0,727781631
ARMC9	-0,727243722
DHRS4L2	-0,719747619

IRF2BP2	-0,718136936
AGMAT	-0,713869923
CCDC28B	-0,701482768
TFPT	-0,700782662
CHRNA5	-0,694944781
FBF1	-0,692907695
LOC100288798	-0,691632372
ZNF579	-0,690777975
PLCXD1	-0,679839379
PAQR8	-0,677656828
TCEAL4	-0,666071621
SAMD10	-0,661109007
HMGN5	-0,660315207
TSEN54	-0,650974712
ENO3	-0,627472043
TNFSF14	-0,627095776
RGS14	-0,612808893
IL27RA	-0,610075512
PAPLN	-0,610045927
DYNC2LI1	-0,605865069
ZYX	-0,605734265
DFNA5	-0,591353973
CHST14	-0,562117689
SGSM2	-0,560536559
SNX29	-0,559131507
DHFRL1	-0,558731672
C7orf60	-0,548820342
ORAI3	-0,542068536
TSPYL2	-0,538576114
ITPK1	-0,523947744
PCED1A	-0,509294676
NSMF	-0,50892269
ENKD1	-0,50647274
SVIP	-0,501844564
PABPN1	-0,496986174
MSANTD2	-0,489084179
PCBP4	-0,484517461
SEPT9	-0,475717041
MAPK12	-0,468604824
SSBP4	-0,468154824
C6orf47	-0,467971865
PIP5K1C	-0,43898694
FAM78A	-0,432060812
SYS1	-0,424351687
AGAP3	-0,423414368
PLGRKT	-0,420939534
ZNF234	-0,41369165

DAPP1	-0,407971125
ACADS	-0,404501869
LRRC45	-0,395588688
PFN1	-0,388938227
TRAPPC5	-0,385175031
CALM3	-0,383137793
CEPT1	-0,372491989
MOAP1	-0,366765878
RAI1	-0,365456397
ZNF747	-0,364041204
ERCC2	-0,340860367
TMC6	-0,335980908
SMARCE1	-0,325172882
FBXL19	-0,317709543
STX4	-0,308278856
TAF15	-0,306720678
RPS6KA4	-0,279091063
CARM1	-0,277411759
PBX2	-0,275975009
TFEB	-0,272262597
PPP1R18	-0,271449611
TRAF2	-0,227926474
MED15	-0,222251468

Up-regulated

Gene	log2FoldChange
SP3	0,190769035
CAPZA1	0,1979337
PTPN1	0,23613938
EZR	0,243686068
FGFR1OP2	0,256394129
ZNF639	0,258830824
SYVN1	0,266055783
BRPF3	0,28399453
RPRD1A	0,301180111
ZNF562	0,302910669
ERO1A	0,307180226
PNPLA8	0,307821568
ATP11C	0,30891426
PPT1	0,319410306
GNA13	0,323979658
MSH3	0,329159011
CASP3	0,345202148
NGLY1	0,350582607
CLSTN1	0,354648433
SDE2	0,362495128

CASC4	0,363484763
TTC37	0,380965531
CALU	0,382180173
ZNF136	0,384122644
CLDND1	0,394033835
GLCCI1	0,398693683
SEC24D	0,399739208
ELF1	0,399812548
ARID2	0,409698521
JOSD2	0,411871871
LMTK2	0,422750971
FAM91A1	0,422876253
USP48	0,426079334
LIMD1	0,436116183
LAMP2	0,458095169
HERPUD1	0,458497151
TMEM59	0,462526785
RAP1B	0,470067907
GNG7	0,47089141
NLK	0,476124539
LMAN1	0,4768773
RNF19A	0,480257351
CHPF2	0,486672707
GNE	0,491271448
HSP90B1	0,494578022
MTRF1L	0,49932408
ASPHD2	0,506343781
KLHL21	0,514643918
TRAM1	0,525107339
CLIC4	0,525504501
TXNRD1	0,525813225
C15orf57	0,525958174
AFF4	0,528554309
SEMA4B	0,529211218
NDFIP1	0,535915056
SEC24A	0,535987439
POLE4	0,539415301
CCPG1	0,541198345
IFNLR1	0,54648845
GNS	0,553022331
ICAM2	0,56057534
IGF2R	0,563152733
IL10RA	0,565274258
TPD52	0,5653677
ELL2	0,568091756
ENTPD4	0,570821382
GCLM	0,580705187

CD99L2	0,582696818
MBNL2	0,584380999
PPP3CC	0,589952867
PTPN22	0,594586432
FAM214A	0,59592332
UBE2J1	0,600524069
CLIP4	0,600829063
C16orf54	0,603812847
MDM2	0,605670475
HSPA13	0,616950905
MAP4K3	0,633180229
SLC41A2	0,643180423
FAM69A	0,648439813
HELB	0,650055069
TSTD1	0,67283654
CCDC134	0,674492078
TXNDC11	0,676298574
KIF1B	0,688050191
FRRS1	0,700971823
HECA	0,707740737
EDEM3	0,724216038
RPS18P9	0,737417108
ACP2	0,745815929
CCDC88A	0,754318167
ZNF784	0,772285329
ERC1	0,773127477
BACH1	0,774148579
PRDM1	0,781737861
PAM	0,786873518
PDK1	0,789907592
DERL3	0,801829739
MANEA	0,803452733
BCAS1	0,805571235
RRAGD	0,838170322
MAN2A1	0,846587198
MXI1	0,856660721
XBP1	0,879555788
MAN1A1	0,884890023
RNF103	0,891837844
NR1D2	0,895212807
TYMP	0,899483678
ATXN7L1	0,912810828
SLC26A11	0,916000465
ERN1	0,98818956
CPEB3	0,994378547
SOCS2	1,0279E+13
TTC39A	2,13298E+13

A2M	3,42779E+13
FNDC3B	1,02244E+14
SRXN1	1,02954E+14
KCNA3	1,04621E+14
KCNK6	1,05016E+14
STAC3	1,0983E+14
TUBB2B	1,10287E+14
FOSL2	1,12307E+14
SNX16	1,25076E+14
CFAP54	1,25514E+14
FAAH	1,29942E+14
CUEDC1	1,30957E+14
GNB4	1,35185E+14
TMEM169	1,40502E+14
C12orf74	1,40726E+14
KIAA1671	1,45204E+14
DSG2	1,46554E+14
CES4A	1,4667E+14
POU4F1	1,50725E+14
TRPV3	1,67222E+14
MIAT	1,67313E+14
EPS8L1	1,72755E+14
PFN2	1,80733E+14
ACOXL	1,81003E+14
IFNG-AS1	1,96845E+14
HMOX1	1,97876E+14
NEUROG2	1,98359E+14
RAB3B	2,01046E+14
EMP2	2,06236E+14
NRN1	2,06247E+14
GAS6	2,1093E+14
ZNF208	2,18514E+14
KIF5C	2,21651E+14
TMPRSS3	2,59201E+14
SHTN1	2,59765E+14
ADAM21	2,69173E+14
SIX1	2,96739E+14
SIX3	3,01118E+14
C8orf31	3,05596E+14
LRRN2	3,13726E+14
ZNF311	3,18272E+14
PRKD1	3,32053E+14
COL1A2	3,50796E+14
LOC646762	3,67762E+14
MSR1	5,3289E+14
PROSER2-AS1	6,39965E+14

Supplementary Table 5. Differentially expressed genes (up- and downregulated) in EP cell lines carrying missense variants compared to controls.

Down-regulated

Gene	log2FoldChange
LCN8	-6,15549E+14
TRIM31	-5,48946E+14
SNCA	-5,43678E+14
BCHE	-4,86024E+14
STMND1	-4,77016E+14
CRTAM	-4,51216E+14
HMX3	-4,46263E+14
OR4C6	-4,43755E+14
CTNNA2	-4,24047E+14
FKBP10	-4,23994E+14
RNF217	-3,94098E+14
HIC1	-3,80143E+14
NRP1	-3,56545E+14
OSBPL10	-3,47246E+14
MYO7B	-3,46769E+14
C14orf132	-3,37102E+14
ANKRD18A	-3,36782E+14
LOC100130298	-3,3651E+14
CREB5	-3,32466E+14
BMP4	-3,2767E+14
TPD52L1	-3,27095E+14
GPM6A	-3,20539E+14
PDE1C	-3,18292E+14
TUSC1	-3,11627E+14
ADGRA3	-3,07795E+14
FAM201A	-2,99978E+14
RND3	-2,99939E+14
MYRF	-2,89436E+14
PLXNA2	-2,89244E+14
MAN1C1	-2,86863E+14
VIL1	-2,80528E+14
PRKCH	-2,72996E+14
NPIPA5	-2,69786E+14
APBB1	-2,62601E+14
MAST4	-2,59738E+14
DISP2	-2,48637E+14
EIF5AL1	-2,44662E+14
LOC729737	-2,35069E+14
TRPC1	-2,33533E+14
ANKRD36BP2	-2,31329E+14

ADGRE2	-2,31183E+14
DPP4	-2,1843E+14
NGFRAP1	-2,16016E+14
SORBS2	-2,11036E+14
C1orf54	-2,04756E+14
NHSL1	-2,03113E+14
KCND2	-1,79905E+14
AMZ1	-1,78121E+14
PTK2	-1,78038E+14
ROBO1	-1,75476E+14
PYGL	-1,73809E+14
PCGF2	-1,72379E+14
CRYM	-1,69587E+14
TNFRSF19	-1,64044E+14
GRPR	-1,63431E+14
LYPD6B	-1,63069E+14
GPRC5C	-1,62255E+14
HNF4G	-1,62231E+14
SDC3	-1,61709E+14
MICAL3	-1,58098E+14
SEPN1	-1,55015E+14
CLIC6	-1,54104E+14
SERINC2	-1,5244E+14
BHLHE22	-1,50964E+14
ANKRD34A	-1,36636E+14
IL6R	-1,27178E+14
ERICH5	-1,21828E+14
TRERF1	-1,13436E+14
GUCY1A3	-1,11778E+14
NFATC2	-1,07335E+14
BHLHE41	-1,06532E+14
LOC613266	-1,05817E+14
RNF144A	-1,01557E+14
TIMP1	-1,0024E+14
MIR646HG	-4,76648E+13
ITGA5	-3,13912E+13
SMO	-1,49684E+13
PON2	-0,989368902
VANGL1	-0,927698308
DHRS4L2	-0,888381534
ST3GAL1	-0,886256256
ETS2	-0,860179321
ZMIZ1	-0,820657289
HMGN5	-0,802059482
PFKFB3	-0,791483293
ARHGEF5	-0,775704715
VCL	-0,773092785

NCKAP1	-0,758736001
ARHGAP18	-0,724148458
IKZF2	-0,718496959
LMO7	-0,717021806
FAM86DP	-0,714572401
CHD3	-0,691170166
AGAP3	-0,686363679
PSMD5-AS1	-0,673754068
FCGR2B	-0,645643745
SMC1A	-0,637159742
ERMP1	-0,62070133
BRD3	-0,603492425
CTH	-0,582570933
ZNF589	-0,542011207
UNC119B	-0,525044193
TNRC18	-0,516573269
UHRF1	-0,514328742
SVIP	-0,51429402
SCFD2	-0,510323389
KIF14	-0,508264381
TPCN1	-0,508003507
BUB1B	-0,493982635
IRF2BPL	-0,493889937
TEX2	-0,485588553
FAM78A	-0,483621595
SORL1	-0,482842165
CDC42EP3	-0,473079101
SKP2	-0,470595566
RAI1	-0,468816976
MCM6	-0,455934365
TRIP6	-0,446988078
SMC2	-0,443032895
PKP4	-0,427003003
TOP2A	-0,422098536
TCOF1	-0,418061745
DIAPH3	-0,414764091
UCK2	-0,411688834
HMGXB4	-0,411118669
THADA	-0,404561755
NCAPD3	-0,384078127
WDR62	-0,383888238
C15orf39	-0,360846884
SEPT11	-0,351914863
DCAF7	-0,319069805
SRRM1	-0,273372949
ILF3	-0,262801058

Up-regulated

Gene	log2FoldChange
TMED9	0,326063746
P4HB	0,363157414
B2M	0,413930347
IL2RG	0,442823991
PTRHD1	0,453696987
SKAP1	0,454528208
GLRX	0,456872921
PGD	0,457509852
PI4K2B	0,460693369
CINP	0,468973591
GSTZ1	0,47780936
EHMT1	0,48616495
ZNF107	0,50476354
PTPRC	0,520318866
FAM117A	0,524806153
PPP3CA	0,545432944
F11R	0,55767147
IQSEC1	0,558080954
POLE4	0,560400363
SEMA4A	0,564425205
EVI2B	0,610880226
C10orf32	0,633357439
CDKN1A	0,634024116
LY9	0,6433409
NAPRT	0,657625805
CYTIP	0,675794916
C4orf32	0,690537066
FRRS1	0,7005104
PITRM1	0,712581491
ACYP2	0,713724707
ZNF682	0,717946269
ISCU	0,719630924
ZNF506	0,721453343
WDR25	0,733063774
HHAT	0,73462183
C15orf57	0,743316333
NDNL2	0,757584994
ARSA	0,763401722
CD99L2	0,778965538
DERL3	0,796947154
SIDT1	0,804266044
SRGN	0,804513057
AP1S3	0,811854271
TARSL2	0,826935162

HECA	0,834301168
SERPINB9	0,836941016
MS4A7	0,850784552
PMAIP1	0,851585875
HMCES	0,864630413
TMSB10	0,882364649
MIR22HG	0,889422535
LY96	0,902300753
SPATA20	0,939447315
LGMN	0,974627836
UNC13B	0,996313088
RPS6KL1	1,62732E+12
SLC26A11	1,16168E+13
FAM83H	1,1619E+13
FADS3	1,24342E+13
ADAM19	1,38572E+13
PLEKHG1	1,38735E+13
SERPINB1	1,53982E+13
LOXL2	1,87985E+13
SMA4	1,92779E+13
ATAD3C	2,01563E+13
PTGER4	2,04475E+13
CHST6	2,07198E+13
PVRL4	2,62873E+13
CPEB1	3,02677E+13
LAMP5	3,78288E+13
INPP5J	3,85247E+13
OVCH1-AS1	4,32124E+13
ATF3	1,02836E+14
SDSL	1,06406E+14
BLVRA	1,06679E+14
TSTD1	1,07382E+14
GNB4	1,08172E+14
CPEB3	1,10102E+14
SOCS1	1,13021E+14
ABCA3	1,15779E+14
BMS1P20	1,1644E+14
TYMP	1,18224E+14
CDKN2A	1,18804E+14
SAT1	1,19362E+14
GAS7	1,21193E+14
GSN	1,21443E+14
GAL3ST4	1,24229E+14
PQLC3	1,24355E+14
PIM2	1,24367E+14
XXYLT1-AS2	1,26515E+14
P2RX5	1,30409E+14

INSIG1	1,31503E+14
PLK2	1,37409E+14
TTC22	1,39804E+14
MMP25-AS1	1,44041E+14
GTF2IRD2	1,48468E+14
PLEKHB1	1,53831E+14
HCAR3	1,54723E+14
CEP70	1,54827E+14
PTPRO	1,58182E+14
PLTP	1,5823E+14
CCL25	1,60507E+14
ADAP2	1,65787E+14
CELSR1	1,67687E+14
FAM90A1	1,70748E+14
ACOXL	1,71269E+14
TUBB2B	1,71967E+14
CEACAM1	1,73037E+14
ADCY9	1,79613E+14
CSPG4	1,80338E+14
FCER1G	1,85477E+14
MUC20	1,9076E+14
FAAH	1,92146E+14
GAB3	1,93697E+14
SH2D4A	1,98416E+14
ZP3	2,0445E+14
MOXD1	2,07397E+14
TYW1B	2,10478E+14
LMTK3	2,10822E+14
MT2A	2,10939E+14
HOMER2	2,1101E+14
SYNPO2	2,12295E+14
CLEC2B	2,13951E+14
TLDC2	2,15392E+14
HAPLN3	2,22016E+14
UNC13C	2,23797E+14
PER3	2,37483E+14
PTPRN2	2,41422E+14
ST5	2,43321E+14
LINC01150	2,45415E+14
XIRP1	2,48852E+14
CCND1	2,52838E+14
S100A10	2,54653E+14
ST14	2,56201E+14
CES4A	2,6115E+14
IFNG	2,62545E+14
RORA	2,63154E+14
AMBP	2,647E+14

POMC	2,66089E+14
EMP2	2,67399E+14
B4GALNT3	2,68904E+14
ASMT	2,80934E+14
POU4F1	2,81455E+14
MT1E	2,83162E+14
EID3	2,87693E+14
PRKCZ	2,9275E+14
FAM189A1	2,99654E+14
TRPV3	3,00969E+14
EPB41L4A	3,10602E+14
LINC00987	3,13081E+14
ST6GALNAC2	3,28424E+14
EEF1A2	3,63054E+14
IL12B	3,99896E+14
LINC00908	4,02194E+14
SOX18	4,06801E+14
MYO18B	4,85801E+14
LAMP5-AS1	4,89051E+14
LIX1	5,39895E+14
CLEC4C	5,42295E+14
AKR1C3	5,56017E+14
USP44	6,24218E+14
ACTN3	6,4765E+14
PROSER2-AS1	6,6128E+14

Supplementary Table 6. Differentially expressed genes (up- and downregulated) in EP cell lines carrying nonsense variants compared to controls.

Down-regulated

Gene	log2FoldChange
PLXDC2	-7,64409E+14
TSPAN18	-6,94157E+14
PCDH7	-6,93184E+14
PLS3	-6,44279E+14
NRG3	-6,43486E+14
TBX20	-6,34309E+14
RPRM	-6,29361E+14
UGT2A3	-6,22747E+14
INSM2	-6,20868E+14
WSCD1	-5,94135E+14
CADPS	-5,76505E+14
CLDN10	-5,43758E+14
KCNJ3	-5,42473E+14
FLRT3	-5,31061E+14
ITGA11	-5,27685E+14
KCNJ2	-5,26937E+14
ST8SIA1	-5,22884E+14
SDPR	-5,22847E+14
FAM86B1	-5,15565E+14
LINC01605	-5,10901E+14
TNIP3	-5,05826E+14
KCNJ12	-4,93469E+14
PRKCQ-AS1	-4,91508E+14
MYT1	-4,80464E+14
GAREM	-4,77918E+14
EDIL3	-4,68892E+14
DLX1	-4,63926E+14
MMP7	-4,62985E+14
SLC39A12	-4,61779E+14
FRMPD3	-4,55582E+14
NTN4	-4,45707E+14
IRX6	-4,37299E+14
LINC01320	-4,30616E+14
ROBO3	-4,12137E+14
CDC42BPA	-4,04076E+14
FAXDC2	-4,02225E+14
SBSN	-3,97632E+14
LURAP1	-3,94779E+14
CTNNA2	-3,92623E+14
FAM198B	-3,91051E+14

ACPP	-3,9002E+14
OTOGL	-3,89295E+14
MTL5	-3,89153E+14
GPC4	-3,85801E+14
SHANK2	-3,76602E+14
PCP4L1	-3,72768E+14
TOX	-3,68549E+14
CFTR	-3,66814E+14
RBPMS	-3,66638E+14
PRKCH	-3,59192E+14
SSC5D	-3,58172E+14
PALLD	-3,50285E+14
PMCH	-3,47724E+14
MYH10	-3,4716E+14
GPR87	-3,45042E+14
SCD5	-3,35312E+14
MMP9	-3,352E+14
PDE4C	-3,24505E+14
MYRIP	-3,22165E+14
NRXN3	-3,19697E+14
INTU	-3,157E+14
CR1	-3,13597E+14
EDARADD	-3,13397E+14
PCDHGA5	-3,1327E+14
PHOSPHO1	-3,12785E+14
RPSAP58	-3,07708E+14
NAP1L3	-3,06572E+14
C2orf78	-3,01822E+14
HOXC5	-2,99701E+14
CNKSR2	-2,97849E+14
CASP14	-2,96413E+14
ABCC9	-2,9576E+14
CR2	-2,85446E+14
SH3RF3	-2,85297E+14
COLEC12	-2,82881E+14
LOC101927815	-2,82424E+14
MYO1F	-2,79807E+14
LGR4	-2,79618E+14
SEMA5A	-2,75537E+14
PCDHGB6	-2,73968E+14
OTX1	-2,72894E+14
HOXB6	-2,72771E+14
FAM89A	-2,71954E+14
PTAFR	-2,61349E+14
HS3ST1	-2,58671E+14
ID2	-2,53349E+14
MAK	-2,4839E+14

TPM2	-2,41021E+14
IER5L	-2,38709E+14
CMTM7	-2,37734E+14
MS4A14	-2,35437E+14
POU3F1	-2,35381E+14
GIMAP7	-2,35073E+14
TPBG	-2,35014E+14
PDE1C	-2,33485E+14
ACTN1	-2,33227E+14
MYOF	-2,32926E+14
MARVELD1	-2,29832E+14
WWTR1	-2,29652E+14
CD244	-2,26241E+14
RAB37	-2,24917E+14
GIMAP1	-2,24207E+14
C15orf27	-2,21748E+14
SPINK2	-2,21713E+14
EPHB2	-2,19775E+14
DHRS3	-2,18652E+14
C17orf51	-2,16719E+14
LRRC16A	-2,15154E+14
PCDHGB2	-2,14676E+14
COL16A1	-2,13263E+14
RCOR2	-2,10961E+14
PARD6G	-2,10894E+14
IL2RA	-2,0989E+14
CROCC	-2,08758E+14
CXXC4	-2,07925E+14
GRHL3	-2,03897E+14
OR2T3	-2,03013E+14
SIX4	-2,02701E+14
PTGER2	-2,02597E+14
SNX21	-2,01999E+14
GPR153	-1,99667E+14
HOXB7	-1,99335E+14
GPR68	-1,97819E+14
ARHGEF17	-1,97582E+14
PEX5L	-1,97298E+14
FCRL4	-1,97125E+14
SCARF1	-1,96395E+14
ZNF608	-1,95891E+14
WDR17	-1,94972E+14
C1orf106	-1,94495E+14
TRO	-1,92878E+14
MCC	-1,92241E+14
HDAC11	-1,91184E+14
P2RY1	-1,90853E+14

LRP1	-1,87739E+14
CALCRL	-1,85295E+14
TPM1	-1,80896E+14
TLN2	-1,79526E+14
CDKL5	-1,79495E+14
ZBTB47	-1,77898E+14
TBC1D8B	-1,72797E+14
TGM2	-1,72654E+14
BMP1	-1,70568E+14
ZNF469	-1,66444E+14
MNX1	-1,64931E+14
PI4KAP1	-1,64229E+14
MAP3K4	-1,63864E+14
LOC102724094	-1,62726E+14
TP53BP2	-1,61312E+14
MEX3A	-1,61304E+14
METRN	-1,60957E+14
RABL2A	-1,60936E+14
BEND4	-1,5988E+14
GOLGA2P7	-1,59563E+14
PHC1	-1,58781E+14
CABYR	-1,58458E+14
EPHA2	-1,57883E+14
FGFR1	-1,56999E+14
TGFBR2	-1,56898E+14
CSPG4	-1,56231E+14
PCGF2	-1,55742E+14
IRAK2	-1,54285E+14
MERTK	-1,52935E+14
PIK3IP1	-1,52365E+14
PRDM11	-1,51215E+14
SIGLEC10	-1,49539E+14
EPB41L5	-1,49476E+14
ZNF205	-1,47659E+14
CCDC136	-1,47369E+14
SDC4	-1,47273E+14
LRRC49	-1,47179E+14
CREB5	-1,47059E+14
THBS3	-1,44856E+14
LAMP3	-1,44123E+14
MNS1	-1,43735E+14
CCDC92	-1,43034E+14
GRAMD1B	-1,42249E+14
KIAA0754	-1,41587E+14
KIF16B	-1,41191E+14
LMO2	-1,40974E+14
CFAP57	-1,40464E+14

VWCE	-1,39734E+14
RP9P	-1,3947E+14
TNFSF12	-1,38935E+14
STRIP2	-1,37686E+14
MRC2	-1,37336E+14
L3MBTL4	-1,36607E+14
CASKIN2	-1,35982E+14
NFATC2	-1,35493E+14
C15orf62	-1,35336E+14
C1orf198	-1,35297E+14
NRG4	-1,35047E+14
LINC00877	-1,33476E+14
ADM5	-1,32856E+14
CCL22	-1,32626E+14
SLC16A10	-1,3242E+14
KIF3C	-1,32346E+14
TTC12	-1,32158E+14
KIF26B	-1,32148E+14
CDC14A	-1,31899E+14
SCML1	-1,31183E+14
GIPC1	-1,30456E+14
WDR63	-1,2969E+14
C2orf74	-1,29052E+14
ILDR2	-1,28488E+14
BMI1	-1,28435E+14
PSTPIP2	-1,27324E+14
SOX9	-1,27071E+14
LOC642361	-1,26397E+14
TRIM6	-1,2582E+14
SLC25A53	-1,23475E+14
SAPCD2	-1,2343E+14
SLC25A29	-1,22089E+14
DTX4	-1,21859E+14
FAM109A	-1,20525E+14
LRRC56	-1,1969E+14
LINC00926	-1,19551E+14
ITGA3	-1,19183E+14
WWC3	-1,17867E+14
ACER2	-1,17813E+14
AGRN	-1,17564E+14
PPP1R13B	-1,17456E+14
GBE1	-1,17166E+14
PKP2	-1,16967E+14
TTYH3	-1,16953E+14
XRRA1	-1,16294E+14
ATP6AP1L	-1,1622E+14
TRIB2	-1,15771E+14

FBXO44	-1,1567E+14
MYL9	-1,15242E+14
CBX2	-1,14855E+14
AIM1	-1,14599E+14
PCTP	-1,13648E+14
PTK2	-1,13352E+14
IFIT2	-1,13128E+14
DHX58	-1,12787E+14
GAMT	-1,12072E+14
PPFIBP1	-1,1156E+14
SLC19A2	-1,11113E+14
MYLIP	-1,11002E+14
ETV4	-1,1076E+14
TSC22D3	-1,10489E+14
ETV5	-1,10459E+14
PVR	-1,10172E+14
TTC39C	-1,09539E+14
SNN	-1,09532E+14
ASRGL1	-1,08787E+14
YY2	-1,08532E+14
OCLN	-1,07124E+14
FAM65A	-1,06953E+14
PTMS	-1,05945E+14
NID1	-1,05911E+14
ITGB2-AS1	-1,05516E+14
LGALS14	-1,0467E+14
ROGDI	-1,04379E+14
FAM86C2P	-1,04261E+14
SYNGAP1	-1,04106E+14
ENO3	-1,0361E+14
ABTB2	-1,0212E+14
BCAT1	-1,01847E+14
PAG1	-1,01107E+14
FAM86DP	-1,0104E+14
CHD3	-1,00712E+14
KSR1	-1,00446E+14
PITX2	-6,75939E+13
PRKG2	-5,83049E+13
OLFML2A	-5,08366E+13
CACNA2D1	-4,25281E+13
PTK7	-4,18247E+13
GRB7	-3,69162E+13
ZNF467	-3,65499E+13
RBFOX2	-3,02363E+13
SLC35G2	-2,94821E+13
FSD1	-2,81519E+13
FILIP1	-2,68771E+13

DLG4	-2,28159E+13
FGFR4	-2,265E+13
CYP1A1	-2,21372E+13
RTN4RL2	-2,11146E+13
NFAM1	-1,83983E+13
PHLDA1	-1,81166E+13
MYBL1	-1,74107E+13
SNPH	-1,70321E+13
NPNT	-1,66213E+13
CCDC74A	-1,56851E+13
DLG5	-1,53632E+13
SPR	-1,50529E+13
FOXO3	-1,48775E+13
PARM1	-1,47584E+13
LOC729737	-1,43645E+13
TBKBP1	-1,29296E+13
SMIM3	-1,24775E+13
EMX1	-1,22388E+13
MFGE8	-1,17945E+13
BCL9L	-1,13904E+13
CPNE4	-4,92256E+12
MREG	-0,998271446
F8	-0,997504347
CCL5	-0,99364316
HMGN5	-0,986190892
REC8	-0,986041419
MAPKAPK3	-0,985384649
PAQR8	-0,980574114
LOC257396	-0,978412484
PCNXL2	-0,967552672
CNR2	-0,949136207
ITPR1	-0,94832192
MARCKSL1	-0,947521229
CLEC17A	-0,947505037
SOX12	-0,946638117
KIF21A	-0,942821758
LPIN1	-0,942437944
PNMA1	-0,940695025
MARVELD2	-0,935966895
TMEM198B	-0,929038761
PTP4A3	-0,916721091
DYNC2LI1	-0,909668926
OCEL1	-0,896835815
MAP3K12	-0,896278233
YBX3	-0,887094201
DUSP16	-0,884941652
SIPA1L1	-0,884619688

RALGAPA2	-0,884402297
DCAF4	-0,881369558
HOXB4	-0,880170956
PSMD5-AS1	-0,874522949
MFI2	-0,874411889
SEMA7A	-0,873465369
NEIL2	-0,869206502
KIF13A	-0,865246364
CD22	-0,854083973
WDR19	-0,850911976
HAAO	-0,843597236
RNF144A	-0,837906528
IL16	-0,830602351
QSOX1	-0,828599075
PHLDB3	-0,826302038
STK33	-0,82303391
TET3	-0,822926396
NOL4L	-0,8215099
IFT81	-0,810138158
ZNF446	-0,808157401
DYRK1B	-0,805568922
CD55	-0,804852469
LUZP1	-0,798447388
RDX	-0,796201499
DRAM1	-0,787740704
PACS2	-0,787162242
RALB	-0,784911039
CHST14	-0,782585327
CHDH	-0,781951684
ECHDC2	-0,781684253
UBXN7	-0,780159519
LINC01278	-0,777713339
ZFAS1	-0,76949832
LOC100506746	-0,768956423
SARM1	-0,765953867
FMNL3	-0,760778183
SIDT2	-0,757495762
TCEAL4	-0,752840947
ELOVL6	-0,744665391
SLC1A1	-0,744317361
CNNM4	-0,743549185
HACD2	-0,740273087
LTBP4	-0,737256739
PIDD1	-0,736483183
FAM213B	-0,732721156
RBM38	-0,732701447
PHF14	-0,729520901

ARHGAP21	-0,725232845
ZNF496	-0,722790373
HDGFRP3	-0,722107163
SLX4IP	-0,722080336
MAPK12	-0,719155094
TFAP4	-0,718372872
NUB1	-0,715134502
TRAF3IP1	-0,713092843
MIPEP	-0,711045976
LRRC20	-0,709243648
NUTM2B-AS1	-0,708292569
RCSD1	-0,706896122
TNIP1	-0,706863119
CRAMP1L	-0,70483775
ICK	-0,704529422
CEPT1	-0,69960848
STK36	-0,692086668
TULP3	-0,69120109
GALNT7	-0,688709468
ARID5A	-0,686489957
ZNRF1	-0,685511395
RRM2B	-0,684686854
TTC27	-0,684175518
IRF8	-0,679170815
ITPKB	-0,677045778
IFT172	-0,674713855
RHOB	-0,674407199
TOB1	-0,673805193
SNX22	-0,673783188
MFHAS1	-0,671813598
JAK1	-0,671354858
MOSPD3	-0,670813691
PAQR7	-0,668850695
RABL2B	-0,666063013
NFIC	-0,665680983
TGFBRAP1	-0,665298716
TM7SF3	-0,664046676
CRTC1	-0,663549386
USP40	-0,661944749
ERF	-0,661698985
FAM212B	-0,661651955
STK3	-0,660742212
KDM6B	-0,658469705
PEX26	-0,655514237
DNAJB5	-0,655402667
ZNF827	-0,654871164
SGSM2	-0,65321742

LCP2	-0,651464918
ETV6	-0,650826425
KLF9	-0,650553923
CPOX	-0,647952889
LDLRAD4	-0,647344858
PCED1A	-0,647320296
TRIM22	-0,646817394
ROCK2	-0,646391902
CSNK1G1	-0,644233428
LSP1	-0,643545262
PHLDA3	-0,641487439
LIX1L	-0,641042582
F8A1	-0,639199397
ZNF609	-0,638035302
LYSMD2	-0,637602697
ZBED6CL	-0,63719646
MBOAT7	-0,631499765
GNA12	-0,628127874
TMEM159	-0,626079823
RALGDS	-0,625852877
BRF1	-0,620555691
ASB1	-0,61868453
PPM1F	-0,616523356
HDGFRP2	-0,6160822
HEXIM1	-0,610565446
TPCN1	-0,609146744
LYRM4	-0,607095759
GADD45B	-0,606449947
ZBED1	-0,603585552
ABI2	-0,602695715
VPS41	-0,602522312
SUSD6	-0,602001439
MSC	-0,601497324
ARHGAP35	-0,599582221
PRKAB1	-0,599422277
MLLT10	-0,598370022
NUDT16	-0,598348874
NPIPB5	-0,597790673
MDFIC	-0,597383635
TNFSF9	-0,595929969
MGAT3	-0,594883654
PIAS3	-0,594177868
ZNF768	-0,593802132
FAM160B2	-0,593173971
GSDMD	-0,589261686
TRAF3IP2	-0,58875066
SASH3	-0,58875021

CD44	-0,583147746
VGLL4	-0,582447537
SPATA20	-0,579806368
PRRC2B	-0,578237509
C9orf69	-0,577628695
SFI1	-0,577361677
TOB2	-0,57717749
STAMBP	-0,576809778
WDR43	-0,576331392
ABI3	-0,574937994
PDLIM7	-0,574139627
MYO1G	-0,573473161
CCNG2	-0,573443304
FBXO22	-0,573227856
MLLT4	-0,572707931
AMPD2	-0,572316738
PSIP1	-0,5720843
AMER1	-0,571040834
BAX	-0,570133633
DNMT3A	-0,56994628
CYFIP2	-0,569900314
WHAMM	-0,56717955
ST3GAL2	-0,566566749
POM121	-0,565977127
DYNC1I2	-0,564868371
ALDH4A1	-0,564235624
ETS1	-0,563917613
PIP4K2A	-0,561486702
STRN	-0,561138232
CYFIP1	-0,559160938
ABR	-0,557550326
PHF8	-0,556353698
TP53BP1	-0,556034068
ZNF512	-0,5553717
IKZF3	-0,553828742
SMG6	-0,552590613
MAD1L1	-0,550273467
ZNF281	-0,550265497
MS4A1	-0,548669535
CNTROB	-0,546594426
PEX6	-0,545089579
CEP68	-0,544819879
OLA1	-0,544758592
PISD	-0,541151419
DFFA	-0,539923722
CCDC93	-0,539473313
MIDN	-0,538959972

ATP1A1	-0,537513361
BLCAP	-0,535416521
TACC1	-0,535258664
SORL1	-0,533280941
POLR1A	-0,531511871
EIF4B	-0,529328045
SLC16A1	-0,526531135
NCDN	-0,524814024
CUX1	-0,524706599
ASMTL	-0,521286899
DCAKD	-0,518654141
ALDH1B1	-0,518278058
PHKA2	-0,517849912
EIF2AK4	-0,51635349
AKNA	-0,516311678
TMEM69	-0,515295622
SMARCC1	-0,513979763
NFKB1	-0,512474387
CUL3	-0,511705133
ELK1	-0,511700257
TCF12	-0,511565132
MTHFD1L	-0,511191423
RASGRP3	-0,510958979
MBNL3	-0,508589606
BRD4	-0,508019631
BTBD10	-0,507733877
ZBTB44	-0,507541718
DOCK2	-0,505891124
TRIM41	-0,505230969
PLEKHO2	-0,503133963
LUC7L2	-0,502283869
CCNY	-0,502112784
FOXK1	-0,502008144
BATF	-0,50184515
POM121C	-0,500009956
DIAPH2	-0,499434254
FOCAD	-0,498186215
ANP32A	-0,496264915
CYTH1	-0,496055943
NISCH	-0,494423008
ZFP36L2	-0,494236391
ANKRD27	-0,491594956
ANXA6	-0,491104776
TIPARP	-0,490280564
THAP9-AS1	-0,48892627
TAF15	-0,488416185
MGAT5	-0,487792752

RBMX2	-0,487379755
UPF3B	-0,485970979
MED28	-0,484879411
PFN1	-0,483277246
CCNK	-0,483119672
DEGS1	-0,480989362
AP1S1	-0,479401031
EFHD2	-0,479097251
SUMO1	-0,478556253
FAM78A	-0,477309903
ZC3H4	-0,474631774
GATAD2A	-0,473744103
PFKM	-0,471932693
MOB3A	-0,470341361
OTUD4	-0,469940109
ATP11A	-0,466776949
YLPM1	-0,466501232
RNF219	-0,464745593
TP53	-0,463832577
GRIPAP1	-0,463695494
NCBP2	-0,461654762
PACS1	-0,460859825
FAM168A	-0,456976466
PLEKHG2	-0,453231107
CAPN15	-0,452712108
SH3KBP1	-0,452181002
STAT5B	-0,4515917
RBM17	-0,451331553
KDM4B	-0,450834574
C11orf57	-0,449731123
FAM13B	-0,446363382
HMG20B	-0,446337537
EIF5B	-0,445395308
TSR2	-0,444706733
SEPT2	-0,444347087
VASP	-0,443845398
STK11	-0,440443068
CNOT6	-0,439731827
RBM8A	-0,439679403
TMEM57	-0,435756786
MYC	-0,435283398
ST13	-0,435224521
NCOR2	-0,43384975
TAF1	-0,433636477
TTL	-0,431669515
ODF2	-0,43138823
HTT	-0,431373212

CAD	-0,43086404
ATP11C	-0,430382021
SARS	-0,430246973
LPXN	-0,429423554
RPS2	-0,424109959
MEN1	-0,424065318
CABIN1	-0,423322582
ERICH1	-0,423218459
HNRNPH3	-0,42278067
FAM168B	-0,422415893
SCRIB	-0,422234197
TRIP12	-0,418801608
RPS6KA4	-0,418001447
PRPF40A	-0,415835159
CAPNS1	-0,414449153
REXO1	-0,413911097
MTA1	-0,413444447
IL17RA	-0,411467717
GNAI2	-0,4114011
SZRD1	-0,409399426
MLLT6	-0,40725263
PIP4K2B	-0,405701919
ARID3B	-0,401374328
SF1	-0,40003214
DROSHA	-0,399324426
EML3	-0,395710716
LRRFIP1	-0,395517545
OXSR1	-0,394870216
RFX7	-0,389690618
HDLBP	-0,38821861
C9orf114	-0,386902216
SF3A1	-0,38570875
SIN3A	-0,384756777
MGRN1	-0,383932879
SMARCE1	-0,380661221
DENND1C	-0,379071732
MED15	-0,377156285
SUPT16H	-0,374438783
GTF2F1	-0,373087569
SRRM1	-0,364846714
STAT6	-0,36483538
PPP1R18	-0,360690614
EIF3D	-0,359288711
AHCYL1	-0,355521922
MSN	-0,353946259
STK26	-0,353256328
MEF2C	-0,351732456

FLII	-0,351437744
ILF3	-0,351224364
PSD4	-0,349349345
PRRC2A	-0,330883512
TLN1	-0,314104034

Up-regulated

Gene	log2FoldChange
CD53	0,305702767
PDXK	0,348747429
MAP2K1	0,359567537
GANAB	0,36422689
ATL3	0,371693872
SDF4	0,380553728
PICALM	0,380858111
CANX	0,382526448
ATP13A1	0,39619729
CASP3	0,400326624
HAX1	0,401411515
B2M	0,401536887
LRPAP1	0,410047965
ATP11B	0,410528706
SELT	0,415061563
TPP1	0,415499468
PAK1	0,419008153
ARF1	0,422001389
ERGIC2	0,422204833
KIAA2013	0,424666444
HLA-B	0,424714315
SS18	0,430167042
NUCB1	0,430484409
ANKRD28	0,431425791
SUMF2	0,431508842
SEC23B	0,431761276
MBD1	0,434162033
TMEM263	0,438943233
ZMYND11	0,441652819
CHSY1	0,441958425
DNASE2	0,442384734
MORF4L2	0,443017743
HSH2D	0,44430423
HAUS6	0,447086363
TBC1D1	0,447173646
ATP2A3	0,450297278
C16orf62	0,451161307
CLPTM1	0,451367822

ABI1	0,451847153
STT3B	0,453013464
CD79A	0,460959932
RPUSD1	0,464439841
TBL1XR1	0,466729655
KIAA1551	0,468561875
YIPF2	0,468655347
GOLPH3	0,470983101
TXNDC15	0,472154935
KLHL5	0,479440515
TXNDC12	0,481043124
HSPB11	0,482567337
ATP2A2	0,4826752
OS9	0,484704968
LAT2	0,488411895
RCBTB2	0,489058539
ARF4	0,4895235
SLC10A3	0,490565387
ENTPD4	0,491170284
SFT2D1	0,493666024
TMEM214	0,495437889
SGSM3	0,495781247
CLCC1	0,495802798
NARS	0,496212265
TES	0,496457985
SEC13	0,49726642
CCM2	0,49750851
GOLGA3	0,498608257
VAPA	0,498730272
COG3	0,503068333
FGFR1OP	0,503720835
MPDU1	0,504311145
USP48	0,505593416
AARS	0,50606509
CIB1	0,508601584
ATP6AP1	0,51009738
RUFY1	0,511045252
FANCA	0,512102258
HEXA	0,515461109
AMFR	0,516280681
GALNT1	0,516633615
TM9SF2	0,518281889
CCBL2	0,522890485
PLOD1	0,52321147
TMED4	0,523496984
MYL12B	0,524249218
PARP2	0,526155619

BAK1	0,527391155
METTL23	0,527561077
MIS12	0,527625219
ADPGK	0,527753562
PREB	0,529680494
TXNL4A	0,532095033
AFF4	0,534179938
ZNF587	0,538805988
COLGALT1	0,541237016
PMM1	0,541502481
ATP2C1	0,541894475
SLC35B3	0,541981016
LONRF1	0,542561434
RPS6KB2	0,543564484
PPT1	0,544869043
CHPF2	0,546180537
DNAJC1	0,54663114
RAB30	0,547920436
SMCHD1	0,548186491
MUT	0,548284561
RLF	0,549186967
IL12RB1	0,549801458
GZF1	0,551254541
NXPE3	0,552934771
GLT8D1	0,558141651
SSR2	0,559865135
MBD4	0,560930846
NAGK	0,562014282
TMED5	0,56641436
ADNP2	0,568426278
SLC38A2	0,569003394
CHID1	0,569284887
CYBA	0,569699456
MYL12A	0,570465531
CISD2	0,572346377
ZNF652	0,574615329
CCDC109B	0,576186798
SLC38A10	0,57632519
EMC7	0,577809731
ADGRE5	0,57797111
ATP6V1A	0,578242561
SPAST	0,580345005
PNPLA8	0,580966944
SLC3A2	0,581242834
LAMP2	0,586299116
MTG2	0,590110078
PLOD3	0,594103202

MGAT2	0,595736711
SEC61G	0,59608463
AP1S3	0,596701345
C12orf4	0,597086503
ALG12	0,597719613
PSMG2	0,59793313
BMF	0,598079701
NAPG	0,599194292
NGLY1	0,60071926
NAGA	0,600777345
EMC3	0,601229059
CDKN1B	0,603386525
UNC13D	0,603521127
GNE	0,604396526
CREB3	0,606007972
KLHDC10	0,607378284
CTSD	0,607667272
LMBRD1	0,608425215
PRDM15	0,608694415
SEMA4A	0,609060774
GNPTG	0,610052564
ATP6V1D	0,610101989
SCPEP1	0,611679941
ATOX1	0,612801499
B4GALT4	0,613653929
ING1	0,615090541
ZNF331	0,616874803
ADK	0,618596574
NCAPH2	0,619299747
RPS19BP1	0,620514475
NAA50	0,622101596
GBA	0,622995071
GRK6	0,623052255
MICB	0,623935197
RPRD1A	0,624277635
SRPRB	0,624884683
FAM50B	0,625606943
SLC52A2	0,626264262
MELK	0,627527368
SPNS1	0,628450782
ME1	0,629049094
DXO	0,629146803
MFSD12	0,63018644
NEMP2	0,63170639
MFSD11	0,640184284
NIPSNAP3A	0,642310207
GLA	0,642465544

RHOQ	0,643847796
SRPR	0,644029346
ATF7IP2	0,644639828
PELO	0,646177597
GMPPA	0,646221614
SPTY2D1	0,646804624
ST7	0,648288924
SUB1	0,649363621
ANKRD12	0,649833507
P2RY10	0,649888256
RRNAD1	0,651890222
ALG2	0,652046515
SEP15	0,65284664
CAMKK2	0,656762046
SLC35C1	0,658874117
RAD9A	0,660845925
TTC14	0,661457186
TMED1	0,661613394
CD99L2	0,662071681
TMEM39A	0,662168634
GNS	0,667399421
STS	0,667408379
ZFP36	0,667990471
ABCB6	0,66809479
HDHD2	0,669293181
INSIG2	0,669987552
NMRAL1	0,670854587
FUCA2	0,674595814
SLC17A9	0,67597793
ITGA4	0,67783862
CCDC53	0,679963084
CENPN	0,680935673
ALG8	0,685074215
NCKAP1	0,685101464
ZNF275	0,686051579
RAB24	0,690101265
ZNF296	0,690622363
UQCC2	0,691022051
C10orf32	0,691245947
SPCS1	0,692176476
YIPF6	0,692352204
FAM214A	0,694351649
ENTPD7	0,696437079
ITCH	0,698311688
OSTC	0,702850732
SLC10A7	0,70285712
ALDH3A2	0,705593576

CPD	0,70573161
ALG5	0,705877401
NANS	0,708439541
CAMK4	0,710264505
ZNF701	0,711317209
PLD3	0,712651398
LYSMD3	0,712751805
TAPT1	0,713970752
SEC14L1	0,717107682
DPAGT1	0,718077185
BTLA	0,718671294
ASF1A	0,719082637
SMPD1	0,721703377
KPTN	0,722490595
RFC3	0,722937515
CTBS	0,727097392
FAM63B	0,728024467
ARMCX3	0,728501166
CYB561D2	0,728520964
EDEM2	0,739157735
CALU	0,741372569
NDUFV2	0,742536036
SDCBP	0,742667836
VEGFA	0,742911482
CARD11	0,746318802
ASPHD2	0,747463309
FNDC3A	0,747490898
NOMO1	0,749878758
FAM8A1	0,751918099
KIR3DX1	0,752485678
TAP2	0,763991597
C16orf54	0,765683919
RHBDD1	0,769097798
JTB	0,770349439
EIF2B3	0,774563925
LEPROT	0,776929891
NEMP1	0,777287177
PSENEN	0,777577914
FAM174A	0,778112032
CDK2AP2	0,780692994
PSAT1	0,781027484
STAMBPL1	0,78327099
ZDHHC4	0,783737049
SPCS3	0,783738144
COX7A2	0,785776092
SIL1	0,78599946
RAB31	0,786958904

HLA-DPA1	0,787036693
CSGALNACT2	0,787271931
CMC2	0,788752745
TMEM184B	0,791951519
WDR45	0,792545101
NEU1	0,792650784
RAPGEF2	0,796337313
AGPAT2	0,797331641
PPAPDC1B	0,797745196
KNTC1	0,798610658
C18orf8	0,799192937
DALRD3	0,799891999
LINC00467	0,807287807
CDC25B	0,807422525
TP53I13	0,809249579
CD320	0,815759578
SEC24A	0,818464376
CITED2	0,819167674
DOK3	0,819347875
TMEM208	0,819624846
SEMA4B	0,820426984
SEL1L	0,822123631
LPIN2	0,823087891
ABCA7	0,82661397
ACP2	0,826697364
CCDC50	0,827843463
CIITA	0,829232303
EIF2AK3	0,831292142
FAM117A	0,833809421
PPP3CC	0,839960614
EPB41	0,840359976
JOSD2	0,842146519
NRIP1	0,842471523
PRKXP1	0,846032382
ENO2	0,846056586
PLA2G16	0,847561918
ZNF486	0,847583255
PRDX1	0,848145153
DNASE1L1	0,85014169
POLQ	0,850230848
ZNF841	0,85230424
ZNF397	0,852979944
E2F2	0,858148365
EMP3	0,863350804
BCORL1	0,864789301
KIAA0040	0,865717332
CEP128	0,866584966

JAK2	0,872699385
WFS1	0,873525472
RNF149	0,879325997
RAD51AP1	0,880397818
IER3IP1	0,88148907
TAF4B	0,88347096
CDC42BPB	0,885679304
CDK14	0,888188511
SKA1	0,888948677
SLC41A2	0,891573569
ATP6V0B	0,894632554
HLA-DPB1	0,898266629
TMEM70	0,899514712
ZNF320	0,899641929
HSPA13	0,899657955
SLC35B1	0,900363502
FICD	0,908527954
EAF2	0,910434845
SMCO4	0,911607334
MRPL14	0,912995166
LSR	0,92147062
TCAF2	0,928330158
STAP1	0,942148593
QPCTL	0,946630135
PLP2	0,947587257
TCF19	0,953057183
P2RX4	0,95447122
FBXO16	0,95826053
TMEM106A	0,959535791
C5orf30	0,968298049
HIPK2	0,96961605
PRAF2	0,971930669
CLPTM1L	0,979912259
CBFA2T3	0,979923205
HLA-DMA	0,983894629
DEF8	0,984950704
B3GNT9	0,992955626
GFI1	0,995767572
SRGN	0,996446522
KCNA3	0,997084732
HLA-DRA	0,998476882
ZBTB20	0,999480079
GMNN	0,999656648
NEK3	1,34689E+12
ERC1	1,39412E+12
MUC20	2,81605E+12
SLC6A9	1,04566E+13

TPST2	1,08914E+13
HIST1H2BK	1,18221E+13
KIAA1549L	1,25846E+13
FAM46C	1,30318E+13
EGR1	1,40463E+13
GALC	1,47652E+13
SHROOM1	1,49463E+13
TMEM45A	1,50977E+13
CRY1	1,57273E+13
ENPP5	1,58398E+13
CD72	1,66071E+13
CPM	1,71156E+13
MIXL1	1,79214E+13
MYH15	2,43173E+13
TEX15	3,19762E+13
GATA4	3,20173E+13
LOC101928767	3,3115E+13
ARHGEF37	3,36565E+13
CLIC5	3,38792E+13
SERPINA9	3,97592E+13
SEL1L3	4,07977E+13
T	4,10358E+13
FAM174B	4,53935E+13
DCC	5,04839E+13
ZNF354C	5,23442E+13
BMP8B	5,43232E+13
PBX4	5,47194E+13
CFAP43	5,76575E+13
ADAD2	5,8713E+13
LOC646762	5,9904E+13
GLYATL2	6,02308E+13
NLRP11	6,5684E+13
LDLRAD2	6,57565E+13
PHYHD1	7,60877E+13
XIST	9,32236E+13
SHCBP1	1,00119E+14
CAPG	1,00136E+14
DNASE1	1,00178E+14
SDHAP1	1,00837E+14
MANEA	1,01492E+14
HYI	1,0218E+14
VNN2	1,02352E+14
CEACAM21	1,02385E+14
ATF5	1,02528E+14
RUFY3	1,02552E+14
INO80C	1,02735E+14
CISD3	1,02808E+14

NCF4	1,03057E+14
GGH	1,03198E+14
BIN2	1,03235E+14
NUCB2	1,03374E+14
ANKRD37	1,03654E+14
CCR10	1,03845E+14
STAP2	1,04631E+14
IGFLR1	1,05247E+14
GPR155	1,05393E+14
C7orf13	1,06259E+14
ZNF844	1,06977E+14
HLA-DRB1	1,08526E+14
CCPG1	1,09293E+14
ABHD6	1,09322E+14
ZNF714	1,09335E+14
MSL3P1	1,09638E+14
CYB561A3	1,09949E+14
CYP1B1	1,10099E+14
SRXN1	1,12029E+14
ZFP82	1,1229E+14
ABCD2	1,13015E+14
TYMP	1,13538E+14
DNLZ	1,13771E+14
ANK2	1,13902E+14
ITM2C	1,14492E+14
ARRDC3	1,14693E+14
ASS1	1,15483E+14
ANXA1	1,15874E+14
SLC16A3	1,16007E+14
KIAA0513	1,16176E+14
PLIN2	1,16427E+14
B3GALT4	1,16428E+14
GPR55	1,17939E+14
CYB561	1,18203E+14
RNF157	1,18251E+14
ASPH	1,18885E+14
LRRC8B	1,19166E+14
AGMAT	1,19691E+14
WNT10A	1,19751E+14
ZNF681	1,19806E+14
TNFRSF17	1,20095E+14
APOL1	1,20766E+14
TWSG1	1,2115E+14
CLEC2D	1,2121E+14
TM6SF1	1,22339E+14
C17orf96	1,2252E+14
CD68	1,23602E+14

ZNF229	1,23705E+14
LINC00996	1,23822E+14
MICAL2	1,24012E+14
RN7SK	1,24196E+14
FOXO3B	1,24532E+14
SNX18	1,25123E+14
CLDN14	1,26938E+14
LIME1	1,27743E+14
LRFN4	1,28251E+14
HLA-DOB	1,29304E+14
LINC00152	1,29387E+14
LINC00324	1,29844E+14
GNB4	1,29864E+14
LTBP3	1,30396E+14
MIR22HG	1,31077E+14
P2RX1	1,31495E+14
RNASE6	1,31825E+14
UNC13B	1,32313E+14
SLC48A1	1,3311E+14
FNDC3B	1,33928E+14
BTD	1,34094E+14
NADK2	1,34265E+14
PINLYP	1,34913E+14
GALNT3	1,35146E+14
TCN2	1,36666E+14
SLFN11	1,37528E+14
MTSS1	1,38006E+14
RWDD2A	1,38738E+14
VASH2	1,39006E+14
ARHGEF35	1,39757E+14
ZYG11A	1,40058E+14
NPDC1	1,40765E+14
RNF122	1,41624E+14
SIK1	1,42658E+14
DDX12P	1,43074E+14
TUBB2B	1,43424E+14
HMSD	1,43984E+14
HLA-DQA1	1,4485E+14
ARHGEF5	1,45046E+14
SPATS2L	1,45118E+14
DHRS13	1,45294E+14
MYO3B	1,45321E+14
SBF2-AS1	1,46806E+14
ZNF665	1,47056E+14
SLC26A11	1,48095E+14
KCNK1	1,48763E+14
PRICKLE1	1,49302E+14

SERPINB10	1,49539E+14
TLR7	1,49675E+14
NOL3	1,50158E+14
GPNMB	1,5028E+14
LINC01480	1,50576E+14
MLC1	1,50631E+14
SAMSN1	1,51617E+14
KL	1,51837E+14
FKBP11	1,51957E+14
CELSR2	1,53055E+14
TFR2	1,5434E+14
KIAA0226L	1,54806E+14
HSPA5	1,54847E+14
F12	1,55407E+14
HSBP1L1	1,55936E+14
ZNF571-AS1	1,56902E+14
DEPDC7	1,576E+14
SLC27A2	1,58245E+14
LBX2-AS1	1,58938E+14
KCTD12	1,59026E+14
IL12RB2	1,61501E+14
TMEM44-AS1	1,61609E+14
AHNAK	1,61908E+14
HIST1H4H	1,6205E+14
ABCA3	1,634E+14
SLC30A4	1,64392E+14
DNAH17	1,65765E+14
MIR5195	1,67279E+14
ESR2	1,69414E+14
DCHS1	1,69535E+14
PVRIG	1,69885E+14
SOWAHD	1,71097E+14
LOXL2	1,71977E+14
ARHGEF34P	1,72475E+14
GPR19	1,73319E+14
CKAP4	1,73326E+14
SPTBN4	1,79171E+14
ZBTB8A	1,79582E+14
NOTCH2	1,81185E+14
LOC613266	1,81934E+14
KIAA1217	1,82404E+14
FCRL5	1,83042E+14
KCNK6	1,83251E+14
COL4A4	1,83694E+14
LOC729603	1,84583E+14
ZFYVE9	1,86495E+14
FAAH	1,86571E+14

ERN1	1,86628E+14
MIR4539	1,86677E+14
C1orf162	1,86884E+14
BTBD19	1,86906E+14
PTPRN2	1,87093E+14
MPZ	1,87832E+14
AEBP1	1,88255E+14
GAB1	1,88263E+14
NEFH	1,88264E+14
NFIX	1,90176E+14
INPP5F	1,90904E+14
EPS8L1	1,91165E+14
HCAR3	1,94438E+14
DIP2C	1,97247E+14
RGCC	1,97658E+14
COL4A3	2,01834E+14
CBARP	2,04982E+14
CHST6	2,06348E+14
CCR1	2,06451E+14
NOD2	2,08574E+14
IRF6	2,0903E+14
LIPG	2,11005E+14
LRP12	2,11457E+14
LINC00539	2,1209E+14
BCAR3	2,12451E+14
TMEM65	2,13467E+14
CD9	2,14218E+14
ZNF793-AS1	2,15072E+14
EVI2A	2,15727E+14
MUC4	2,15826E+14
ARHGAP42	2,18118E+14
PDGFA	2,19047E+14
BCL2L10	2,1966E+14
LINC00528	2,19945E+14
CLEC2B	2,20226E+14
MT2A	2,20264E+14
CFAP54	2,23559E+14
PDE9A	2,25257E+14
MAFF	2,26499E+14
HSPA7	2,269E+14
BAIAP3	2,28385E+14
SSTR3	2,33535E+14
CCDC144B	2,35323E+14
TPTE2	2,44311E+14
PRKCZ	2,46299E+14
LGALS3BP	2,46327E+14
ZNF711	2,46894E+14

LYPD6B	2,47619E+14
PC	2,48864E+14
GLB1L2	2,49711E+14
RIMBP2	2,50329E+14
RGAG1	2,51029E+14
PDE6G	2,52863E+14
CEBPA	2,54359E+14
ADAP2	2,5552E+14
IL32	2,56503E+14
MIR4538	2,56509E+14
POU4F1	2,57061E+14
TNFRSF18	2,59448E+14
LAD1	2,59452E+14
C17orf107	2,62084E+14
ZBP1	2,65359E+14
HRASLS2	2,67372E+14
SERPINB2	2,70461E+14
PTPRS	2,70502E+14
PLEKHA7	2,70597E+14
MAP1LC3A	2,74522E+14
IRS2	2,7581E+14
ESPNL	2,78251E+14
SPTA1	2,80273E+14
RAB36	2,83668E+14
ST14	2,83961E+14
MYO1D	2,84347E+14
ACRBP	2,84431E+14
CTBP2	2,89189E+14
LMCD1	2,91448E+14
ST3GAL6	2,9308E+14
RARRES2	2,93242E+14
NDFIP1	2,93563E+14
SERPINF1	2,95109E+14
CKB	2,97377E+14
FAM109B	2,97591E+14
ITGAX	2,97668E+14
C11orf63	2,97846E+14
JCHAIN	2,98778E+14
COTL1	2,99097E+14
TIMD4	3,01162E+14
TCL6	3,01927E+14
CD180	3,02032E+14
FAM171A1	3,02134E+14
BTN1A1	3,02442E+14
FHOD3	3,02743E+14
MZB1	3,04149E+14
NSUN7	3,06086E+14

TESC	3,09034E+14
PECAM1	3,10503E+14
INPP5J	3,10563E+14
ESRP2	3,10835E+14
ZNF208	3,12503E+14
PCBP3	3,14235E+14
RNF5P1	3,16595E+14
LDOC1L	3,16666E+14
IFI27	3,18555E+14
CASP1	3,20406E+14
LNX1	3,22206E+14
ASMT	3,23345E+14
CUEDC1	3,23592E+14
RNASE4	3,24453E+14
PYHIN1	3,28529E+14
LAMA5	3,30662E+14
PROSER2	3,3112E+14
ARHGEF10	3,4008E+14
ZNF300	3,40976E+14
NEURL1	3,41792E+14
COL6A1	3,41969E+14
DLGAP2	3,43122E+14
ADAMTS17	3,43491E+14
DNAH17-AS1	3,45317E+14
TRPS1	3,45647E+14
EVC	3,4575E+14
TRIM47	3,49554E+14
MCOLN3	3,52079E+14
PRR18	3,5403E+14
FAM129C	3,5489E+14
RHBDF1	3,58876E+14
GAS6	3,59898E+14
LINC00242	3,61483E+14
LOC441666	3,62484E+14
KCNK5	3,66615E+14
SYT12	3,67259E+14
GABRR2	3,68702E+14
DERL3	3,68918E+14
GJB2	3,69788E+14
CTGLF12P	3,71848E+14
ARHGEF10L	3,72574E+14
USP44	3,72745E+14
RASGEF1A	3,73061E+14
MARC2	3,75196E+14
PCSK6	3,83591E+14
SIT1	3,90684E+14
ITGA6	3,9085E+14

IGF2BP1	3,93778E+14
PTPN21	3,95753E+14
CDHR1	3,97514E+14
CRNDE	3,99158E+14
HORMAD2-AS1	4,05066E+14
ADAMTSL2	4,05657E+14
SCGB3A1	4,09664E+14
MTCL1	4,11213E+14
SYDE2	4,12212E+14
DENND2C	4,20681E+14
ANKRD36BP2	4,21624E+14
PDCD1	4,31577E+14
TEAD1	4,41137E+14
FMNL2	4,4727E+14
HMX2	4,52718E+14
A2M	4,53166E+14
ZNF492	4,54519E+14
WFDC2	4,56199E+14
PXDN	4,60727E+14
CCNI2	4,61603E+14
KLB	4,65206E+14
XIRP1	4,65642E+14
GPR141	4,66867E+14
ADTRP	4,66933E+14
LHFPL1	4,68921E+14
ZNF542P	4,69438E+14
LINC00540	4,79017E+14
GSTM3	4,81769E+14
SYBU	4,83002E+14
CHST4	4,91477E+14
ITM2A	4,92279E+14
SLC6A12	4,94743E+14
ITGB5	5,02846E+14
SOX18	5,05506E+14
PIEZO2	5,06019E+14
EPB41L4A	5,07744E+14
ARSD	5,27059E+14
PPP1R27	5,29453E+14
NUAK2	5,2986E+14
XCL1	5,30707E+14
CLEC4C	5,34988E+14
ACSBG1	5,3946E+14
ADGRE1	5,4039E+14
EDNRA	5,40568E+14
ELFN1-AS1	5,50508E+14
AMPD1	5,50908E+14
MARK1	5,54398E+14

SCT	5,56716E+14
TSPAN1	5,60955E+14
ACE	5,61052E+14
ANKK1	5,65482E+14
LRRN2	5,67854E+14
EGFR	5,70722E+14
XKRX	5,82863E+14
KGFLP1	5,82955E+14
LONRF3	5,85823E+14
TMEM52B	5,88831E+14
NUP62CL	6,05523E+14
LRP3	6,07769E+14
THNSL2	6,0808E+14
IFNG	6,19331E+14
COL4A2	6,21845E+14
SAMD13	6,22488E+14
TSPAN7	6,25838E+14
LIX1	6,2885E+14
KDELR3	6,33684E+14
SLC8A1	6,36907E+14
MAP1B	6,43971E+14
SLC32A1	6,52996E+14
GIMAP4	6,57335E+14
EDNRB	6,70032E+14
HHEX	6,7595E+14
CCR2	6,90284E+14
APP	7,06132E+14
PRSS21	7,29639E+14
TLE1	7,30108E+14
TCL1B	7,46692E+14

Supplementary Table 7. Differentially expressed genes (up- and downregulated) in EP compared to CdLS cell lines.

Down-regulated

Gene	log2FoldChange
CHIA	-6,7219E+14
ITGA11	-6,29338E+14
C1orf21	-5,83974E+14
PAX8-AS1	-5,21556E+14
PLCB1	-5,18647E+14
SIGLEC15	-5,08284E+14
SCHIP1	-5,06417E+14
CA4	-4,97667E+14
PPP2R2C	-4,70739E+14
CRTAM	-4,68034E+14
CTTNBP2	-4,46948E+14
RIN2	-4,40295E+14
MIR548D1	-4,35559E+14
CORO2A	-4,35007E+14
CNTNAP3	-4,22921E+14
JAKMIP2	-4,20219E+14
FOXG1	-4,1198E+14
NPY	-4,11822E+14
CBR3	-4,11084E+14
ATP10A	-4,09979E+14
ZNF462	-4,01483E+14
DIP2A-IT1	-3,99539E+14
WWTR1-AS1	-3,84611E+14
SNORD33	-3,81519E+14
CALML6	-3,77748E+14
USP32P2	-3,57384E+14
LINC00977	-3,55836E+14
PRKCQ	-3,5335E+14
PKP2	-3,44477E+14
TPM2	-3,35093E+14
SNORD47	-3,26738E+14
APP	-3,20254E+14
TOX	-3,11856E+14
PDE3B	-3,03428E+14
SNORA65	-2,97458E+14
GRAP2	-2,89353E+14
RHPN1	-2,81952E+14
PEX5L	-2,79186E+14
SNORD42A	-2,7587E+14
C17orf97	-2,66034E+14
DAPK2	-2,52685E+14
WWC1	-2,48382E+14

AXIN2	-2,43853E+14
LOC101929574	-2,42077E+14
PAPSS2	-2,40193E+14
JAKMIP1	-2,39781E+14
GABRB2	-2,39198E+14
FAM89A	-2,37491E+14
SPNS3	-2,37395E+14
TMEM178B	-2,37031E+14
HS3ST1	-2,32481E+14
ADRB1	-2,26531E+14
FAM110B	-2,22008E+14
CNKSR2	-2,20927E+14
MCC	-2,19875E+14
LOC729737	-2,09445E+14
DLSTP1	-2,04065E+14
JAM3	-2,02552E+14
DHRS3	-1,98917E+14
ARHGEF17	-1,97952E+14
SNORD45C	-1,97707E+14
STXBP1	-1,87536E+14
DOCK4	-1,80635E+14
ITGB3	-1,79781E+14
HEY1	-1,7908E+14
SLC23A3	-1,78908E+14
HPSE	-1,7004E+14
CCDC74A	-1,6139E+14
ERP27	-1,59873E+14
SYNJ2	-1,59841E+14
KLF5	-1,54593E+14
ZFP92	-1,54378E+14
WDR17	-1,54102E+14
EDARADD	-1,50885E+14
PTGER4	-1,49703E+14
TP53BP2	-1,40328E+14
LOC730183	-1,36988E+14
SATB1	-1,32142E+14
AMZ1	-1,31262E+14
FAM222A	-1,31225E+14
CAPN2	-1,30142E+14
ACY1	-1,28331E+14
SNORD5	-1,26404E+14
FOXD2-AS1	-1,20733E+14
APOBR	-1,20586E+14
ZMIZ1	-1,15967E+14
MTHFS	-1,07525E+14
EIF1AY	-1,06589E+14
CDCA7	-1,02483E+14

ACCS	-1,01567E+14
TMIGD2	-6,1429E+13
S100A9	-5,25753E+13
NCCRP1	-4,68797E+13
LOC339874	-4,10344E+13
MMEL1	-4,01215E+13
SNORD28	-2,80383E+13
MIR3191	-1,91922E+13
MIR8072	-1,50849E+13
GIMAP6	-1,4734E+13
GBGT1	-0,991629029
S1PR1	-0,956967139
CRYBB2P1	-0,950009039
PIK3C2B	-0,872317706
TMTC4	-0,871211323
GTF2H2B	-0,842139439
KLF12	-0,834163393
NAV2	-0,833767628
MACROD1	-0,799665593
SLC39A10	-0,748598408
RGS16	-0,727575882
E2F8	-0,711600512
SAMD4A	-0,710303595
ROCK2	-0,708501016
ELOVL6	-0,702595978
ENTPD1-AS1	-0,6790245
RAI1	-0,673841151
NFATC2	-0,663377388
SLC35G1	-0,658210214
FAM72D	-0,658181103
MCM6	-0,656319861
SPAG16	-0,649405197
MARCKS	-0,633470248
UHRF1	-0,628238831
SLC4A7	-0,621013878
BARD1	-0,619758636
LY75	-0,61668858
CEP78	-0,612746287
ARL5A	-0,602596871
TAF1B	-0,600528708
DUSP7	-0,595429284
CENPL	-0,588905817
E2F1	-0,585308241
MBLAC2	-0,57927944
TMPO	-0,570727056
BLM	-0,570326118
CORO1A	-0,568704098

LRRC20	-0,563134293
MCM7	-0,5609095
SPTLC2	-0,560172331
RIF1	-0,556013301
POLR3G	-0,554767366
CPOX	-0,553435415
C4orf46	-0,552731706
LRRC58	-0,549113019
PLD6	-0,547216895
SLC20A2	-0,546805297
ARL13B	-0,545895779
ENTPD5	-0,545527125
POLA1	-0,543710035
ANP32E	-0,532397138
SMC4	-0,523458889
UBE2D1	-0,516653811
MSH2	-0,510476384
OSBPL8	-0,505319755
ECT2	-0,504786457
CCNF	-0,504493682
CD3EAP	-0,503109428
ARHGAP11A	-0,500944099
SNRNP48	-0,499649339
MZT1	-0,496486935
CDCA4	-0,493990868
MTHFD1L	-0,490389793
IPMK	-0,486844057
ITPK1	-0,484379833
PTMA	-0,481538761
SRSF1	-0,481522789
PRKAA1	-0,471070577
GINS4	-0,46843495
XPO4	-0,466670282
SCAI	-0,465920781
NUCKS1	-0,460591192
CHD7	-0,460270597
PFAS	-0,456891286
DCTPP1	-0,454998493
GPR180	-0,451341394
CEP135	-0,450718636
PMS1	-0,450418728
TRIM33	-0,450080042
ZNF100	-0,448303926
DPY19L4	-0,445386016
SUZ12	-0,443781246
DHX33	-0,441760773
FAM122B	-0,439882387

GMEB1	-0,438002706
AGPS	-0,437312941
SFMBT1	-0,43662119
MFNG	-0,434960724
MTFMT	-0,427170515
ACOT7	-0,425746574
HNRNPD	-0,425585315
PARPBP	-0,425264721
TRUB1	-0,424703446
GNPNAT1	-0,424577368
FAM78A	-0,424283149
RANBP1	-0,424161654
MSH6	-0,423691097
FBXO45	-0,421101264
RCL1	-0,419838133
RFC2	-0,419085923
LIG3	-0,417112216
RPGR	-0,41491393
KNOP1	-0,414878998
TMEM110	-0,414151965
ZDHHC17	-0,413916619
TWISTNB	-0,413555286
ALG10B	-0,411350349
BAG4	-0,411014278
TMEM201	-0,409448482
LIG1	-0,408128099
SRSF2	-0,408048949
GMFB	-0,406728799
LMNB2	-0,406391452
GABPA	-0,405722485
RRS1	-0,405327204
TMEM170A	-0,403714075
YTHDC2	-0,401268091
PABPN1	-0,397773027
SCOC	-0,393840916
ZNF619	-0,393108482
NAA25	-0,3929099
TP53	-0,391801778
ERI1	-0,388812001
HDAC2	-0,386707789
AEBP2	-0,385985972
PIGW	-0,383324505
TTLL12	-0,382083593
SLC16A1	-0,380917833
HNRNPA3	-0,380233192
LINC00265	-0,376345026
ARID3A	-0,375638943

NCL	-0,374772578
MBNL1	-0,373213099
NOP9	-0,37301745
PTER	-0,372253594
CENPB	-0,371191791
IPO7	-0,370812559
TIMM23B	-0,367833653
ESF1	-0,366848074
GEMIN6	-0,365835229
SLMO2	-0,364790843
FUS	-0,361208701
UCK2	-0,360257677
HNRNPA2B1	-0,359611521
CASP2	-0,35937506
CELF1	-0,357320017
GOLT1B	-0,356810915
TRMT5	-0,356801385
HDGF	-0,356477463
SORD	-0,355657012
SAP30	-0,353838663
LYPLA1	-0,353108729
YWHAQ	-0,351086167
PPP1CB	-0,349338018
SMNDC1	-0,34777243
TUBA1B	-0,347440496
B4GALT2	-0,347412487
IKZF3	-0,347072722
LIMS1	-0,346543956
PCK2	-0,346401843
KPNA3	-0,346393215
MRTO4	-0,345624831
MOSPD1	-0,345550025
KLHL42	-0,343325411
FANCL	-0,343299808
HN1L	-0,343159327
CABLES2	-0,342926027
PAPD5	-0,341784389
SHMT2	-0,340914844
RAD18	-0,339883777
DPP8	-0,339433326
PURB	-0,337797471
SREK1IP1	-0,337710272
TSEN15	-0,337398792
PGGT1B	-0,337196583
GNA11	-0,336801964
NIPA2	-0,33676931
TRA2B	-0,335313075

C12orf65	-0,331914499
BAZ1A	-0,328261361
TRA2A	-0,328069719
PROSER1	-0,326103484
UNG	-0,324203963
RBM14	-0,323540928
PKNOX1	-0,323074623
SLC35A3	-0,322590142
NUDT21	-0,319794458
ZNF326	-0,319059419
MAZ	-0,318449726
SET	-0,31838869
KPNB1	-0,318180142
GATAD2A	-0,317679043
HNRNPH3	-0,317550057
ANP32A	-0,315048635
MED27	-0,313143576
PA2G4	-0,31207199
SF3B3	-0,311863679
HNRNPM	-0,311780647
KIAA0020	-0,311769566
C9orf114	-0,311605089
HNRNPR	-0,307811364
MRE11A	-0,307417133
TTC33	-0,307174056
C2orf44	-0,300951227
PDAP1	-0,300509748
AKT1	-0,300054401
SDCCAG3	-0,29615538
WDR12	-0,295096678
FUBP1	-0,294266401
TAF6	-0,290059763
SLC25A51	-0,288499004
HNRNPH1	-0,287497977
TFAM	-0,287468175
GABPB1	-0,287289063
CREB1	-0,287116951
NSUN2	-0,286045763
NCOA5	-0,284218838
EWSR1	-0,283765598
NUP50	-0,283637038
TSNAX	-0,283417069
PPAT	-0,281538135
ILF3	-0,280306185
NIP7	-0,278486214
HNRNPUL2	-0,27814224
BYSL	-0,277854261

MTF2	-0,27739736
CCT5	-0,277197626
LSM12	-0,273987254
DR1	-0,270576109
MRPL42	-0,269280811
UBE2K	-0,268788359
LSM14A	-0,268717567
CBX3	-0,267958069
MAT2A	-0,267358165
ZRANB2	-0,267090443
SRSF10	-0,26557541
ATAD1	-0,262817798
MPRIP	-0,260403428
CARM1	-0,260141561
BLMH	-0,257950709
ACTR2	-0,25786633
SNRNP40	-0,254062935
ABCE1	-0,253881921
STK35	-0,253678501
SPIDR	-0,253594616
SERBP1	-0,250668161
STAM	-0,248468307
HIRA	-0,246906641
HNRNPU	-0,244841927
DAZAP1	-0,243981978
CPSF3	-0,243542386
NUDCD1	-0,243206144
FAM210A	-0,242402172
PPP1R8	-0,242014076
CPSF6	-0,237890375
TFCP2	-0,234396276
SF3A3	-0,233179425
HAUS2	-0,228367805
SRF	-0,221293197
LEO1	-0,220931086
NONO	-0,219601351
PCNP	-0,21786925
SYNCRIP	-0,215750532
NRAS	-0,212779754
THUMPD1	-0,211427783
RNPS1	-0,207032912
GTPBP4	-0,205096639
CDC123	-0,194097337
PITPNB	-0,185785986
RAVER1	-0,176385949
WBP11	-0,166448471
KHDRBS1	-0,164665512

ATXN2L	-0,157866285
AKT2	-0,153035792
ZNF207	-0,151296938

Up-regulated

Gene	log2FoldChange
GPBP1	0,179066855
TMBIM6	0,199276014
UBC	0,209094956
SNX17	0,25197902
ZKSCAN5	0,253953306
C9orf156	0,254478608
SQRDL	0,259028717
NDEL1	0,266253807
SPG7	0,269191442
TMEM115	0,273171189
ARL2BP	0,274456701
COQ5	0,28227352
SNAPIN	0,283147497
ASPSCR1	0,293232865
CCDC22	0,30076485
CINP	0,303480176
MGAT4B	0,305428324
NR1H2	0,305549829
NDUFA4	0,311315334
KIAA1191	0,313273853
ITFG2	0,317875412
SYNGR2	0,318577766
DEDD2	0,319045021
B4GALT7	0,327183626
R3HDM4	0,329359259
TM2D3	0,330183097
ZNF761	0,344056185
ZNF717	0,349973424
PNPLA8	0,351699975
EMC3	0,357530178
ANKRD42	0,359686002
TCTA	0,362925215
NDUFB2	0,365871878
RNF14	0,371488434
C19orf60	0,373407639
CD99L2	0,373897033
ORMDL2	0,380335303
BAD	0,385604917
PARP6	0,390301558
TMC6	0,397735638

ZNF18	0,403280189
PDE4DIP	0,40427584
MFSD11	0,406371587
TMEM129	0,406970298
FBXL15	0,409599968
POLE4	0,413665152
FAM98C	0,419866877
CCM2	0,431687012
RMND5B	0,434931873
WDR45	0,439467946
MTIF3	0,443617305
PAK1	0,444503822
TRPT1	0,44534882
SERINC1	0,445743159
ZNF671	0,453578901
TMED9	0,464015731
GNS	0,465882783
WDR83OS	0,466177282
PLA2G6	0,466632511
TMEM216	0,466985824
TPP1	0,472377255
KPTN	0,473817969
LOC100131564	0,486787645
IFT43	0,493751186
SLC46A3	0,494004461
ZNF700	0,494225053
TPT1-AS1	0,494371119
PLA2G15	0,495872847
PSTPIP1	0,497234298
KCTD21	0,497654194
LOC285074	0,4994021
EVI5	0,501755839
PGAP3	0,503574612
DLEU1	0,504804516
PHTF1	0,514603403
CCDC159	0,524519161
TBC1D17	0,529338359
PSENEN	0,529991417
TMEM99	0,532242163
LIPT1	0,533560477
CHPF2	0,533778623
ACADM	0,535654522
PHF1	0,53650866
NUDT17	0,54069888
FLJ37453	0,54260512
BIN1	0,548284219
CYB5D2	0,559042317

PNPLA4	0,559175501
SGSH	0,562063463
GM2A	0,574749745
SLC31A2	0,578986153
H1FX	0,579506583
LYSMD1	0,581430976
TCAF2	0,583032423
GLT8D1	0,585066405
SPATA2L	0,593172974
DHRS12	0,611162473
VAT1	0,613400512
C2orf81	0,618423613
IGFLR1	0,622942195
C5orf45	0,629883031
DGKQ	0,630661218
NDNL2	0,637426347
SQSTM1	0,655592913
ZNF559	0,659155845
WASH3P	0,6616276
PPP2R5B	0,667897385
ZNF837	0,719438836
MAP3K14-AS1	0,721112007
FLJ20021	0,722141401
LOC728743	0,72578161
JOSD2	0,741221238
MIR22HG	0,775774481
ABCA2	0,784173897
SDCBP2-AS1	0,809526402
MYL5	0,81621216
CTTN	0,827992972
TYMP	0,831850757
ZNF763	0,836741024
ZNF699	0,84655015
SCAMP1-AS1	0,881764631
B3GALT4	0,887743786
ABHD4	0,896938644
GPNMB	0,921696884
PKIG	0,926865177
GABARAPL1	0,931549418
EMILIN2	0,951420352
TMEM44-AS1	0,956187168
NPIPB4	0,971274593
KIAA0226L	0,991814487
DDR1	0,996368592
RUSC2	1,51855E+12
ETV2	1,14632E+13
GSTA4	1,5133E+13

TPTE2	1,59254E+13
HHLA2	2,33951E+13
PRODH	2,34508E+13
CX3CL1	4,01769E+13
CPEB3	1,00112E+14
SLC26A11	1,02564E+14
ANGPTL2	1,03295E+14
OSER1-AS1	1,03853E+14
RAP2C-AS1	1,04362E+14
LIN7B	1,06578E+14
ZNF880	1,07334E+14
C14orf79	1,08429E+14
MIR5195	1,0846E+14
LOC100507283	1,09463E+14
SLC16A5	1,09877E+14
KLHL6	1,1056E+14
LY6G5C	1,10722E+14
UXT-AS1	1,1103E+14
LOC728392	1,15851E+14
TTC22	1,22495E+14
TTC39A	1,37953E+14
GPR157	1,38069E+14
SLC7A7	1,38112E+14
YTHDF3-AS1	1,39581E+14
RRAD	1,4116E+14
MIR3064	1,41531E+14
HEPH	1,47215E+14
HMOX1	1,48438E+14
PVRL4	1,50655E+14
PFN4	1,51551E+14
PTPRF	1,53362E+14
KIAA0895	1,55647E+14
ITGAM	1,57596E+14
DNM1P46	1,62663E+14
SH3BGRL2	1,64137E+14
CHRNE	1,65273E+14
CACNA1E	1,65475E+14
FAM167B	1,66498E+14
TMEM51	1,66767E+14
C20orf194	1,70689E+14
PLEKHG6	1,7102E+14
EDN1	1,71541E+14
POU4F1	1,7326E+14
GABBR1	1,73868E+14
HCN2	1,87329E+14
LARP6	1,90091E+14
GUCY2C	1,98495E+14

DENND2C	2,05185E+14
INCA1	2,05339E+14
SEMA3B	2,08052E+14
PIWIL2	2,21341E+14
TTC7B	2,26177E+14
SGK2	2,30811E+14
HPCAL4	2,3325E+14
LINC00540	2,37784E+14
NRN1	2,38082E+14
PCDH8	2,40565E+14
OSBPL6	2,43551E+14
LINC00925	2,43788E+14
HAL	2,50636E+14
UTS2R	2,51E+14
ADGRA3	2,70363E+14
DRC7	2,72599E+14
SEPP1	2,83571E+14
RASD1	2,8955E+14
LOC730102	2,90396E+14
ARHGEF10L	2,99544E+14
TCTE1	3,02987E+14
PAX9	3,34621E+14
FAM46B	3,35461E+14
EGFL6	3,58334E+14
LOC100506860	3,58852E+14
PAX3	3,7936E+14
KIF17	3,79976E+14
INHBB	4,01232E+14
GUSBP3	4,03097E+14
AHSG	4,10712E+14
TMEM176B	5,25843E+14
LINC00221	9,60697E+14

Supplementary Table 8. Differentially expressed genes (up- and downregulated) in EP versus CdLS cell lines, both carrying missense variants.

Down-regulated

Gene	log2FoldChange
LINC01115	-7,49312E+14
TLE1	-6,93177E+14
GZMH	-6,61912E+14
NETO1	-6,09623E+14
EML5	-5,94021E+14
KCTD15	-5,93567E+14
CBR3	-5,62118E+14
ZFX-AS1	-5,56557E+14
CRTAM	-5,16042E+14
MAGI2	-4,7322E+14
GRIA1	-4,6603E+14
SNORD47	-4,53412E+14
AXIN2	-4,34965E+14
C17orf97	-4,17491E+14
SPTSSB	-3,49986E+14
IL17RC	-3,44633E+14
DLSTP1	-2,70394E+14
LOC729737	-2,6578E+14
SPNS3	-2,6196E+14
DOCK4	-2,10965E+14
PHKA1	-2,09937E+14
FCGR2C	-2,09611E+14
MAN1C1	-2,04229E+14
KLHL13	-1,9062E+14
HLA-DQB1	-1,86144E+14
PALD1	-1,86005E+14
ZNF818P	-1,74512E+14
NLRP2	-1,66248E+14
FAM86B3P	-1,63769E+14
HLA-DQA1	-1,54727E+14
AMZ1	-1,53514E+14
WDR17	-1,51911E+14
ITGB3	-1,49035E+14
STC2	-1,27302E+14
KCTD12	-1,11262E+14
ZNF584	-1,08477E+14
MYB	-1,02139E+14
JAKMIP1	-3,19922E+13
EIF5AL1	-2,38558E+13
CTH	-0,998662919

PHGDH	-0,979837369
PSAT1	-0,968122819
UHRF1	-0,904708037
CCDC126	-0,901470442
HDAC4	-0,898122368
NDC1	-0,857162636
SPAG16	-0,849866252
PKP4	-0,832765622
MCM7	-0,827767061
TFAP4	-0,807011831
TAPBPL	-0,805193861
SLC25A10	-0,802819493
SMC4	-0,797174425
RBL1	-0,79430949
SLC19A1	-0,793968727
SMC2	-0,792414163
LZIC	-0,792189711
DNAJC15	-0,786470876
CEP78	-0,781968075
MMS22L	-0,772762245
POLA1	-0,770340951
MCM3	-0,758595957
TMPO	-0,757591077
RIF1	-0,754040057
ARHGAP11A	-0,753330268
MCM4	-0,736658475
MZT1	-0,735469051
SLC4A7	-0,726032675
NUP155	-0,719818523
PRDM10	-0,719268622
PFAS	-0,71746258
XPO4	-0,713952009
SRSF1	-0,706830422
MZT2A	-0,706150832
CBFB	-0,704266057
CEP57L1	-0,69979738
ARHGAP19	-0,695034906
CASC5	-0,692039054
MKI67	-0,691483333
WDR76	-0,689425128
LRRC58	-0,687356993
CHML	-0,684050777
MCM5	-0,675909032
ST3GAL1	-0,67478489
MCMBP	-0,670748887
MARCKS	-0,666214144
COLGALT1	-0,664882004

PAG1	-0,662280758
ITPRIPL1	-0,66082516
ANP32E	-0,654057258
FAM122B	-0,64563338
TOP2A	-0,644914381
IRAK1	-0,642328471
WDR4	-0,641819102
NAA15	-0,640278059
WHSC1	-0,631384427
CENPU	-0,631322422
MIPEP	-0,629554865
TCOF1	-0,62097737
MFNG	-0,620383692
XPOT	-0,616611679
MCM2	-0,615932743
RNF138	-0,610128797
MTHFD1L	-0,608551052
HNRNPD	-0,601290636
NAA50	-0,597949516
SLC7A1	-0,596215735
NCL	-0,595900491
SLC7A5	-0,595667647
NOL8	-0,590613007
APIP	-0,590031205
HNRNPA3	-0,576455512
BRIP1	-0,573440444
RFC2	-0,572909455
OSBPL8	-0,572878708
PARPBP	-0,57267797
RAI1	-0,569237959
PRKDC	-0,568630678
DIAPH3	-0,56840732
SMC1A	-0,567399222
HNRNPA2B1	-0,566760236
DDX21	-0,56556733
GPR180	-0,559515283
AMD1	-0,558464895
DHX33	-0,558084017
NUP160	-0,557786124
C10orf2	-0,552601798
MEF2A	-0,546614095
SUZ12	-0,541928541
NUCKS1	-0,535665488
MAZ	-0,530164395
TCERG1	-0,527909101
LIG3	-0,525520194
BAG4	-0,524720734

GMFB	-0,521276696
DHX9	-0,511409529
PSPH	-0,5098762
ANP32B	-0,508083613
ESF1	-0,507905886
DOCK8	-0,506175699
HK2	-0,504540134
TTLL12	-0,503033128
TP53	-0,498264991
DOCK7	-0,496504844
SRSF10	-0,49390015
TRA2B	-0,493535436
XPO1	-0,492474328
TTLL4	-0,49242609
SF3B3	-0,491139379
SSRP1	-0,48705857
LIG1	-0,486436385
FBXO41	-0,485087738
HDGF	-0,478749471
LPGAT1	-0,473975854
BOP1	-0,470458557
RUVBL1	-0,469690828
TMEM123	-0,468823805
NUP153	-0,464783258
BAZ1A	-0,463753307
KIAA0196	-0,462732666
KPNA3	-0,462006717
SET	-0,46083482
PPP1CB	-0,459418269
ZNHIT6	-0,453222226
NOL11	-0,453206888
NOLC1	-0,452368264
CCT5	-0,44384123
RNF219	-0,440263208
HNRNPH3	-0,437512944
IPO7	-0,437440272
UCHL5	-0,437128039
ARMC10	-0,436448853
KHSRP	-0,433488124
STX7	-0,433465753
GPATCH4	-0,433201232
MBNL1	-0,430874311
PURB	-0,430318723
TCP1	-0,424575147
RBM14	-0,424014547
CELF1	-0,423737092
HNRNPM	-0,422172466

WDR36	-0,422043224
LARP4	-0,42126076
IDH3A	-0,420450265
KPNB1	-0,420208835
SNRNP27	-0,419994913
CBX3	-0,419118741
HNRNPR	-0,418360907
WDR3	-0,413650576
ILF3	-0,41108704
HSPD1	-0,41105277
EIF1AX	-0,410583855
BAZ1B	-0,409584366
ARHGAP18	-0,408361908
LSM14A	-0,407470969
IPO4	-0,402176896
RBBP8	-0,400975812
MPRIP	-0,398891077
HNRNPH1	-0,396581442
KIAA0020	-0,390772644
HSP90AA1	-0,390421524
RBM25	-0,388539108
PES1	-0,384958896
NUP50	-0,374819341
SERBP1	-0,372476699
CACTIN	-0,369392874
NPM1	-0,36850778
C15orf39	-0,35855081
SRRM1	-0,354573492
SENP1	-0,353357761
IARS	-0,353102556
NUPL1	-0,3504704
DAZAP1	-0,346783096
HNRNPU	-0,345991534
ABCF2	-0,345937112
UBE2K	-0,341531823
ZRANB2	-0,340712929
EIF2S2	-0,339664288
NACC1	-0,336104371
SF3A3	-0,331109719

Up-regulated

Gene	log2FoldChange
CTSA	0,384553823
SLC25A1	0,389285919
GPX4	0,410899146
TRAFD1	0,424447721

NCSTN	0,448821905
SHISA5	0,453262697
NDEL1	0,455169458
PSENEN	0,460976937
IRF9	0,466435819
CCND2	0,475330582
F11R	0,478185587
IL2RG	0,482963624
HLA-E	0,486188913
MCOLN2	0,493717168
AVEN	0,497362547
CST3	0,502490068
TRAF1	0,517186497
PNOC	0,527698073
EHMT1	0,539252259
SKAP1	0,543128761
TTYH3	0,545837538
ICAM3	0,545985471
ACP2	0,546309276
SERINC1	0,547289579
THEMIS2	0,548280521
PVT1	0,578494413
LAPTM5	0,579700429
ZNF581	0,584963139
INPP1	0,596203513
BBC3	0,599580867
CD99L2	0,603136887
SPRYD4	0,604025768
DTX3	0,608800272
ALOX5AP	0,612229331
LIPA	0,616615429
TMEM164	0,618431558
MICAL1	0,620282441
PIGV	0,624810353
ZNF331	0,629877047
CFLAR	0,636966145
RGS20	0,640097101
MVD	0,640864208
RAB9A	0,643151636
ACADM	0,652926943
DNAJB2	0,65918492
HAAO	0,659373664
B4GALT3	0,668237155
FCER2	0,689213705
FAM117A	0,703190049
SERPINB8	0,714867166
TMOD1	0,718556538

TM7SF2	0,725378884
SGSH	0,727856603
MKNK2	0,730338218
ARSA	0,747934452
CRTC1	0,755508352
IGFLR1	0,759851953
ZC3H12D	0,765013324
RGL1	0,779926731
CCDC102A	0,781546323
CCDC64	0,781846696
PNKD	0,790636788
TNFSF13B	0,797379593
ATHL1	0,799672081
IKZF1	0,805957917
RASGRP1	0,809690346
CDKN1A	0,816454132
ATF3	0,823814064
LGALS3	0,830816468
ABHD4	0,832787057
CHRNB1	0,84768966
FDXR	0,850291947
HMCES	0,851230807
TBC1D17	0,857495232
PITRM1	0,87425056
FBXO44	0,876883032
CD83	0,901424804
RN7SK	0,903248363
ISCU	0,9056246
PHLDA3	0,907688788
SOCS1	0,908678614
CHDH	0,911694008
ASRGL1	0,91517423
KLK1	0,921746687
CTTN	0,922670371
YPEL3	0,935515301
STARD10	0,95129929
RTN2	0,955289226
TUBB2A	0,957732164
PIM2	0,96023619
HHAT	0,986226803
ENDOV	1,0039E+13
TMEM25	1,15974E+13
PLXNB1	1,23626E+13
CAB39L	1,24806E+13
CNR1	1,26652E+13
B3GALT4	1,28699E+13
B3GNT9	1,29385E+13

HECW2	1,36148E+13
PLTP	1,37574E+13
ANXA1	1,82192E+13
BCAS1	2,05096E+13
SLC32A1	2,44528E+13
ZNF503	2,44947E+13
STEAP2	2,63505E+13
MSRB3	2,79704E+13
SNPH	2,90132E+13
ESPN	4,39682E+13
SDPR	6,64161E+13
AOC1	1,00279E+14
QPRT	1,0091E+14
ASTN2	1,02234E+14
KIAA1217	1,04637E+14
GABARAPL1	1,08344E+14
MYL5	1,10241E+14
ST3GAL6	1,11665E+14
PKIG	1,13491E+14
SULF2	1,13669E+14
MAP3K12	1,14642E+14
SYNPO	1,15293E+14
CLECL1	1,16775E+14
TNFSF4	1,16906E+14
LACC1	1,17266E+14
PMS2P5	1,18248E+14
SDCBP2-AS1	1,20721E+14
EVA1B	1,22118E+14
SHF	1,22868E+14
GAMT	1,24572E+14
SCAMP1-AS1	1,26357E+14
SPATA20	1,28518E+14
NTRK2	1,296E+14
APOL1	1,3035E+14
GPR15	1,32007E+14
WNT10A	1,32471E+14
LINC00936	1,35197E+14
ETV7	1,37009E+14
CLIP3	1,37178E+14
ABCA3	1,37198E+14
TMEM140	1,38226E+14
TK2	1,39383E+14
KLHL6	1,39405E+14
CCR7	1,42287E+14
CKB	1,4235E+14
GAL3ST4	1,43763E+14
GUCY1A3	1,44927E+14

XXYLT1-AS2	1,45229E+14
ADAM19	1,47516E+14
S100A4	1,49702E+14
SLC7A7	1,53637E+14
ZNF880	1,53871E+14
PERP	1,5482E+14
DOK4	1,57577E+14
ST3GAL6-AS1	1,58159E+14
IGFBP4	1,58517E+14
FAM46A	1,58799E+14
CHST6	1,59808E+14
GAREML	1,60466E+14
MOXD1	1,62391E+14
MT2A	1,6443E+14
CDKN2A	1,64929E+14
PLK2	1,65587E+14
CSPG4	1,6677E+14
LNX1	1,6804E+14
F2R	1,70841E+14
LTBR	1,72081E+14
MAB21L3	1,73492E+14
TTC22	1,74416E+14
ABCA9	1,7489E+14
CYP1B1	1,75789E+14
ELF3	1,79125E+14
LIPH	1,81358E+14
MAL	1,83069E+14
RRAD	1,859E+14
EMX1	1,91103E+14
HCN2	1,92528E+14
SPINT2	1,96425E+14
EPHA2	1,97373E+14
HES2	1,98092E+14
SERPINB1	1,99894E+14
ENPP2	2,0518E+14
GLIS3	2,05922E+14
TLN2	2,08662E+14
CLEC2B	2,09397E+14
OSBPL6	2,1087E+14
TCN2	2,12553E+14
C10orf10	2,14355E+14
CYSLTR2	2,15994E+14
PDE6G	2,1643E+14
STEAP1	2,1927E+14
CXCR5	2,19998E+14
JUP	2,27343E+14
C20orf194	2,28079E+14

EPHB1	2,28595E+14
TIGIT	2,28694E+14
SERPINB10	2,29404E+14
ITGAM	2,354E+14
EDN1	2,36738E+14
IFNG	2,37152E+14
LOC100190986	2,37491E+14
LAG3	2,38014E+14
PLEKHG6	2,39778E+14
TNFRSF4	2,41079E+14
MUC13	2,4137E+14
NAALADL1	2,44462E+14
MAP7D2	2,52512E+14
ABCA12	2,52872E+14
ST14	2,58061E+14
GTF2IRD2	2,59027E+14
SYTL2	2,59253E+14
ZNF578	2,59406E+14
HLA-DQA2	2,5996E+14
ADGRA3	2,63012E+14
DLGAP1	2,63472E+14
LINC00176	2,6573E+14
ANO3	2,67899E+14
DDR2	2,69253E+14
RUSC2	2,69692E+14
SEPP1	2,82432E+14
CACNB2	2,8313E+14
POU4F1	2,84463E+14
FAM167B	2,86236E+14
PCDHGB5	2,88506E+14
CALD1	2,88992E+14
DTHD1	2,90801E+14
OR2T3	2,90935E+14
MOCS1	2,91326E+14
PLCL1	2,96139E+14
HOMER3	3,02053E+14
LINC01150	3,02983E+14
RYR3	3,04053E+14
PHEX	3,06481E+14
LINC01258	3,16131E+14
PRODH	3,16626E+14
HPCAL4	3,16888E+14
LOC101930010	3,24743E+14
AMBP	3,26739E+14
NINL	3,27754E+14
LINC00987	3,30934E+14
SLIT1	3,35207E+14

ASPA	3,40634E+14
SLC4A4	3,45134E+14
HHLA2	3,52924E+14
CREB3L3	3,58671E+14
NAP1L3	3,67292E+14
LINC01320	3,68264E+14
POMC	3,76991E+14
LOC730102	3,91074E+14
LHFPL3-AS2	3,97057E+14
LRRN3	3,98183E+14
WFDC2	4,00476E+14
WNT7B	4,07489E+14
CPA4	4,34219E+14
MIR4507	4,51656E+14
LINC00689	5,20609E+14
KIF17	5,30967E+14
THEMIS	5,3812E+14
CX3CL1	5,49747E+14
OR5H6	6,2858E+14
CLEC4C	6,33978E+14
ACTN3	6,88642E+14

Supplementary Table 9. Dysregulated genes (both downregulated and upregulated) identified upon comparison of ataluren EP1-treated cells versus untreated controls.

Down-regulated

Gene	log2FoldChange2
MIR4785	-6,3E+14
LOC283440	-5,7E+14
SNORD18B	-5,4E+14
LDB2	-5,2E+14
EFCAB9	-5E+14
C1orf189	-5E+14
CASC19	-5E+14
PDCD1	-4,8E+14
LOC101929473	-4,8E+14
LOC102723517	-4,8E+14
ABCG1	-3,1E+14
CXCR2P1	-2,9E+14
RBM5-AS1	-2,9E+14
KCNQ5-IT1	-2,8E+14
CCL3L1	-2,7E+14
LST1	-2,5E+14
INSM1	-2,4E+14
LOC100130872	-2,4E+14
XCL1	-2,2E+14
CYP51A1-AS1	-2,1E+14
SREBF1	-2,1E+14
OLMALINC	-2E+14
C1orf228	-2E+14
PTGER2	-2E+14
RUFY4	-1,9E+14
LINC01176	-1,9E+14
PIPOX	-1,9E+14
ULBP2	-1,8E+14
MIR6774	-1,8E+14
TAS2R4	-1,8E+14
MIR4517	-1,7E+14
SCD	-1,7E+14
NPW	-1,7E+14
PNPLA3	-1,7E+14
LOC100506801	-1,6E+14
MST1P2	-1,6E+14
TMEM191B	-1,6E+14
GRAMD1B	-1,6E+14
KLHL29	-1,6E+14
LOC100506457	-1,5E+14

TSNAXIP1	-1,5E+14
SCML1	-1,5E+14
SNORD14D	-1,5E+14
EDN1	-1,5E+14
KCNA1	-1,5E+14
LOC102724596	-1,4E+14
GPR84	-1,4E+14
EGR3	-1,4E+14
SETBP1	-1,4E+14
SLC29A2	-1,4E+14
PDGFA	-1,4E+14
LOC646471	-1,4E+14
HOXB9	-1,4E+14
LINC01126	-1,4E+14
DHRS9	-1,4E+14
THY1	-1,4E+14
AK1	-1,4E+14
SNHG25	-1,3E+14
PCYT1B	-1,3E+14
TPTE2P5	-1,3E+14
HES6	-1,2E+14
ZBED3-AS1	-1,2E+14
HIST4H4	-1,2E+14
ALDH8A1	-1,2E+14
SPON2	-1,2E+14
PCSK4	-1,2E+14
CD4	-1,2E+14
FAM129C	-1,2E+14
SEMA6C	-1,2E+14
RAB33A	-1,2E+14
CHRNA10	-1,2E+14
LINC00106	-1,2E+14
SSSCA1-AS1	-1,2E+14
LINC00504	-1,2E+14
CFAP46	-1,2E+14
DLGAP4-AS1	-1,1E+14
LOC105377348	-1,1E+14
MYO1F	-1,1E+14
C1QTNF6	-1,1E+14
AK4	-1,1E+14
FCRL5	-1,1E+14
CCDC24	-1,1E+14
TMEM145	-1,1E+14
EFEMP2	-1,1E+14
NPIPB15	-1,1E+14
BMPR1A	-1,1E+14

SMPDL3B	-1,1E+14
FCRL3	-1,1E+14
MC1R	-1,1E+14
NRARP	-1,1E+14
PLAUR	-1,1E+14
MIR34A	-1,1E+14
MOK	-1,1E+14
GATA3-AS1	-1,1E+14
PLEKHG6	-1,1E+14
SYT17	-1,1E+14
NPHP1	-1,1E+14
WHAMMP1	-1,1E+14
SNAI3-AS1	-1E+14
SNHG19	-1E+14
HCN3	-1E+14
CCDC74A	-1E+14
FBXL8	-1E+14
IL13RA1	-1E+14
NPFF	-1E+14
CFHR4	-5E+13
C11orf91	-5E+13
LOC100130417	-4,9E+13
H1FX-AS1	-2,5E+13
LOC103908605	-2,2E+13
ZDHHC1	-1,8E+13
SNORA63	-1,5E+13
GALM	-1,3E+13
LINC00957	-1,2E+13
FSCN2	-1,2E+13
RIMKLB	-1,1E+13
NPPA-AS1	-1,1E+13
ACSS2	-1,1E+13
HIST1H1E	-1E+13
AK7	-1E+13
LOC401557	-5,1E+12
GRIN1	-1,6E+12
NR4A1	-1,2E+12
PALD1	-1,2E+12
ANKRD6	-0,99729
BMS1P5	-0,99588
TMEM198	-0,99401
KLHDC1	-0,98807
CLCN6	-0,98612
TTLL3	-0,98312
PFKFB4	-0,98254
C5AR1	-0,98082

LINC01311	-0,98021
GUCA1B	-0,97816
TMEM9B-AS1	-0,97179
EPHB2	-0,97155
ACAD11	-0,96445
MFSD2A	-0,96381
CPNE7	-0,96024
MIR4292	-0,95737
ARHGAP24	-0,9571
GEM	-0,95511
MIR3064	-0,95479
URB1-AS1	-0,94771
CD69	-0,94597
LBHD1	-0,94098
SNORD104	-0,94009
FER1L4	-0,93252
SNORD2	-0,92929
KIF6	-0,92884
KIAA0226L	-0,92837
GABBR1	-0,92188
TUBB3	-0,91684
RBMS1	-0,90975
LOC100270804	-0,90964
MIR1914	-0,90543
LOC644656	-0,9044
ARHGAP39	-0,89967
ANKRD24	-0,8973
RARG	-0,89269
TSPAN32	-0,88891
TPBG	-0,88889
ETV7	-0,88784
PAN3-AS1	-0,88729
RGS3	-0,88634
MYCBPAP	-0,88533
SPTBN5	-0,87613
WHAMMP3	-0,87531
GIPR	-0,87079
TMEM44-AS1	-0,8686
RHOV	-0,86688
TMEM150A	-0,86478
COL4A3	-0,86319
DUOX1	-0,85959
MST1R	-0,85922
HAPLN3	-0,85667
TGM1	-0,85361
LOC101927740	-0,84712

INTS6-AS1	-0,83914
RGS6	-0,83764
PRICKLE4	-0,8357
ZNRD1-AS1	-0,82704
BTNL9	-0,82687
CTC-338M12,4	-0,81819
ZBTB10	-0,81789
ANKRD13B	-0,81415
LINC00494	-0,81186
TMEM136	-0,80692
PROCA1	-0,80676
RPSAP9	-0,80364
MIR22HG	-0,80029
KIAA1875	-0,79802
CELF6	-0,78288
CCNI2	-0,78074
C8orf44	-0,77889
DBNDD1	-0,77699
MNDA	-0,77404
SNHG9	-0,77401
COL9A2	-0,76887
ICAM5	-0,76836
IDUA	-0,76762
FAM53A	-0,76638
PPP1R32	-0,76413
DHRS2	-0,76394
HSD17B7	-0,7619
SLCO4C1	-0,7615
CORO1B	-0,76017
HAGHL	-0,75547
SLC26A11	-0,75382
ZSWIM6	-0,75323
LZTFL1	-0,74866
PLEKHG1	-0,74704
ARRDC3-AS1	-0,74251
SNORD58C	-0,74235
CBLN3	-0,7399
C14orf79	-0,73896
CREB5	-0,73833
WBP1	-0,73111
CD72	-0,72962
TUBB2B	-0,72893
GOLGA6L10	-0,72862
ZC3H12C	-0,72626
C19orf71	-0,72413
QRICH2	-0,72072

AMY2B	-0,7198
TCEB3-AS1	-0,71901
RPARP-AS1	-0,71639
AMT	-0,7148
APTR	-0,71328
TNFAIP2	-0,71192
TFAP2A-AS1	-0,70991
CAPN3	-0,70807
BCORP1	-0,70455
SERPINB1	-0,7016
NLGN2	-0,69965
LMO2	-0,69948
GSTM2	-0,69706
MAP3K14-AS1	-0,69482
MXI1	-0,69435
MORN2	-0,6943
RPL36A	-0,69316
LOC102724814	-0,69173
NPDC1	-0,69137
PRR7	-0,69006
ZNF846	-0,68737
NPIPA1	-0,68463
C16orf93	-0,68444
RTKN	-0,68013
PATL2	-0,67845
SAP25	-0,67624
ASMTL-AS1	-0,67192
LOC100506127	-0,66885
CD40	-0,66871
SENP8	-0,66619
LINC01138	-0,66502
ST20	-0,66477
CBWD3	-0,66181
C12orf77	-0,66163
SNHG11	-0,65937
KCNC4	-0,65892
C12orf79	-0,65823
PRORSD1P	-0,65396
PAQR6	-0,65359
NT5M	-0,6488
NPHP3	-0,64747
MZF1-AS1	-0,64283
FSTL3	-0,64214
SPAG4	-0,64206
NFYC-AS1	-0,64023
RDH14	-0,63985

PPT2	-0,63955
IFT20	-0,63786
RAB11B-AS1	-0,63675
HIST1H3E	-0,6361
DNHD1	-0,63609
SRI	-0,63403
TSPO	-0,63201
MFSD10	-0,62945
IDH1	-0,6285
MERTK	-0,6279
SNHG10	-0,62502
LINC01089	-0,62321
CD200R1	-0,6228
GPR89B	-0,62075
ANKDD1A	-0,61754
PTK2	-0,61501
ELMO3	-0,61495
LOC100049716	-0,61471
MYH3	-0,61289
DLL1	-0,6127
ODF3B	-0,61263
TNFRSF9	-0,61223
LINC01004	-0,6109
SMG1P7	-0,60983
THBS3	-0,6091
CROCCP3	-0,60705
NSDHL	-0,60642
STK19	-0,60613
PAX6	-0,60461
LOC100506258	-0,60113
ANKHD1	-0,60083
ALOX12P2	-0,6007
LINC01534	-0,60057
SLC2A6	-0,60057
THEMIS2	-0,59979
EMILIN2	-0,59624
LONRF1	-0,59564
L3HYPDH	-0,59401
LRRC26	-0,59276
PPP1R3E	-0,59095
RAD51-AS1	-0,58957
SORBS3	-0,58939
CRIP1	-0,58718
SFN	-0,58449
PCYT2	-0,58336
ARRDC1	-0,58222

RABGGTB	-0,58114
LOC101929709	-0,58018
CTTN	-0,57873
FAHD2CP	-0,57857
LOC728323	-0,57816
SCAMP1-AS1	-0,57508
RRAGD	-0,57482
LINC00674	-0,57101
LYSMD4	-0,57071
ZNF529-AS1	-0,56933
PTOV1-AS2	-0,56909
RPL32P3	-0,56704
PPM1K	-0,56684
PLEKHM1P	-0,56605
COL11A2	-0,5654
DND1	-0,56511
SQLE	-0,56496
WRAP73	-0,56465
BOLA1	-0,56415
FBXL15	-0,56395
C2orf76	-0,56339
NPIPA5	-0,56313
TCF7	-0,56257
LINC01160	-0,56248
PCBP1-AS1	-0,56241
NFKBIA	-0,56155
RPH3AL	-0,56068
TPCN2	-0,56014
LOC102606465	-0,55911
CIB1	-0,55892
MPST	-0,55825
DDX26B	-0,55825
PARGP1	-0,55771
DBI	-0,55716
ANKRD16	-0,55673
LOC100128398	-0,55648
FAM216A	-0,55354
ZGLP1	-0,55289
CEBPB	-0,55272
ZFYVE19	-0,55264
LOC728613	-0,55243
LOC729737	-0,55179
MAPKAPK5-AS1	-0,55086
LOC100507006	-0,55064
MAMDC4	-0,5505
ENTPD2	-0,55016

SEMA4C	-0,54789
TRIP10	-0,54642
DPM3	-0,54604
RPL23AP82	-0,54495
CLCF1	-0,54448
IER2	-0,53554
TRIM52	-0,53508
LTB4R2	-0,53347
MAPK11	-0,53254
STARD4	-0,53101
GTF2IP20	-0,52954
SNHG4	-0,5253
SLC26A6	-0,52415
SUZ12P1	-0,52394
MIR142	-0,52365
LOC155060	-0,52227
ABCA2	-0,52164
PDXDC2P	-0,52056
SLC27A1	-0,51812
SUSD3	-0,51713
SPATA24	-0,51702
ARHGEF17	-0,51617
MMP25-AS1	-0,51604
LHX4-AS1	-0,51542
HMGCR	-0,51524
CCDC120	-0,51334
RNF215	-0,51315
EHD1	-0,51284
PIK3AP1	-0,51275
TNF	-0,51153
RRN3P1	-0,51032
ZFP3	-0,5093
SPSB3	-0,50822
TPT1-AS1	-0,50821
NFKB2	-0,50727
SLC50A1	-0,50571
SEC61A2	-0,50564
PIGBOS1	-0,50532
RASSF4	-0,50491
AGAP9	-0,50445
ACHE	-0,50417
PIK3IP1	-0,50391
TOPORS-AS1	-0,5014
SNORA40	-0,50108
ALOX12-AS1	-0,50102
TMEM129	-0,50045

ZSCAN16-AS1	-0,49951
C2orf81	-0,49892
MAP3K8	-0,49862
TNFRSF14	-0,49767
SLC29A3	-0,49731
CCDC136	-0,49703
RSAD2	-0,49683
IFNGR1	-0,49671
FBXO6	-0,49576
GLUD1P3	-0,49545
MKNK2	-0,49542
AGER	-0,49333
DUSP10	-0,49105
FBXL19-AS1	-0,49083
CSF1	-0,49046
PIM3	-0,48934
PHYKPL	-0,48926
LRRC27	-0,48839
EPHB4	-0,48643
NPR2	-0,4864
TRPV1	-0,48628
RPL17	-0,48419
RRN3P2	-0,48239
UPB1	-0,48192
NFKBIE	-0,48187
IL4R	-0,48099
OVCA2	-0,48097
LRMP	-0,48003
TMEM161B-AS1	-0,47972
MIR17HG	-0,47912
TMEM80	-0,47838
UNC119	-0,47592
VPS9D1	-0,47514
LGALS3	-0,4749
DMPK	-0,47479
S100A6	-0,47433
KCTD13	-0,47385
P2RX5	-0,47177
GPR75	-0,47114
STX1A	-0,47032
LMBR1L	-0,46976
ABTB2	-0,46974
ZBTB32	-0,46944
CSTB	-0,46832
EMID1	-0,46769
IFI44L	-0,46747

ZNF222	-0,46722
MAFIP	-0,46695
SNHG7	-0,46516
TRADD	-0,46426
CASC10	-0,46255
ATAT1	-0,46229
LINC00493	-0,46225
ATG16L2	-0,46143
CLIC4	-0,46046
SIAH2	-0,46034
PSMG3	-0,45952
ZNF593	-0,4582
ADAT2	-0,45793
ERV3-1	-0,45708
LUC7L	-0,45456
RAB11FIP1	-0,45332
ID2	-0,45292
IFITM1	-0,45223
DKFZP434I0714	-0,45176
HLA-L	-0,4517
HERC2P9	-0,45063
TARBP1	-0,45062
NBR2	-0,45048
C15orf40	-0,44945
SRGN	-0,44785
ADAP1	-0,44703
TP53I13	-0,44573
MAP4K3	-0,4443
PMS2P3	-0,44409
IL6R	-0,4438
C11orf71	-0,44335
MIR3916	-0,44334
FBXW9	-0,44265
TNFAIP3	-0,44259
DVL1	-0,4421
GRAMD1A	-0,44166
MICA	-0,44103
POR	-0,43983
TNFRSF13C	-0,43946
HOOK2	-0,43894
LYSMD2	-0,43842
MCOLN2	-0,43841
DGKQ	-0,43836
COMMD3	-0,43782
GGA1	-0,43777
ARRDC1-AS1	-0,43774

DEXI	-0,43772
KPTN	-0,43744
ABCA10	-0,43736
TMEM55B	-0,43714
SH3BP2	-0,43707
METTL22	-0,43604
TCTN1	-0,43541
DPP7	-0,43345
NUPL2	-0,43266
PGBD2	-0,43192
IFIT2	-0,4312
C5orf45	-0,4302
PCGF1	-0,4301
ANKZF1	-0,42956
IRX6	-0,42722
PLXNA3	-0,42588
ARID5A	-0,42519
ERO1B	-0,42504
PHC1	-0,4247
TESK2	-0,42468
EBI3	-0,4238
LIN37	-0,42371
PPIEL	-0,42369
OSBPL7	-0,42348
HOXB3	-0,42317
PGBD4	-0,42285
TSPAN15	-0,42281
DNAAF2	-0,42249
FKBP14	-0,42103
SNHG15	-0,41992
PDE6D	-0,41928
PTRH2	-0,4182
FAM73B	-0,41737
GRHPR	-0,41722
CD58	-0,41675
PLD2	-0,41674
ZC3H12A	-0,41649
WASH7P	-0,41638
C19orf66	-0,41596
ANKRD23	-0,41591
VIMP	-0,4148
CD46	-0,41464
NECAB3	-0,41251
NSMF	-0,41196
EBP	-0,41149
LINC-PINT	-0,41094

ELP5	-0,41087
DHRS1	-0,41082
NPRL2	-0,41068
PPP1R12C	-0,41053
CTSZ	-0,41016
NAT14	-0,40799
PLXNB1	-0,40751
RSAD1	-0,40742
LOC441242	-0,40736
C9orf72	-0,40732
ATP6AP1L	-0,40359
VAMP5	-0,40336
ZNF446	-0,4031
C21orf91	-0,40278
RFNG	-0,40249
ARHGAP33	-0,40241
BISPR	-0,40228
TMSB10	-0,40202
PSMG4	-0,40187
RTN2	-0,40141
TFAP2A	-0,401
OSGEPL1	-0,4009
GUSBP1	-0,40027
SYNGAP1	-0,40009
DPY19L2P2	-0,3999
SS18L2	-0,39963
ABCA7	-0,39699
DENND3	-0,395
LZTR1	-0,39425
KLC4	-0,39415
CDKN2A	-0,39336
DYNC2LI1	-0,39315
INAFM2	-0,39197
COA5	-0,39178
FAM173A	-0,39139
SS18L1	-0,39116
NAT9	-0,39043
ALPK1	-0,38891
HNRNPU-AS1	-0,38863
CYTH2	-0,38861
YPEL3	-0,38846
DUS4L	-0,3876
FASTKD3	-0,38666
UAP1L1	-0,38598
SNHG5	-0,38545
TRIB3	-0,38505

KDM5D	-0,38392
RRAGB	-0,38321
DUSP11	-0,38142
TMEM243	-0,38071
ZNF839	-0,38051
ISG20	-0,37991
EIF1	-0,37987
KIAA1407	-0,37922
BTN2A2	-0,3788
VMAC	-0,37865
CCDC92	-0,37848
TMEM63B	-0,37732
HDHD3	-0,37716
MIF-AS1	-0,37683
TSNARE1	-0,37588
LOC440434	-0,37585
FAM60A	-0,37562
ECHDC2	-0,37552
WDR19	-0,37526
COQ10A	-0,37498
MED7	-0,37484
LINS	-0,37472
SUPT7L	-0,37427
PPP4R1L	-0,37411
FAM89B	-0,37399
NR2C1	-0,37371
RRAS	-0,37333
STAG3L4	-0,37281
NFKBID	-0,37235
CALCOCO1	-0,37019
TAGLN	-0,36962
WASH1	-0,36938
ERMARD	-0,36858
HTRA2	-0,36822
LOC100507195	-0,3677
BSDC1	-0,36668
CCNG2	-0,36564
QPCTL	-0,36554
ACTR1B	-0,36532
PKD1P6	-0,36484
FASTK	-0,36462
HSH2D	-0,3645
TMEM216	-0,36398
FADS3	-0,36385
TAZ	-0,36339
C6orf1	-0,36259

GPR137B	-0,36222
NUMBL	-0,36163
CLK2	-0,36149
P4HTM	-0,3611
USP18	-0,36026
DHX58	-0,36026
PCMTD2	-0,35915
FLYWCH2	-0,35909
EZH1	-0,35817
ELMOD3	-0,35771
NCBP2-AS2	-0,35753
IFT140	-0,35742
FAM195B	-0,35676
MAPKBP1	-0,35672
TRIM41	-0,35529
ENDOG	-0,35526
DCUN1D2	-0,35486
XPNPEP1	-0,35455
ORMDL1	-0,35422
TMEM175	-0,35402
HIST1H2AC	-0,35372
LRP8	-0,35361
SLC25A37	-0,35319
CD22	-0,35275
TYMP	-0,35248
SFI1	-0,35246
LAT2	-0,35168
SH3YL1	-0,35162
P2RX4	-0,34995
AFMID	-0,34984
ZDHHC8	-0,34892
FLOT1	-0,34878
POP5	-0,34826
N4BP2L2	-0,34773
ago-04	-0,34734
CYP4V2	-0,34697
PPAPDC1B	-0,34627
SLC12A9	-0,34624
WDR5B	-0,34576
PEX16	-0,34533
DDX5	-0,34518
NADSYN1	-0,34495
REC8	-0,34479
MAT2A	-0,34468
STARD3NL	-0,34431
FBXO44	-0,34428

HSBP1	-0,34398
C9orf142	-0,34396
GALE	-0,34393
ZFC3H1	-0,34336
CD80	-0,34228
CYB5A	-0,34145
STAT6	-0,34107
NOP10	-0,34103
NUDT16L1	-0,34076
RANGRF	-0,34055
LINC01215	-0,33959
BCS1L	-0,33916
GBA2	-0,33906
CD274	-0,33881
HMG20B	-0,33809
LHX2	-0,3379
POLM	-0,33783
UTP6	-0,33727
PDCD5	-0,33719
PGS1	-0,33716
LINC00623	-0,33697
FANCL	-0,33675
TJAP1	-0,33635
OFD1	-0,33593
ACSF2	-0,33573
ZNRD1	-0,33555
CCDC142	-0,33545
PAX8-AS1	-0,33533
COX10-AS1	-0,33453
RPL22L1	-0,33412
TRMT10B	-0,33341
FAHD2A	-0,33226
UBL5	-0,33224
CCDC85B	-0,33071
RPL39	-0,33054
ANKRD13D	-0,33035
LRSAM1	-0,33017
ZNF75D	-0,33016
OXLD1	-0,32945
ZNF251	-0,32936
LAMTOR2	-0,32899
ACAP3	-0,32883
C19orf60	-0,32687
KAT2A	-0,32684
ZNF581	-0,32653
WASH3P	-0,32646

SLAMF1	-0,32595
RBM48	-0,32593
PTS	-0,32559
MAP3K10	-0,32454
MARCH9	-0,32378
ZFAS1	-0,3236
TIMM23B	-0,32341
RNF170	-0,32273
ACYP1	-0,32251
SGTB	-0,32166
RAB40C	-0,32122
CHMP5	-0,32114
ZBTB26	-0,32092
NBPF8	-0,32008
IKBKE	-0,31991
WDR91	-0,31972
ARFIP2	-0,31955
ARNTL	-0,31842
NR6A1	-0,31822
RRN3P3	-0,31819
MPG	-0,31748
CCDC159	-0,3171
ANKRD10	-0,31689
CBWD5	-0,31657
CCDC14	-0,31637
NBPF11	-0,31637
IP6K2	-0,31527
PSMA3-AS1	-0,31504
UGCG	-0,31492
N4BP2L1	-0,31434
PI4KAP2	-0,31411
TUBE1	-0,31402
EMC6	-0,31375
DALRD3	-0,31348
PARP6	-0,31336
NIT1	-0,31321
SELO	-0,31311
TRAF4	-0,31277
BTAF1	-0,31275
TRMT61B	-0,3126
C11orf49	-0,31259
WDR45	-0,31211
MRPL14	-0,31095
BTN2A1	-0,31089
RPL36	-0,31058
PLSCR1	-0,3098

PLEKHF2	-0,30947
MRPL33	-0,30942
MXD4	-0,30867
NEK8	-0,30862
CHPT1	-0,3086
DIMT1	-0,30848
MPLKIP	-0,30797
TBCK	-0,30502
ALKBH6	-0,30473
ZNF83	-0,30343
FBXO9	-0,3028
GEMIN7	-0,30257
IFI44	-0,30185
LINC00909	-0,30181
ARL16	-0,30179
QTRT1	-0,30161
MAGEF1	-0,3016
CCDC84	-0,3015
USMG5	-0,30112
FCHSD1	-0,30094
TMEM43	-0,30082
ALKBH7	-0,30066
C17orf75	-0,30021
ABCC10	-0,30002
RHOQ	-0,30002
C21orf59	-0,29898
AKTIP	-0,29874
SNRPD2	-0,29841
ISG15	-0,29716
DNAJC19	-0,29654
SRSF5	-0,29634
ANAPC10	-0,29561
AP4M1	-0,29531
RPL35	-0,29522
TIMM8B	-0,29485
CRYBB2P1	-0,29457
MRPS21	-0,2944
MICAL1	-0,29393
RIC8B	-0,2937
RRP7BP	-0,2936
RBX1	-0,29329
MKS1	-0,2929
MED30	-0,29283
RAB11FIP3	-0,29281
ZNF226	-0,29199
CLSTN3	-0,29144

APBA3	-0,29108
FNBP4	-0,29088
GSKIP	-0,29054
C16orf13	-0,29048
CDK7	-0,29048
DFFB	-0,29017
C21orf33	-0,28979
SPATA20	-0,28964
GSTK1	-0,2892
TMEM134	-0,28897
TMEM161A	-0,28873
ASB16-AS1	-0,2887
RBCK1	-0,28862
ARV1	-0,28856
ZNF428	-0,28845
LINC00094	-0,28831
BBS2	-0,28812
SAT2	-0,28672
DNAJB9	-0,28596
APIP	-0,28578
TRABD	-0,28577
AFG3L1P	-0,28515
AKR1A1	-0,28496
PPP3CC	-0,28483
IKBKB	-0,28432
ANKLE1	-0,28419
AUP1	-0,28414
ATP6V1F	-0,28401
ZNF639	-0,28393
GABARAPL2	-0,28362
DUSP12	-0,2836
PRKAB2	-0,2834
VCPKMT	-0,28333
ZNF558	-0,28293
UBE2B	-0,28288
MYO19	-0,28261
TMEM205	-0,28257
IRF7	-0,28182
TSPAN31	-0,28084
ORAOV1	-0,28002
ATP8B2	-0,27966
CREBZF	-0,27917
UBXN11	-0,27881
ZNF783	-0,27858
C1orf27	-0,2785
DTX3	-0,27811

WDR59	-0,27749
POLR2L	-0,2772
TMEM161B	-0,27717
SNAPC4	-0,27672
PIGQ	-0,27619
HIP1R	-0,27595
CSNK1G2	-0,27533
QSOX2	-0,27491
E4F1	-0,2743
ATP5J2	-0,27414
C8orf59	-0,27399
GAS5	-0,27388
PTRHD1	-0,27374
CAPRIN2	-0,27373
NIPAL2	-0,27306
DCAKD	-0,27276
AKAP17A	-0,2726
PPCS	-0,27253
TRMT2A	-0,27184
TRAF5	-0,27166
TRMU	-0,27071
TOP1MT	-0,27032
BIN2	-0,26995
GTPBP2	-0,26901
C9orf16	-0,26893
ADAM8	-0,26796
ZNF500	-0,26753
FAM58A	-0,267
LINC00938	-0,26698
ZNF589	-0,2668
SDCCAG3	-0,26661
STX2	-0,26607
DHPS	-0,26606
C2orf47	-0,26591
IL17RB	-0,26536
DDX17	-0,26493
SPG7	-0,26471
DXO	-0,26466
NXF1	-0,26436
IRF9	-0,26426
POLL	-0,2641
ISL2	-0,26372
UCKL1	-0,2636
MUS81	-0,26342
C19orf25	-0,26312
MRPL54	-0,26293

GFOD2	-0,26272
ADCK4	-0,26255
ARHGEF1	-0,26251
NSUN5	-0,26244
OAZ2	-0,26115
HOXB4	-0,26054
LARP1B	-0,26027
PAN2	-0,25996
TBRG1	-0,25929
CASZ1	-0,25913
SDCBP	-0,2584
C19orf24	-0,25838
ANKRD49	-0,25701
SLC25A28	-0,25636
MIEN1	-0,25584
P3H1	-0,2555
NT5C	-0,2551
UGGT2	-0,2549
DCAF8	-0,25486
TRIT1	-0,25436
MOAP1	-0,25405
TAF10	-0,25373
NPHP4	-0,25346
RPL29	-0,25285
TBCC	-0,2528
TMEM120A	-0,2525
PSMB8-AS1	-0,25247
USP45	-0,25239
CBWD2	-0,25237
LTBP4	-0,25227
UNC50	-0,25099
JRKL	-0,25086
MPV17	-0,25045
IRF3	-0,24985
RPL38	-0,24943
ZNF600	-0,24927
SIN3B	-0,24892
RPGRIP1L	-0,24853
EXOSC5	-0,24837
LRRC14	-0,24806
CCDC66	-0,24771
RBM5	-0,24743
CHMP1B	-0,24718
C5orf24	-0,24683
MIB2	-0,24674
PIKFYVE	-0,2465

ZNF655	-0,24572
PRPSAP2	-0,24562
CCDC88B	-0,24523
KRCC1	-0,24514
POMGNT1	-0,24502
KIAA0141	-0,24477
THOP1	-0,24456
OCIAD2	-0,24442
CNTNAP1	-0,24393
RPS18	-0,24392
ALG13	-0,2438
AP1G2	-0,24374
MTG1	-0,24337
RPL31	-0,24262
LYPLAL1	-0,24205
ZNF580	-0,24167
CCNDBP1	-0,24154
TBCB	-0,24153
FKBP3	-0,24149
RBM6	-0,24114
ZBED5	-0,24098
IFFO1	-0,24057
TAF11	-0,24023
GLT8D1	-0,24017
LSM7	-0,23909
KATNB1	-0,23903
PLEKHJ1	-0,23888
SSSCA1	-0,23855
NXT1	-0,23847
POLR2I	-0,23842
SLC25A29	-0,23811
EBLN3	-0,23805
XAF1	-0,238
SH3GLB2	-0,23752
COMMD6	-0,23739
PNPLA2	-0,23661
ILKAP	-0,23659
RAB11FIP2	-0,23628
RAB24	-0,23597
FLAD1	-0,23592
POLD4	-0,23589
CD48	-0,23531
NECAP1	-0,23524
TOP3B	-0,2342
ATAD3B	-0,23419
ZRANB2	-0,23281

STK25	-0,23233
GRAP	-0,23214
GTPBP3	-0,23206
RPL32	-0,23198
RPL18A	-0,23191
C19orf53	-0,2315
ZNHIT1	-0,23125
VPS28	-0,23111
NUDT22	-0,23074
PAXBP1	-0,23069
PFDN5	-0,2293
ZNF76	-0,22919
ZNF830	-0,22879
ZNF512B	-0,22853
CHCHD7	-0,22784
RCCD1	-0,22763
DMAP1	-0,22696
CLCN7	-0,22679
DGUOK	-0,22654
PNKP	-0,22598
IQCB1	-0,22562
DHX34	-0,22538
TOMM6	-0,22533
ACTR10	-0,22507
NDUFAF7	-0,2246
INTS3	-0,22439
IFI6	-0,22422
ULK1	-0,22371
RXRB	-0,2237
TNFRSF10B	-0,22353
MRPL43	-0,22349
TXNDC9	-0,2233
PLK3	-0,22327
MRPS25	-0,22237
SNX22	-0,22148
RNF19A	-0,22122
NGRN	-0,22107
RPL37	-0,22082
SNHG16	-0,22021
VMP1	-0,21982
ATP6V1E1	-0,21944
ACAA1	-0,21914
CISD2	-0,21815
PRPF39	-0,21799
GNL3	-0,21722
MTERF3	-0,21711

CHFR	-0,21687
CD70	-0,21568
MAP3K13	-0,21528
C19orf48	-0,21498
RPL41	-0,21442
ABCC5	-0,21439
SHARPIN	-0,21265
STX8	-0,21252
GPR108	-0,21201
TAF7	-0,20999
COPS7B	-0,20942
CD19	-0,20911
DRG2	-0,20542
ATG4B	-0,20529
COX6B1	-0,20454
RPL12	-0,20433
PHF11	-0,20408
HAX1	-0,20222
CPNE1	-0,20155
LINC00667	-0,20056
COX7A2	-0,20038
ATG16L1	-0,20004
OAZ1	-0,19943
RPS21	-0,19919
WDR11	-0,19849
EMC4	-0,19717
PPIA	-0,19706
IGSF8	-0,19573
JAK3	-0,19485
TKFC	-0,19457
RNF126	-0,19455
ZBTB40	-0,19424
NDUFB7	-0,19386
EXOSC9	-0,19298
PPP1R21	-0,19115
WDR74	-0,19044
CHD1L	-0,18931
DYNLL1	-0,18841
MRPL38	-0,18786
RBM39	-0,18772
MTERF4	-0,18644
THOC1	-0,18412
ARHGAP4	-0,18309
PPP6R2	-0,18147
C7orf73	-0,18094
LIG4	-0,18087

RELT	-0,18033
PSMB10	-0,1796
ERCC3	-0,1783
GSDMD	-0,17448
RPS27	-0,17394
TRIM22	-0,17367
MCRS1	-0,17358
LIMD2	-0,17315
ZC3H11A	-0,17314
SRSF11	-0,1718
MFF	-0,16973
LILRB1	-0,16815
EML3	-0,16317
COX7B	-0,15908
PPP5C	-0,15824

Up-regulated

Gene	log2FoldChange
LARP1	0,138036716
WASF2	0,139405955
KPNB1	0,139409952
SNX29	0,139845894
API5	0,140742285
KLF13	0,142972624
KHDRBS1	0,144399429
SUZ12	0,145034067
SEPT11	0,146677341
CAD	0,148254218
SETD1A	0,149252754
WDR82	0,149348754
KCTD20	0,150359206
ATP2A2	0,150495085
LONP1	0,152143157
IPO5	0,152596706
RRM2B	0,152615555
GTF3C1	0,153206703
KRR1	0,153703361
SEC63	0,155025741
SMCR8	0,155616674
GALNT2	0,157172778
DUSP4	0,158361605
STK10	0,15893962
GATAD2A	0,159934103
CUL3	0,160324022

WDFY4	0,160327658
NUP153	0,160816747
SLC38A1	0,161050589
SHOC2	0,161258776
IBTK	0,161333958
CRTC3	0,161771369
CNTRL	0,162022186
ICMT	0,163499937
SYNCRIP	0,16365999
ACTR2	0,164058351
SUPT16H	0,164200637
CDK12	0,164479029
RAVER1	0,164944257
PAK2	0,16533603
TNPO3	0,165660853
USP9X	0,165666411
YWHAH	0,165720796
HDGF	0,165844565
BTBD10	0,166003314
MICU1	0,166111511
CREBBP	0,166119035
LSP1	0,166168736
BMPR2	0,166434936
SLC7A1	0,166501618
CHST11	0,167170275
ATF7	0,167902059
NOM1	0,168287705
ELF4	0,16916826
PRRC1	0,169503608
SLC16A1	0,169800209
TRIP12	0,169907692
MTHFD1	0,170139269
TFDP2	0,1701595
ARHGEF12	0,170626981
BCL9L	0,170665499
MED16	0,170704694
FAF2	0,17100597
ANAPC1	0,171245534
PREX1	0,171339223
APC	0,171504555
SAP130	0,172592683
G3BP2	0,172742182
RNF219	0,17339556
MTA2	0,174316658
USP7	0,174738793
B4GALT1	0,175403543

CLTC	0,175647503
CAND1	0,175657181
MED13	0,176360438
PDE4B	0,176722936
STAG2	0,176826588
TNRC18	0,176831488
PTPN7	0,177077841
SF3B3	0,177512935
HSPD1	0,177598236
PRRC2B	0,178138615
AARS	0,178283752
GTF3C4	0,178354844
C15orf39	0,178446135
KIAA0100	0,1795532
GIGYF2	0,179970099
CDK6	0,180130957
RAB3GAP1	0,18081978
CADM1	0,181026711
POM121	0,181215273
UBTF	0,18177924
ANKRD52	0,182255009
GOT2	0,183109066
STAU1	0,183293608
GPR107	0,183695288
WIPF2	0,183695392
PJA2	0,184561131
NUCB1	0,185149863
PIK3R1	0,185445943
PVRL1	0,185793927
GPI	0,186070126
PTBP3	0,186621436
SSH2	0,186916819
POLR2A	0,187045404
SH3KBP1	0,187305959
LAPTM4A	0,189226775
SPTLC2	0,18923193
PDK3	0,189251902
ORAI2	0,189838958
ZAK	0,190242973
RPRD2	0,190991213
QSER1	0,191035826
TRIP11	0,19105732
FOCAD	0,191086285
LMAN2	0,191223837
NUP188	0,191564216
RANBP2	0,192874619

TAF4	0,193779477
KIF1B	0,193826714
CACYBP	0,19400155
ZNF766	0,194290028
IQGAP2	0,194326685
SUPT6H	0,194344558
RAPGEF6	0,194489913
SON	0,194701539
HIRA	0,195593957
CAMSAP2	0,195802315
NUDT21	0,196389178
STAG1	0,196600654
SF3B4	0,196803485
RAB3D	0,197569589
IQSEC1	0,197658382
CYB5R3	0,197896156
TBC1D5	0,19792294
NCOR2	0,198100206
CHD8	0,198115891
LDHA	0,198200505
SBNO1	0,1984543
GBF1	0,19851371
SPTAN1	0,198636299
SLC9A3R1	0,198745723
WBSCR16	0,198868812
EIF4EBP2	0,198904092
LRRC58	0,199548638
RERE	0,199672074
ARHGAP1	0,199806231
KDM3B	0,200033493
SERTAD2	0,20037047
POLR1A	0,200756354
ZYX	0,201874429
NXPE3	0,20222112
SLC7A11	0,202985238
ANKRD17	0,202989956
SENP1	0,203055058
GPATCH8	0,203734668
RIF1	0,204620309
ZFAT	0,204703593
CLPB	0,205004021
HEG1	0,205203085
KDM5A	0,205209563
PIGN	0,205729885
TRAF3IP2	0,206318393
PER2	0,206481828

TRIM24	0,206545401
MAP3K1	0,206829439
SMG6	0,20700636
AMER1	0,207072033
SLK	0,207259803
PGM1	0,207436524
SP1	0,207444092
RFWD3	0,208036731
ZC3H4	0,208948918
RBM27	0,208994025
DESI2	0,209010835
SMG7	0,209036891
GNS	0,209075412
SNX10	0,209285658
MIB1	0,209459128
RBPJ	0,209545216
ARRB1	0,209785854
TNIK	0,209794775
MBNL1	0,209868025
SP3	0,210118514
SELL	0,210629937
CREB1	0,210655063
CELF2	0,210787719
PPT1	0,210890353
TAF15	0,211090938
UHRF1BP1	0,211166847
IPO8	0,211404874
ARID1A	0,211536015
C1orf216	0,211558842
LIMS1	0,211590611
MARCH8	0,211693199
AKAP13	0,212671741
ago-01	0,214073074
RPN2	0,214133632
GEMIN4	0,214333004
HELZ	0,214498879
TRIM32	0,214917388
NRF1	0,215932518
NAV2	0,217239011
KIAA0586	0,217930965
H2AFZ	0,218283209
CSE1L	0,218362092
HSP90AA1	0,218703702
PBRM1	0,218724378
UTP20	0,219194557
PARP1	0,220303781

PEX5L	0,220949601
KIF21B	0,221685537
ARID2	0,22230467
MYH9	0,222525209
NR3C1	0,222977018
PARP4	0,224505453
HNRNPM	0,224770672
TUBB	0,225226615
MBTPS2	0,225293632
ZMAT3	0,225388369
ENC1	0,225601756
ZBED1	0,225747727
ALDH5A1	0,225926295
CEP55	0,225935214
CREB3L2	0,226577323
MED1	0,226984669
POM121C	0,227180873
BRI3BP	0,227788607
ago-02	0,227855139
SMARCC1	0,228299631
CCNK	0,228713592
DIAPH1	0,228946206
FAM129A	0,229206698
BCOR	0,229387379
HTATSF1	0,229473758
F8A1	0,229715582
TIMP1	0,229826575
UBR4	0,23016631
TMEM41A	0,230433924
MECP2	0,230485723
NF1	0,230635719
KIAA0040	0,230679925
SEC62	0,230688878
TACC1	0,230782
INO80D	0,230795364
TLN1	0,231293533
SPEN	0,231313932
CDS2	0,231465712
IKZF3	0,232143002
TOR1AIP1	0,232726674
TRIM56	0,232754224
GMPS	0,233449231
CTDSPL2	0,233507838
IL17RA	0,233968579
CPOX	0,234424376
KMT2E	0,234844752

PHGDH	0,234854451
CNOT1	0,235204161
MFSD6	0,235680036
C19orf47	0,235757818
NCOR1	0,235933576
ZNF28	0,23624676
NDST1	0,236580403
EP300	0,236669037
IQGAP1	0,236822266
HNRNPU	0,23687303
PRRC2C	0,238269821
HNRNPUL1	0,238830389
TTYH3	0,238905078
ALKBH8	0,23903266
GDE1	0,239644322
FAM168A	0,23977653
TNRC6C	0,241532394
SLC30A6	0,24170496
ZNF609	0,242196011
GOLIM4	0,242203628
CLP1	0,242683096
PIGK	0,243314587
ADCY1	0,243342789
PDZD8	0,243375713
RNF157	0,24358185
CNKSR3	0,243599282
TMEM245	0,244396157
ZNF124	0,244444954
LRR1	0,245264374
GVINP1	0,245825708
ACAT1	0,246139133
PLD1	0,246504518
ESYT1	0,246996033
USP37	0,24788872
FECH	0,248135184
IFNAR1	0,248371157
CRTAP	0,248924967
PLK1	0,249016992
SRBD1	0,249131981
DCLRE1B	0,249294906
CPD	0,249766411
SETX	0,25036826
PTCH1	0,250871135
PRR12	0,251002473
CHAF1B	0,251224771
MACC1	0,252463464

IGF2R	0,252592259
MLH1	0,252918919
NDC1	0,253826607
DOCK8	0,254464153
KCTD1	0,254550598
CBL	0,255209506
TMEM201	0,255384724
CHD9	0,255585672
YLPM1	0,256563518
POLA1	0,257027013
GUCY1A3	0,257147682
HMMR	0,257366447
PRPF8	0,257653355
GPD2	0,257888511
DIP2B	0,258129316
FAM13B	0,258423205
SEC16A	0,258615361
NIPBL	0,259090589
ARHGEF6	0,259193099
PIK3R3	0,259203734
SACS	0,259990635
NUP210	0,261084054
NBAS	0,261629828
MYO18A	0,261714159
LMNB1	0,262970609
PPDPF	0,265559348
KIAA1671	0,265790098
NUP155	0,266193001
WDR7	0,266206642
MEF2D	0,266553647
GTF2A1	0,266759
SMAD5	0,267105242
NCAPD2	0,267111136
POLD3	0,267229132
MPP6	0,268811183
TTC39C	0,268985507
MSN	0,269058295
C10orf54	0,26979358
PLP2	0,270327123
EI24	0,270412873
HMGN5	0,270591422
TXNRD1	0,270987166
UHRF1	0,271038374
WNK1	0,271815161
NOMO2	0,27275246
CHAMP1	0,274126389

LRBA	0,274331611
IRS1	0,275044471
MAP3K9	0,275058057
APOBEC3B	0,275885616
MGA	0,275996762
LIMA1	0,27640792
IPO11	0,276734671
TUBB6	0,277116269
MCM6	0,277134295
NFIC	0,277157362
MAD2L1	0,277261598
LASP1	0,2775517
RAD54L2	0,278624398
SLC1A4	0,27890272
COPG2	0,279303168
CALM3	0,279683731
DSG2	0,280008951
ZNF407	0,280177619
IKZF2	0,281356935
SRCAP	0,281390844
NEDD4	0,282238177
EVI2B	0,282259236
MACF1	0,28292974
CALU	0,283883282
ANP32E	0,284624139
NCOA2	0,285171103
TMX4	0,287033973
BAZ1B	0,287707965
MYCBP2	0,287893891
ARHGAP35	0,289295967
CABLES2	0,289586133
NET1	0,290512023
HPSE	0,291368405
HIPK2	0,29166724
HNRNPD	0,292183882
ZNF675	0,292316246
ARHGAP26	0,292747372
KATNAL1	0,294557569
SLC25A10	0,295000442
USP13	0,29520992
TNRC6B	0,295342475
NTRK2	0,296670417
ABHD2	0,296987002
TLE3	0,297001046
FLNA	0,29721847
PDIA6	0,297528055

SEPT9	0,297629111
MDC1	0,297817082
CXorf21	0,29794868
ENDOD1	0,298071994
WDR1	0,298121563
C3orf58	0,298314461
AGA	0,298316408
IPCEF1	0,298901542
KLF12	0,299500456
FUT8	0,300312569
SMARCA4	0,300594415
MDN1	0,300768941
TFRC	0,301206393
RNF144A	0,301230922
USP34	0,301693763
AKAP11	0,30172819
SEC24A	0,301886123
ZZEF1	0,303646968
RACGAP1	0,303733568
KIF14	0,304135027
CEP128	0,304305443
CCNA2	0,304580806
RNASEH2A	0,304702023
SPRY2	0,305502779
RNF26	0,305870155
FLI1	0,305927722
HNRNPUL2	0,306399254
NUP214	0,306529074
PIK3CG	0,307054164
KCNJ3	0,307363592
CDH2	0,307378911
CTNNAL1	0,307508345
FNIP2	0,307676547
KAT6A	0,308228812
DDI2	0,308492399
TNFRSF11A	0,308619365
KIAA0513	0,308897161
KIAA2018	0,309034867
MGAT3	0,309125239
HDHD1	0,309289662
EP400	0,310751544
UGGT1	0,311527213
PAFAH2	0,313376428
DACT1	0,313422091
GIMAP6	0,313596225
CEP350	0,315760644

ANXA11	0,315887858
SYNJ2	0,316084807
GPAT3	0,316575295
FBXW7	0,317482159
ADPRH	0,317869494
RSC1A1	0,319881595
INCENP	0,32000712
SYNE3	0,321584708
CTCF	0,321836122
C1R	0,322126659
HS3ST1	0,322934086
CENPL	0,325227504
MCM2	0,326387344
ERMP1	0,327569613
CEND1	0,327657536
MCC	0,328563432
LUZP1	0,330741381
PAG1	0,330957467
NCOA3	0,331196671
LAPTM5	0,331357786
CDC25B	0,331754531
HCFC1	0,331785254
FTL	0,331803066
SORL1	0,331847208
ZNF880	0,333405793
DCP2	0,333685963
TMTC1	0,334125571
NSD1	0,336245448
POU2F1	0,337377561
C10orf12	0,338101408
ORC1	0,338438994
DYNC1H1	0,3388466
DST	0,339365735
SIPA1L3	0,33997626
REV3L	0,341919297
HTT	0,343485261
TULP4	0,343825345
ANK1	0,344037934
HDAC9	0,344299909
GIMAP8	0,34507651
ZNF385A	0,345312376
TUBA1B	0,345548331
DTL	0,345878872
MMS22L	0,347858156
KLK1	0,349053625
ABL2	0,349274579

CNOT6L	0,349559348
TPX2	0,349739072
ZNF106	0,34985516
RBFOX2	0,350638496
PPP3CA	0,351176296
ASCC3	0,351478825
DHFR	0,351593599
SLF1	0,351981355
ALG10	0,352427248
MYBPC2	0,352832132
BIRC6	0,352873212
DSCC1	0,353375353
HERC2	0,35394011
ETS1	0,355554822
HERC1	0,356024023
NUDT15	0,356028894
SPTY2D1	0,357644829
MFHAS1	0,359041541
TOP2A	0,359736885
SKA3	0,361545549
ESCO2	0,362419163
WHSC1	0,363658987
OTUD1	0,363670018
SHISA5	0,364239869
FOXRED2	0,36429712
GALNT7	0,365061832
ALMS1	0,365204736
AKAP5	0,365701446
ZFHX3	0,36601546
NNT	0,36672497
PRR11	0,366778422
SPTBN1	0,367814982
PINK1-AS	0,368783768
CKAP2L	0,369458163
CDKN3	0,370264996
RN7SL2	0,370535093
PRKDC	0,372230122
PRKACB	0,374406363
SMC1A	0,376526408
KCTD12	0,376975436
TBC1D9	0,377779899
KIF4A	0,379077133
SHCBP1	0,379616476
IKZF1	0,380661002
CD84	0,382227634
LRP6	0,382360146

UTRN	0,384102533
RAB30	0,385942865
ZNF829	0,386218034
FLJ42627	0,386289337
HIRIP3	0,387262127
FRYL	0,387989092
CDCA2	0,390569267
APOBEC3C	0,39197726
SASH1	0,392159973
PRDM1	0,392379809
MYH10	0,393204324
RBL1	0,393501352
CCDC15	0,394962694
FOXN3	0,395018362
KMT2A	0,397752086
GGH	0,397836447
MBNL3	0,398507202
VANGL1	0,401410551
SLX4IP	0,404557381
LRRC16A	0,404948112
SMC2	0,405605844
RRM1	0,40610047
CORO2B	0,407315862
FAM111B	0,408730119
KMT2D	0,408769899
VPS13D	0,410055132
ITGB3	0,410462241
TLR9	0,411887975
ANK3	0,412044443
PCDHGC3	0,412600388
RAD51	0,418275309
STARD13	0,418483526
PTPRK	0,421787451
ROBO1	0,421997618
CRIM1	0,423022946
SEMA4A	0,424387341
CCDC141	0,424499901
TRRAP	0,425104015
CPM	0,430331532
LOC103611081	0,433018302
ARHGAP11A	0,434141688
ITPR2	0,436287834
AHNAK	0,43731253
FRMPD3	0,438450574
TREML2	0,438972337
LIPH	0,443949475

CLSPN	0,444403126
ZNF462	0,444515162
ZFP36L2	0,446363541
CENPF	0,446462019
GLIPR1	0,448618574
RIMS3	0,449432917
FRAS1	0,450209156
ILDR2	0,452412151
MYBL2	0,455757366
SCARB2	0,458066948
KMT2C	0,459995733
LOC101927550	0,461196391
CD109	0,461661733
KCNV1	0,462853238
ZBTB37	0,466374808
TLN2	0,467561961
CDC42BPA	0,469387929
KCNN3	0,469951894
NEO1	0,480723242
PKI55	0,485921833
FBN1	0,485944931
IER5L	0,486528163
SPSB1	0,486948805
PLXDC2	0,487807466
CABLES1	0,492040072
WFS1	0,492815354
KANK2	0,493540028
PRTFDC1	0,499260637
SOGA1	0,500762333
PALLD	0,502664486
ARHGAP5	0,503110886
TUBA4A	0,508258218
RGL1	0,514234055
AMICA1	0,518699208
NOTCH2	0,519277759
FOXO3	0,519303691
SMIM3	0,523934056
AAK1	0,52681521
WDFY3	0,527862041
SEMA3D	0,529337884
TPRG1	0,529461791
CREB3L1	0,53188822
FOXO1	0,532219291
CA5B	0,533761651
FILIP1	0,534477489
TTN	0,536944782

GDF15	0,539752866
ACER2	0,542979232
ZNF784	0,548077011
MICAL2	0,549224617
KLLN	0,551161768
CBX5	0,551501338
RNF213	0,553529481
TLR3	0,555484049
CPT1A	0,556717085
GPC4	0,556980981
AMOTL1	0,557203682
KLF5	0,559207191
SMPD3	0,570731609
CDCP1	0,571704308
TMEM2	0,571739233
NCKAP5	0,58064654
PEG10	0,582335503
CTTNBP2	0,596873461
CCNE2	0,597078031
MTUS1	0,598557557
FZD7	0,602660361
MITF	0,612372162
BMP2	0,620878928
LINC01358	0,633244719
FAT1	0,637849668
FN1	0,638124098
NKAIN2	0,64592732
CADPS2	0,649986322
MYRIP	0,659399274
KIAA2022	0,662856631
TCAF2	0,664151973
ARHGAP23	0,66510804
AMZ1	0,670797804
TENM2	0,681531833
LOC102723373	0,682695202
UBASH3B	0,684929775
ANXA1	0,693468905
PLXNA2	0,713807996
F2RL3	0,722596431
SIGLEC15	0,736953118
ZNF703	0,741713643
CCNJL	0,759155402
PCDH7	0,767222781
MFAP3L	0,783636654
LRCH2	0,786829051
GNAQ	0,788342851

MAP1A	0,791375931
ADCY9	0,804152332
PTPN14	0,817743693
LIMD1-AS1	0,822805495
FGL2	0,837940237
RASA4B	0,843530833
LRP1	0,865149758
ARHGAP31-AS1	0,869710647
IL1B	0,872835596
DGCR11	0,875390708
PAPSS2	0,878785995
IGFBP3	0,893119388
SLC24A3	0,895408435
MIR5195	0,900245601
SNTA1	0,937785681
AGAP2-AS1	0,941692896
MAGI2	0,966153315
PTRF	0,972831557
CELSR1	0,982844974
FOXP3	0,986968455
ADAMTS8	3,07345E+12
ZBED2	1,07315E+13
RNA28S5	1,14566E+13
NEBL	1,1462E+13
SLC26A7	1,36196E+13
TGFBI	1,41458E+13
BMPR1B	1,52477E+13
UNC13C	1,69251E+13
CNTN6	1,88843E+13
ROS1	2,03975E+13
TRHDE-AS1	2,15835E+13
LINC00508	2,35767E+13
FST	2,52123E+13
ZNF99	2,5691E+13
PCDHB11	2,60248E+13
KRT9	2,69092E+13
LOC101927769	2,71113E+13
LOC100996291	2,75932E+13
TMEM92	3,19726E+13
KIAA1210	3,4517E+13
C1orf137	4,0428E+13
PRKG1-AS1	4,0428E+13
PWRN1	4,0428E+13
LILRA6	4,0428E+13
SULT1C4	4,0428E+13

PCK1	4,0428E+13
LOC101928269	4,0428E+13
SNTN	4,0428E+13
LINC01054	4,84847E+13
LINC00488	1,00626E+14
CYP1A1	1,02529E+14
RNA45S5	1,03291E+14
ADGRV1	1,04146E+14
MYBPH	1,04784E+14
COL4A5	1,05106E+14
SV2B	1,0774E+14
C14orf132	1,10162E+14
GRIA3	1,11999E+14
EHD3	1,12364E+14
NR5A2	1,12436E+14
F5	1,12667E+14
HIST1H2BL	1,12692E+14
MMRN1	1,12791E+14
ARMC2	1,13978E+14
NWD1	1,1442E+14
C1orf226	1,1567E+14
ENPEP	1,1603E+14
SLC8A1	1,18006E+14
OSBPL1A	1,19598E+14
VIL1	1,21682E+14
EFCAB5	1,25611E+14
THEMIS	1,28939E+14
BMP3	1,29414E+14
AKR1C3	1,31754E+14
ARHGEF10	1,32413E+14
SCARNA7	1,34101E+14
ST14	1,36711E+14
GAS1	1,37114E+14
MYOM3	1,38417E+14
KIRREL3	1,39436E+14
GNAT2	1,45562E+14
HMCN2	1,46675E+14
CRTC3-AS1	1,48841E+14
FREM1	1,54575E+14
CDK5R2	1,54782E+14
EREG	1,56322E+14
SLC4A10	1,56419E+14
CCBE1	1,59293E+14
PLXDC1	1,59697E+14
SCUBE3	1,63158E+14
FLT4	1,63441E+14

MET	1,67698E+14
LINC01234	1,70268E+14
VSTM4	1,71646E+14
SLC34A2	1,75359E+14
DRAXIN	1,75739E+14
PAPPA	1,7826E+14
PLEKHD1	1,79384E+14
DEAR	1,84483E+14
DLGAP2	1,87596E+14
OR2T2	1,91259E+14
THSD4	1,91631E+14
GLI2	1,94076E+14
LPPR5	1,94518E+14
IL1A	1,95692E+14
ERICH6	1,96152E+14
C1QL1	1,99842E+14
MTMR7	2,00677E+14
NRG1	2,04113E+14
SPARCL1	2,04564E+14
CUX2	2,05922E+14
STEAP4	2,05968E+14
ZNF704	2,06277E+14
LOC414300	2,07163E+14
MEP1B	2,10392E+14
ANKRD35	2,10466E+14
PCDHGC4	2,11199E+14
CCDC129	2,14811E+14
HSD3BP4	2,15472E+14
PDE10A	2,16771E+14
BIN3-IT1	2,17067E+14
ANKK1	2,17901E+14
PIWIL1	2,18959E+14
ALX4	2,19432E+14
ALDH1A2	2,19432E+14
C1orf94	2,25643E+14
PLSCR2	2,25943E+14
ASPG	2,26415E+14
PEAR1	2,27049E+14
LOC100129697	2,28466E+14
FLG2	2,32867E+14
KCNH7	2,33404E+14
GALNT15	2,35776E+14
IQCA1L	2,41613E+14
LIN28B	2,41979E+14
LINC00521	2,42689E+14
RADIL	2,42689E+14

ADGRF1	2,43408E+14
CDH18	2,44297E+14
CDHR3	2,47275E+14
GNA14	2,50783E+14
SIGLEC8	2,5122E+14
PLD5	2,5176E+14
ADGRB3	2,52869E+14
TECTB	2,55361E+14
JPH3	2,55885E+14
LPCAT2	2,57457E+14
KCNB1	2,59937E+14
CPN2	2,60186E+14
PDZD3	2,62604E+14
CYP4F22	2,62809E+14
LOC101926962	2,63406E+14
COLEC11	2,63826E+14
CLCA4	2,64302E+14
KRT80	2,65543E+14
BEST3	2,67166E+14
C11orf96	2,68177E+14
GOLGA6L17P	2,69475E+14
TPH2	2,69585E+14
CSMD2-AS1	2,70215E+14
ZNF806	2,721E+14
KLHL31	2,74614E+14
CA12	2,76267E+14
S100B	2,77366E+14
SNORD36B	2,77366E+14
AGBL1	2,77798E+14
LINC01182	2,77798E+14
LOC401242	2,77798E+14
CXorf36	2,81207E+14
SPINK5	2,83041E+14
DNAJC22	2,84193E+14
LOC442132	2,86738E+14
LOC101928519	2,87715E+14
TDRD6	2,87715E+14
LOC100133077	2,87715E+14
PAX7	2,87769E+14
SLC5A8	2,89819E+14
VAX1	2,94274E+14
CLCA3P	2,97267E+14
ZDHHC15	3,00262E+14
DCX	3,00363E+14
KCNJ5	3,00557E+14
LOC100128531	3,00557E+14

CYR61	3,03592E+14
OTOP3	3,03592E+14
ST7-OT3	3,03663E+14
TMC4	3,06887E+14
KCNK2	3,09578E+14
SERPINA4	3,12848E+14
CLRN1	3,12848E+14
PNLIPRP1	3,1475E+14
GNAT1	3,1475E+14
ZNF804B	3,15388E+14
TMEM47	3,18172E+14
CFAP221	3,22969E+14
CADM3-AS1	3,24434E+14
LINC01180	3,25655E+14
RBM46	3,2688E+14
SPOCK3	3,2688E+14
TRIM43	3,30067E+14
LOC643542	3,34029E+14
CD1E	3,3517E+14
RNU6ATAC	3,4014E+14
ADH7	3,45286E+14
MMP10	3,47609E+14
SMOC2	3,54992E+14
CDC14C	3,58002E+14
LINC01222	3,60231E+14
LOC283299	3,60231E+14
SACS-AS1	3,60231E+14
REREP3	3,60231E+14
RNU6-10P	3,60231E+14
PRDM14	3,64614E+14
LOC284950	3,65955E+14
NPTX2	3,66065E+14
LINC00964	3,70812E+14
ADRB3	3,72559E+14
LINC01492	3,72559E+14
LEFTY2	3,78001E+14
AKR1B10	3,82179E+14
EPCAM	3,89829E+14
WNT8A	3,89829E+14
LINC01375	3,90265E+14
TRIM49C	3,90627E+14
SIGLECL1	3,96655E+14
GPR37	3,96655E+14
DLX3	4,09747E+14
LOC100506085	4,09747E+14
AFAP1-AS1	4,16788E+14

OR10A3	4,20275E+14
LOC101928778	4,22253E+14
CD3G	4,22253E+14
PSG5	4,22409E+14
PRSS48	4,22409E+14
PLCZ1	4,38597E+14
SULT1B1	4,38597E+14
WNT16	4,38597E+14
CLEC12B	4,39108E+14
LOC101927653	4,39108E+14
GYPE	4,53214E+14
ARSE	4,53214E+14
LINC00554	4,54186E+14
MGC27382	4,66533E+14
KLHL40	4,66533E+14
SERP2	4,67827E+14
TCP10L2	4,67827E+14
CD2	4,78764E+14
OMP	4,80281E+14
MIR30E	4,89315E+14
PDZK1IP1	4,89315E+14
LOC100996263	4,89315E+14
OR51A7	4,89315E+14
GPHA2	4,89315E+14
FAM181A	4,89315E+14
LINC00483	4,89315E+14
MIR216B	4,89315E+14
LINC00489	4,89315E+14
SPINT3	4,89315E+14
LOC101929412	4,89315E+14
NUPR1L	4,89315E+14
TAS2R38	4,89315E+14
DEFA6	4,89315E+14
LINC00208	4,89315E+14
LINC00548	4,98479E+14
KRT4	5,08601E+14
LINC01143	5,08601E+14
KRTAP13-1	5,08601E+14
ARHGEF3-AS1	5,08601E+14
OTOL1	5,08601E+14
TMED11P	5,08601E+14
LOC102477328	5,08601E+14
LOC100128993	5,08601E+14
KLRF2	5,21472E+14
HIST2H2BA	5,2561E+14
FAM163A	5,2561E+14

LOC101927787	5,2561E+14
THPO	5,2561E+14
MEP1A	5,2823E+14
IFNL4	5,40823E+14
SSX5	5,54585E+14
OLAH	5,67147E+14

Supplementary Table 10. Dysregulated genes (both downregulated and upregulated) identified upon comparison of ataluren EP2-treated cells versus untreated controls.

Down-regulated

Gene	log2FoldChange
NELL2	-6,93587E+14
CRX	-6,91785E+14
GPA33	-6,84302E+14
ADGRF5	-6,84302E+14
HYDIN2	-6,79683E+14
SLC9C1	-6,73048E+14
ADAM33	-6,72833E+14
PPP1R9A	-6,72833E+14
SLC14A2-AS1	-6,71866E+14
AMBN	-6,71866E+14
LOC101927666	-6,68217E+14
LINC01492	-6,66947E+14
ZNF366	-6,64592E+14
HEPHL1	-6,6428E+14
CDH3	-6,6217E+14
SLC26A5	-6,62063E+14
ATP1A2	-6,5955E+14
MOG	-6,58244E+14
GLRA2	-6,55143E+14
TSPYL6	-6,52904E+14
LOC442028	-6,52904E+14
NDST3	-6,52904E+14
ENPP3	-6,52904E+14
BPIFB1	-6,51506E+14
KNG1	-6,51506E+14
LOC101927766	-6,50233E+14
WFDC1	-6,50068E+14
XIST	-6,50068E+14
ALS2CR11	-6,46028E+14
SLC47A1	-6,44587E+14
B3GNT3	-6,44587E+14
SYT3	-6,44587E+14
LINC00547	-6,41599E+14
GCSAML	-6,40274E+14
RFX4	-6,38787E+14
MIR124-2HG	-6,35941E+14
PIANP	-6,3576E+14
CCDC170	-6,3576E+14
PCDHA1	-6,34339E+14
LOC101928150	-6,34201E+14

TRPM5	-6,3275E+14
ST8SIA3	-6,31166E+14
LOC284865	-6,31166E+14
GRIA2	-6,31166E+14
IL21-AS1	-6,27978E+14
C5orf47	-6,27978E+14
TMEM255B	-6,26615E+14
CYP4A22	-6,26354E+14
GABRA1	-6,26354E+14
TERT	-6,24872E+14
PKD1L3	-6,24697E+14
KLHL1	-6,23155E+14
MIR8078	-6,23155E+14
GIPC2	-6,22995E+14
ADAMTS14	-6,22995E+14
LGI2	-6,21449E+14
TSG1	-6,21449E+14
FGF1	-6,21231E+14
DKK3	-6,19743E+14
DKFZP434A062	-6,19743E+14
MYOM3	-6,18027E+14
LOC440390	-6,18027E+14
LAMB4	-6,18027E+14
LACTBL1	-6,1629E+14
BMP4	-6,1629E+14
TMC5	-6,1629E+14
HTR2B	-6,1629E+14
CDH18	-6,1629E+14
GRM6	-6,1629E+14
TRIML2	-6,14764E+14
LOC101929488	-6,14764E+14
BDKRB2	-6,1452E+14
ECEL1	-6,1452E+14
CNTN6	-6,1452E+14
ZIC1	-6,1452E+14
EBF2	-6,1452E+14
LOC101927623	-6,1452E+14
ADGRG4	-6,1452E+14
ARMC4	-6,12703E+14
LOC646903	-6,12703E+14
CD163L1	-6,11037E+14
TDRD1	-6,09191E+14
APOA4	-6,09191E+14
LOC283177	-6,09191E+14
FAM181A-AS1	-6,09191E+14
GSG1L	-6,09191E+14

FAR2P1	-6,09191E+14
FOXF2	-6,09191E+14
H2BFM	-6,09191E+14
HTR2A	-6,08841E+14
RGSL1	-6,0734E+14
PROX1-AS1	-6,0734E+14
LINC01561	-6,0734E+14
KRT74	-6,0734E+14
LOC100505918	-6,06613E+14
LINC00482	-6,05469E+14
BPIFB3	-6,05469E+14
SLC36A2	-6,05469E+14
LINC01500	-6,03566E+14
RNF112	-6,03566E+14
ANTXR1	-6,03566E+14
FRMD1	-6,03566E+14
LINC00597	-6,01858E+14
LOC284344	-6,01858E+14
ARID3C	-6,01858E+14
MMP12	-6,01616E+14
SIAH3	-6,01616E+14
ZP4	-5,99826E+14
NEUROD4	-5,99826E+14
GABRD	-5,99598E+14
C16orf89	-5,99598E+14
PCSK2	-5,99598E+14
VSX1	-5,99598E+14
ZIC4	-5,99598E+14
MEPE	-5,99598E+14
GABRR1	-5,99598E+14
MUSK	-5,99598E+14
CSF2RA	-5,99598E+14
MGAT4C	-5,97475E+14
SLC1A6	-5,97475E+14
PSG4	-5,97475E+14
LOC728084	-5,95798E+14
GRB14	-5,95798E+14
GPIHBP1	-5,95798E+14
NR0B1	-5,95798E+14
LINC00839	-5,95087E+14
MSI1	-5,95087E+14
MYL1	-5,95087E+14
SPO11	-5,95087E+14
FZD10	-5,93769E+14
SNHG24	-5,93769E+14
LILRA1	-5,93769E+14

CYP27C1	-5,93769E+14
MLPH	-5,93769E+14
EYA2	-5,93769E+14
FOXP1-AS1	-5,93769E+14
F11	-5,93769E+14
CYP4X1	-5,91709E+14
LOC283214	-5,91709E+14
TMEM132D	-5,91709E+14
BNC1	-5,91709E+14
CCDC144NL-AS1	-5,91709E+14
DUXA	-5,91709E+14
OLIG2	-5,91709E+14
CXCL1	-5,91709E+14
RBM46	-5,91709E+14
FAM87A	-5,91709E+14
LOC392232	-5,91709E+14
LINC01606	-5,89964E+14
AQP4-AS1	-5,89601E+14
OR7A5	-5,89601E+14
KCNJ16	-5,87691E+14
LYPD4	-5,87691E+14
TNFRSF6B	-5,87691E+14
SPATA12	-5,87691E+14
LOC101927374	-5,87691E+14
CLEC5A	-5,87691E+14
LINC01296	-5,87422E+14
TMEM56	-5,85467E+14
LRP3	-5,85133E+14
ZMAT4	-5,85133E+14
HNRNPCL1	-5,83256E+14
CLCNKB	-5,83256E+14
LRRC7	-5,83256E+14
DKFZP434L187	-5,83256E+14
ANKRD30B	-5,83256E+14
DMRTC2	-5,83256E+14
TRPM4	-5,83256E+14
RHAG	-5,83256E+14
LOC101926964	-5,81036E+14
LOC101928436	-5,81036E+14
EPS8L3	-5,81036E+14
GLYATL1	-5,81036E+14
KRT25	-5,81036E+14
OR7E91P	-5,81036E+14
LINC01310	-5,81036E+14
LRRN1	-5,81036E+14

PCDHA10	-5,81036E+14
GREM2	-5,7649E+14
FENDRR	-5,7649E+14
DAW1	-5,7649E+14
LINC01524	-5,7649E+14
VGLL3	-5,7649E+14
CCDC37	-5,7649E+14
SLC51A	-5,7649E+14
GC	-5,7649E+14
KLHL38	-5,7649E+14
OR7E156P	-5,71629E+14
PDLIM3	-5,71629E+14
TRPV6	-5,71629E+14
RNU4-1	-4,29481E+14
RNA28S5	-4,01737E+14
KNDC1	-4,01229E+14
TMEFF2	-3,96834E+14
DTNA	-3,8936E+14
FSIP2	-3,8628E+14
RNU4-2	-3,81867E+14
SVEP1	-3,81475E+14
SLC24A2	-3,78104E+14
SLC4A3	-3,7474E+14
PPFIA2	-3,73902E+14
LONRF2	-3,73902E+14
PTGER3	-3,73016E+14
SLC12A1	-3,71353E+14
DSCAM	-3,67776E+14
LOC100131257	-3,63145E+14
MUC5B	-3,58838E+14
RIMS1	-3,5858E+14
RUNX1T1	-3,57529E+14
IL22RA2	-3,55603E+14
NOS1	-3,54925E+14
ASTN1	-3,50647E+14
RMRP	-3,50106E+14
SLC9C2	-3,47664E+14
XDH	-3,45483E+14
SLIT3	-3,41342E+14
GREB1L	-3,41302E+14
BRSK2	-3,41248E+14
VEPH1	-3,40283E+14
TNC	-3,39117E+14
RBFOX1	-3,39062E+14
STXBP5L	-3,39052E+14
NCAM1	-3,38401E+14

VWA3B	-3,36901E+14
MRO	-3,34727E+14
CDHR3	-3,34633E+14
ZNF704	-3,27664E+14
MICU3	-3,25304E+14
FAM71F1	-3,24099E+14
BEAN1	-3,22901E+14
MROH2A	-3,22845E+14
KIF26A	-3,21705E+14
RIPPLY2	-3,21705E+14
ABCA8	-3,20505E+14
RN7SK	-3,19907E+14
ENPP7	-3,17222E+14
C1orf21	-3,14125E+14
SCN10A	-3,13615E+14
SGCD	-3,12852E+14
ADAMTS2	-3,11836E+14
TPTE2P1	-3,07505E+14
CORIN	-3,05972E+14
CRB1	-3,05299E+14
FAT3	-3,01332E+14
SLC4A10	-3,01029E+14
ABCB11	-2,96025E+14
APOB	-2,95442E+14
SLC4A1	-2,92431E+14
SDK2	-2,8953E+14
CSMD1	-2,89316E+14
LRRC9	-2,89157E+14
ADAMTS18	-2,89157E+14
HYDIN	-2,8706E+14
LOXHD1	-2,85039E+14
TLL1	-2,83862E+14
HIST1H1B	-2,79839E+14
SULF1	-2,77758E+14
ARHGEF4	-2,74793E+14
DPYSL5	-2,7385E+14
TMEM59L	-2,70292E+14
KIRREL	-2,66871E+14
GRM5	-2,66871E+14
ARAP3	-2,66871E+14
CEP126	-2,64876E+14
ERBB4	-2,62394E+14
LOC101929541	-2,53908E+14
SH3TC2	-2,49667E+14
COL20A1	-2,49358E+14
ENAH	-2,47612E+14

FLT4	-2,4676E+14
SGIP1	-2,43357E+14
MYT1L	-2,42457E+14
PTPRQ	-2,41642E+14
RYR2	-2,38309E+14
PKHD1	-2,38084E+14
TMEM54	-2,36785E+14
ESYT3	-2,35965E+14
WNK3	-2,34648E+14
CACNA1F	-2,25377E+14
KSR2	-2,2047E+14
COBL	-2,14769E+14
MYO15A	-2,06521E+14
ARFGEF3	-2,05839E+14
MUC17	-2,04702E+14
BACE2	-1,98845E+14
SLC34A2	-1,96168E+14
ENAM	-1,92461E+14
TCP10L	-1,90354E+14
LAMB2	-1,8299E+14
DNAH3	-1,80991E+14
PLCD4	-1,77921E+14
HIST1H1E	-1,71275E+14
TP53I11	-1,69746E+14
OTOF	-1,57796E+14
LRP2	-1,57359E+14
EML6	-1,54713E+14
CACNA1C	-1,51994E+14
SCARNA7	-1,44407E+14
CCDC30	-1,34631E+14
PTCHD2	-1,33342E+14
DNAH11	-1,31616E+14
RASAL2	-1,25935E+14
DNAH10	-1,23643E+14
SPRED3	-1,1254E+14
PTPRN2	-1,05037E+14
ABCC8	-6,98757E+13
NR2F1-AS1	-6,92747E+13
ACAN	-6,7879E+13
NTRK3	-6,68305E+13
CRTAC1	-6,29579E+13
MGC39584	-6,29579E+13
CARD10	-6,29579E+13
FAM90A25P	-6,29579E+13
GAS2L2	-6,12889E+13
LOC100505716	-6,12889E+13

PRICKLE2-AS1	-6,06223E+13
MGC27382	-5,78787E+13
KRT73-AS1	-5,78787E+13
SP7	-5,78787E+13
PWAR1	-5,78787E+13
PDZD9	-5,78787E+13
KCTD19	-5,78787E+13
RBFADN	-5,78787E+13
LOC641367	-5,78787E+13
SFTPB	-5,78787E+13
GPR149	-5,78787E+13
CNGA1	-5,78787E+13
ADH1B	-5,78787E+13
GRIK2	-5,78787E+13
GHRHR	-5,78787E+13
OPRK1	-5,78787E+13
LINC01289	-5,78787E+13
HAS2-AS1	-5,78787E+13
GYG2	-5,78787E+13
YWHAEP7	-3,71133E+13
MEG3	-3,549E+13
PRSS23	-3,51736E+13
PTPRT	-3,43422E+13
PPP1R1B	-3,32345E+13
COL4A1	-3,08088E+13
KCNC1	-3,04776E+13
PCDH10	-2,4143E+13
DNAH14	-2,25982E+13
ADGRV1	-1,90537E+13
OLFML2B	-5,97812E+12
HOXD3	-5,97812E+12
CNTN3	-5,97812E+12
PCDHA9	-5,97812E+12
LMX1B	-5,97812E+12
AIM1L	-5,74118E+12
CD1D	-5,74118E+12
KERA	-5,74118E+12
EPX	-5,74118E+12
LOC284395	-5,74118E+12
LOC645949	-5,74118E+12
OR5K1	-5,74118E+12
NPY6R	-5,74118E+12
MYH16	-5,74118E+12
NUP210L	-3,36845E+12
LIFR	-2,68541E+12
GLYATL2	-2,49295E+12

ALOX12B	-0,901459356
MYLK4	-0,867525617
SORBS1	-0,76423671
EGR3	-0,724237678
BEX5	-0,709534938
HOXB9	-0,64757502
EGR1	-0,638083241
SNORD104	-0,619891233
MIR17HG	-0,597979123
ABCA3	-0,594069272
WBP1	-0,559173783
JAKMIP2	-0,539021565
SNPH	-0,52496445
LOC728613	-0,499114005
ENOX1	-0,497654786
HIST1H2BC	-0,472010308
RBMS2	-0,454027326
ANKRD42	-0,452790959
AK7	-0,450894901
FAHD2CP	-0,449002007
SPATA7	-0,448593743
ZSCAN2	-0,432506058
C10orf10	-0,419776719
HOXC6	-0,417523808
IER3	-0,41359194
OTX1	-0,392444107
CDADC1	-0,388619994
CNPY4	-0,364404228
PYGL	-0,357157396
BCL2A1	-0,356292456
NAT6	-0,349738143
ENTPD2	-0,344247051
BCL2L11	-0,332552552
PINK1	-0,326803374
DNAJB4	-0,305920001
LXN	-0,302254653
DNAJC24	-0,295039018
TMEM175	-0,293803029
CBR1	-0,291668318
PPP1R16A	-0,287645249
CYP4V2	-0,282404761
ZNF354A	-0,278720934
ARHGEF11	-0,275210001
MCAM	-0,273296352
TCEAL4	-0,268683238
MSX1	-0,262694366

RNF19B	-0,260257452
TARSL2	-0,259157186
IQCE	-0,258535968
LEF1	-0,255185258
KRCC1	-0,254237926
PPP1R13B	-0,248601161
ABHD4	-0,245725682
CETN3	-0,244973312
ZCRB1	-0,244173001
ACKR3	-0,241516989
CBWD1	-0,240256559
KRT10	-0,240157965
CCR7	-0,238201212
DYNC2LI1	-0,237946448
NSRP1	-0,237733178
RNF216P1	-0,236099318
FAM172A	-0,235488959
FAIM	-0,235290429
KCTD13	-0,234574121
ARL2	-0,2333097
MOXD1	-0,233063504
SIAH2	-0,232762059
CYSTM1	-0,232552751
TRAF3IP1	-0,228889871
NKIRAS1	-0,227448905
ARL2BP	-0,225326181
DCAKD	-0,22488584
DLX2	-0,222865686
CHMP4A	-0,222478339
CFDP1	-0,222053738
MYPOP	-0,221444445
NPNT	-0,221366597
CIR1	-0,220869582
CD86	-0,220702959
C4orf32	-0,220650271
ZNF213	-0,218686
TIRAP	-0,218506812
TULP3	-0,217661566
AKT1S1	-0,217092252
WDR60	-0,217061969
UBLCP1	-0,216451938
CALCOCO1	-0,214129764
CEP290	-0,213659023
PIK3R2	-0,212724673
FAM50A	-0,21170732
TMEM63B	-0,211660806

LINC01215	-0,211178603
FOXP4	-0,210335957
CDC14A	-0,210312122
IFT74	-0,210184178
ARID4A	-0,210056791
RAB12	-0,20867208
STX4	-0,208491587
DDX10	-0,208362704
SP140	-0,208355962
RAB29	-0,207985234
GADD45GIP1	-0,206649654
VIM	-0,206648809
R3HCC1	-0,204856645
TOM1L2	-0,204849545
PAPD5	-0,204579686
NABP2	-0,20448612
MIA3	-0,203637704
MSC-AS1	-0,203372233
NELFE	-0,203294588
HGSNAT	-0,203229888
RAB2B	-0,203088121
C12orf65	-0,2028805
BRD7	-0,202228514
TMA7	-0,202154275
FRA10AC1	-0,199509828
LEPROTL1	-0,198616678
MARCH9	-0,198474338
TMEM50B	-0,198437956
STRADA	-0,197773235
BCL2L1	-0,197153726
SRI	-0,196730354
MNAT1	-0,195733278
TMOD2	-0,195383142
FTH1	-0,194925793
CCDC6	-0,194901425
CBWD2	-0,193773789
HIVEP3	-0,193008838
FAM127A	-0,192087456
WAC-AS1	-0,191811509
ZNF768	-0,19126511
EDF1	-0,191172198
CCDC124	-0,189828993
RAB1A	-0,189702971
EIF3J	-0,189560813
ITFG3	-0,18871553
NUFIP1	-0,188349972

CLIP2	-0,188190632
TCEB3	-0,187918662
ZFPL1	-0,187599088
INSIG1	-0,186462613
PGD	-0,185975763
HKR1	-0,185478745
PURA	-0,185368412
BSDC1	-0,184723546
JUNB	-0,184633273
TDRD3	-0,184520348
UPF3B	-0,184254514
TBCK	-0,183730388
PHF14	-0,182848025
RWDD4	-0,182611957
TSPAN3	-0,182364604
UNC119	-0,181858019
SYF2	-0,18183926
DYNLRB1	-0,181303514
UBAP2L	-0,180912437
IK	-0,180555297
DAG1	-0,179589777
BCL3	-0,179213856
PARM1	-0,178972803
TOX2	-0,178547485
NFKBIE	-0,178206056
ST6GALNAC6	-0,178065544
CYB5A	-0,177803627
IFIT2	-0,177543796
YLPM1	-0,177236811
ARHGAP31	-0,176753027
OXTR	-0,176593805
HMGN5	-0,176517408
TRAPPC1	-0,17631988
FAM65A	-0,176206355
RAB11FIP3	-0,176003576
SLC4A1AP	-0,175806319
CDC42EP3	-0,175335288
TUBA1A	-0,174885902
PPID	-0,174682227
PDCD5	-0,174584014
CCSER2	-0,17456625
GOPC	-0,174072425
BTN2A2	-0,172590948
GSK3A	-0,171905913
EBF1	-0,171832661
UBXN1	-0,171085263

BRPF3	-0,17063162
GATAD1	-0,170467438
C7orf73	-0,169921438
CPT1A	-0,169618646
RBM38	-0,169294518
FLNB	-0,169017114
TRIP10	-0,168643786
PRR14	-0,16826743
ZMIZ2	-0,167923203
PPIL4	-0,167445125
SOCS1	-0,167392677
ARL8A	-0,166895792
MESDC2	-0,16688
NFKB2	-0,166797592
CBLL1	-0,166364757
CBX1	-0,165504952
CRIP1	-0,165211319
HMGN3	-0,164771698
LHX2	-0,163941093
TSPYL1	-0,163789739
BRD3	-0,16372136
TMCC3	-0,163048084
TRAPPC6B	-0,162455681
ZNF664	-0,161413215
WBP2	-0,160925977
CIZ1	-0,160837419
ATN1	-0,160747149
BRD2	-0,16031923
PREPL	-0,160049308
GDI1	-0,158872139
RPL23A	-0,158678807
EGR2	-0,158398746
PPDPF	-0,158243263
SHFM1	-0,158227565
ORAI1	-0,158072368
BLK	-0,158014314
LMTK2	-0,157877311
RAB7A	-0,157485624
TOB1	-0,157174996
RELA	-0,156906604
CSTB	-0,156887191
RBM25	-0,156863674
SNRPD1	-0,156725162
HTATSF1	-0,156593693
IER2	-0,156297163
C21orf59	-0,156028774

EVI2B	-0,155294064
TMEM57	-0,155115317
SLAMF1	-0,154503568
SCLT1	-0,154328442
CD2BP2	-0,154326284
NFKBIB	-0,154034358
NPRL3	-0,153953962
PRKACA	-0,153953752
UPF3A	-0,153806535
SUGP1	-0,152924372
NKIRAS2	-0,152826227
R3HDM1	-0,1527246
CD44	-0,152084959
CASC3	-0,151884028
SAMD4B	-0,151832945
CRK	-0,151759803
HNRNPH3	-0,151395477
SOX9	-0,151273467
REL	-0,151267574
NOLC1	-0,150874078
EPM2AIP1	-0,150370045
PIP5K1C	-0,150009166
ERICH1	-0,149842764
SNRNP27	-0,148794695
NCL	-0,148678572
TAX1BP1	-0,148481659
MRPL10	-0,148068697
PRPF38B	-0,147812467
SRRM1	-0,147621709
EIF3A	-0,146952382
KDM2B	-0,146789236
TAF6	-0,146763333
TSG101	-0,146239037
HNRNPR	-0,145999375
MRFAP1L1	-0,144630769
SMARCE1	-0,144256433
EHD1	-0,143667903
PRCC	-0,143581203
MAP3K4	-0,142792843
CD55	-0,142791028
AP3D1	-0,14272508
KLC2	-0,142697062
WIPF2	-0,14239146
CC2D1A	-0,141826062
NEMF	-0,141451248
PITPNM1	-0,141203229

DPF2	-0,140820887
SSB	-0,140190418
DHX38	-0,139869181
ABCF1	-0,139467779
PPM1K	-0,138951126
BCL7B	-0,138497484
AGPAT1	-0,138240701
ATF7	-0,137329654
TERF2IP	-0,136976395
C9orf78	-0,136489717
CNOT3	-0,136207237
ZC3H18	-0,135390017
EIF5B	-0,135303211
KIF1C	-0,135165232
PSMF1	-0,134979997
HECTD3	-0,134320304
SREK1	-0,133938199
ADD1	-0,133736545
HNRNPA2B1	-0,133331801
RUVBL2	-0,133213204
ABI1	-0,133056218
EIF3G	-0,13293562
TOX4	-0,130808666
LSS	-0,130431113
SSU72	-0,130278485
ID2	-0,129976717
BTF3	-0,129947876
CMPK1	-0,129285557
HYOU1	-0,129230814
MYC	-0,128760318
PAF1	-0,128226704
RHOF	-0,128134403
FOXK2	-0,127348052
SAFB2	-0,126002232
CARM1	-0,125934594
GPR183	-0,12585554
WAC	-0,125664938
POLR2A	-0,12484639
PPIG	-0,124755187
TNIP1	-0,124063993
MED15	-0,12394026
SRSF11	-0,123456581
CHERP	-0,12273624
TNFAIP3	-0,122732615
DVL3	-0,122655778
DCAF5	-0,122450895

NDE1	-0,121933528
PPP1R9B	-0,121114438
SUPT5H	-0,120859632
TAPBP	-0,120595131
ATF6B	-0,120167011
TCF25	-0,120150677
SFSWAP	-0,118232829
PROSER1	-0,118066429
CSNK2B	-0,117179444
KMT2E	-0,114821024
MGEA5	-0,112181532
FADS2	-0,112078193
ATF7IP	-0,108566469
YBX3	-0,108369879
FNBP1	-0,107791741
RPL28	-0,104699631
BPTF	-0,10422342
PRRC2C	-0,097153519
RPS26	-0,095561442

Up-regulated

Gene	log2FoldChange
RPL3	0,094952231
NACA	0,09561793
RPL4	0,095906604
HLA-DRA	0,09641374
CAPZA1	0,100246307
PCM1	0,100840676
SEPT9	0,10267629
IGF2R	0,102946263
ETS1	0,103439076
ARPC5	0,103501774
ANXA6	0,10409322
H2AFZ	0,10420576
MTHFD1	0,104570951
STARD7	0,105192137
PMAIP1	0,106191677
RPS28	0,106462924
NEK6	0,107664391
HLA-DQB1	0,107736438
FBL	0,108020305
LPCAT1	0,108404243
CD70	0,109392762
CFL1	0,109623805

GOT2	0,110369947
SRSF3	0,111143038
CTSC	0,111317134
STMN1	0,111356949
RPS21	0,111497438
SNX25	0,1117727
H2AFX	0,112230782
MARS	0,112634863
ADRBK1	0,112653395
PTDSS1	0,113573746
GTF2I	0,11487447
MTDH	0,115091759
GSTP1	0,115490974
MTHFD2	0,115646884
ATP5A1	0,115739738
ANAPC1	0,115996078
LIMD2	0,117706815
IDH3A	0,118220601
BCAT1	0,118221546
VARS	0,118239489
SETX	0,119366347
LRPPRC	0,119904431
YARS	0,119964336
RANBP1	0,120126096
CD52	0,120152944
GALNT2	0,120394712
RBBP4	0,12075484
SHMT2	0,120786935
RPS13	0,120857621
TXNDC11	0,121265358
MCM5	0,121523239
HLA-DQA1	0,121730824
SELT	0,121840149
PAFAH1B1	0,122117097
CD79B	0,122183054
LYPLA1	0,122200111
DDX39A	0,122503785
LGALS9	0,123054016
BUB3	0,123436907
RRM2B	0,123874946
CD53	0,124040459
TOMM20	0,124061149
NCAPD2	0,124384616
MID1IP1	0,12454649
CD164	0,126138454
SPAG5	0,126210868

RSL24D1	0,126228662
USP15	0,127231759
SEL1L	0,127285895
POLD1	0,127360113
RPN2	0,127802307
PHGDH	0,128012749
CTDSP1	0,128259067
PCNT	0,128268465
BUB1	0,128623119
CLTC	0,12872567
STT3B	0,128930454
GM2A	0,129003365
SORL1	0,129532988
FKBP1A	0,129645322
CDK2	0,129693713
CBL	0,12970225
STAT1	0,129838589
PGAM5	0,129926928
CHCHD2	0,130120596
RRM2	0,130178394
CDV3	0,130554199
LMNB1	0,13059168
WHSC1	0,130749073
AKNA	0,130797118
NMD3	0,130857201
SLC5A3	0,131054227
AURKB	0,131677239
MDFIC	0,132058354
FAM78A	0,132532955
SBF1	0,132583828
DHTKD1	0,132667507
ATAD2	0,132819627
RAD21	0,132870533
SEP15	0,132931995
ECHS1	0,133300901
BUB1B	0,134218381
NAA25	0,134332932
IPO5	0,134590902
PRDX3	0,13491449
GANAB	0,134939484
TES	0,135081978
SLC38A1	0,135118071
TBL1XR1	0,135266924
ZNF106	0,135812855
RNH1	0,135816064
PRKDC	0,136251661

CDCA7	0,136496626
FERMT3	0,136861605
RIC1	0,136920697
FLNA	0,137332366
SLC1A5	0,137432693
PLEKHB2	0,137479763
SLC1A4	0,137542669
ATR	0,138162808
RPS6KA3	0,138203706
CCNB2	0,138386966
ASPM	0,138394996
ZFAND5	0,138516094
UCP2	0,13860577
PLEKHO1	0,138644222
POLR1B	0,138874718
MARCH6	0,138893398
COX7C	0,140262895
TIMM13	0,140398629
NREP	0,140790001
STARD4	0,141397563
RPSA	0,141686593
RPL10A	0,141763076
PSMB3	0,141834649
CAND1	0,1421379
ORAI2	0,142254436
RPL15	0,142278104
TCF4	0,142337238
NADK	0,142575398
PGK1	0,142789757
BTBD2	0,142895076
SPG21	0,142982203
MAN1A1	0,143031146
CCM2	0,143508496
FAM49B	0,143544117
GLDC	0,143657305
CST3	0,143859801
KDM4B	0,14399739
NNT	0,144295786
DOCK11	0,144454609
MRPL35	0,144565802
GPC4	0,144747687
OAS1	0,144834978
ACAP1	0,144968695
SYNE1	0,145517577
RB1	0,145521852
PLA1A	0,145787663

NUP205	0,145867998
TMEM30A	0,145928297
ASNS	0,146072052
VRK2	0,146746561
IKZF1	0,146798602
ANXA11	0,14682584
ATP6V0E1	0,147199172
DDIT4	0,14730018
CXXC5	0,147513561
STT3A	0,147739804
RAP1A	0,147838131
ATXN7L3	0,147921073
CKS1B	0,147971764
ZBTB1	0,148046062
ACADM	0,148294013
AKAP13	0,148548985
EIF2AK3	0,148587474
HPS5	0,148629671
TOMM40	0,148787785
KIFC1	0,149148919
NDUFS7	0,14921218
TACC1	0,149257563
MCM4	0,149784508
CLIC1	0,149813684
PI4K2B	0,149827584
RAPGEF6	0,150109912
KIF23	0,150365977
UTP18	0,15052113
ACAA2	0,150648248
NDUFA9	0,150793389
SPTY2D1	0,15081674
GLRX	0,1510406
MMD	0,151169077
PAN3	0,151170486
TEC	0,151173521
NCAPH	0,151319826
HLA-DRB1	0,1513859
LRRK1	0,151749539
SDHC	0,151800602
NCAPG2	0,151932005
SAPCD2	0,15201064
SLC12A2	0,152062441
MYLIP	0,152327589
IFRD2	0,152534394
TMX4	0,152556687
PSMB8	0,152761533

HIST1H1C	0,15284023
ADPRH	0,153101654
CYBA	0,153809953
ATP5B	0,153872688
ARSB	0,154409537
GSTO1	0,154411333
E2F8	0,154433232
SLC2A4RG	0,154656282
LONP1	0,155173595
GINS4	0,155332492
DUT	0,155471496
FANCD2	0,155638132
SETDB2	0,155697799
AKAP11	0,156350664
SLAMF7	0,156570775
RHOC	0,156605971
SYPL1	0,156652068
MDH1	0,156835579
FOXRED1	0,15693496
GMFB	0,157215856
CDC25A	0,157249745
EARS2	0,157566649
ZBTB2	0,158050221
PLS3	0,158194495
MCM2	0,158323337
PICALM	0,159199048
DDX60	0,15936
LPIN1	0,159433035
CECR1	0,159720532
PTPN7	0,159897002
GMPR2	0,159936886
SDHA	0,16027726
AURKAIP1	0,160598272
DAD1	0,160665856
NT5C3A	0,161098845
SLC20A1	0,161160727
NR3C1	0,16136809
COG4	0,161850235
PHF19	0,16239361
DPY19L3	0,162473292
KCNAB2	0,162772659
CARHSP1	0,162896498
TBC1D2B	0,163069143
RASAL3	0,163399042
FOXN2	0,163514542
SAMD9L	0,163612017

EMB	0,164056407
AARS	0,164239979
CDC42SE2	0,164392742
CENPN	0,164601003
COX15	0,165285345
POLE	0,165330486
ZMYND8	0,165701746
SIPA1	0,165815259
ARPC4	0,16632706
EMX1	0,166331528
WDR36	0,167201698
IRF7	0,167223741
ITM2B	0,167320766
B3GNT2	0,167322638
KIAA0101	0,167469413
ATP5D	0,167705603
SUSD6	0,167851539
SEPHS1	0,168146108
XRN1	0,168956012
CCNB1	0,169268278
NUP85	0,170059118
NDC1	0,170706642
TIMELESS	0,170766773
TNFRSF13B	0,170924999
PSMA2	0,171060901
ANKRD28	0,171190804
UBE2S	0,171215631
TK1	0,171320211
PLEKHA2	0,17210752
CXCR4	0,172447417
LY6E	0,172466524
JUN	0,172780195
DACT1	0,172980414
SOX5	0,173615961
FAM214A	0,173759584
ITGB7	0,173857209
ATP8A1	0,174071353
SYNE3	0,174085869
SLC3A2	0,174592448
RFX3	0,174802665
UTRN	0,174804208
PCK2	0,175061851
PMVK	0,175214641
LRRK2	0,175248272
SUMF2	0,175253702
FAM46A	0,17530269

MBNL3	0,175311739
NCOA3	0,175473041
FANCI	0,175603444
IFIT1	0,175620698
SGOL2	0,176185068
NUP155	0,17620098
VPS51	0,176265224
ITGA4	0,17645989
FASTKD2	0,176821719
ABCB10	0,177600188
PTCD3	0,177852545
RNF213	0,178383577
NCF1	0,178654773
STK11IP	0,178740917
MRPS28	0,178821686
HOOK1	0,179459886
KAT8	0,179659406
ACTR1B	0,179887941
DCLRE1A	0,180223907
MIPEP	0,180762306
CD19	0,180894637
C11orf31	0,181131455
SFMBT2	0,181196229
RNASEH2A	0,182119998
APOL6	0,182502585
ORC1	0,182592204
AHNAK	0,183220036
CHDH	0,183313136
MYB	0,18402364
CYB561A3	0,184823728
NFE2L3	0,184835146
GPD2	0,18486461
DTYMK	0,185326885
USP1	0,185732316
FGFR1	0,186262464
PLXDC2	0,186331466
SOGA1	0,18661116
MMP7	0,186976354
WDFY1	0,187515414
ALOX5	0,188326679
PHPT1	0,188959172
ARHGAP6	0,189680071
MMS22L	0,190103115
PTAR1	0,19037221
S1PR2	0,191127022
SCARB2	0,191154511

DOK1	0,191655899
RGS19	0,191676512
UBL4A	0,191702436
ISG15	0,191851874
OSTC	0,192475333
IKZF2	0,19254017
ATL2	0,192990677
GK	0,193262498
RNGTT	0,193445397
TNFRSF1B	0,194262184
SLAMF6	0,194273558
MDM4	0,194453883
CLN6	0,194627283
ADCY7	0,195795201
RPSAP58	0,196132206
COX18	0,196260585
CDKN3	0,196333273
SLC19A1	0,196926214
ATP1B3	0,19748034
SOX4	0,197503479
FAM43A	0,197660744
DFNA5	0,197802193
LZTS2	0,198108955
DUS3L	0,198249357
ALDH16A1	0,199188594
THOC3	0,199281167
NME1	0,199410001
MRPS18B	0,199576327
BMF	0,199632172
CENPV	0,199746071
FCRLA	0,19983588
TEP1	0,200473677
BRCA2	0,201520617
SLC7A11	0,201806569
LIMA1	0,201849793
MRPL1	0,20278121
COL19A1	0,202812926
FIZ1	0,20369808
PNP	0,204077056
MPEG1	0,204305684
COQ2	0,204476091
SIVA1	0,204588029
ABCA6	0,205413893
MACC1	0,205980952
MYO1G	0,206012022
TEX9	0,206484

MTX1	0,207089897
NLRX1	0,207384454
TNFRSF21	0,207715798
ZWILCH	0,207887493
CA2	0,208175919
CSGALNACT2	0,20973165
MRPL23	0,210403591
CLCN5	0,211282915
SLC35E2B	0,21140753
ISOC2	0,212669546
RICTOR	0,212695669
MAD2L1BP	0,212752066
KIAA1671	0,214213039
ANK1	0,214445657
ARHGAP4	0,214594253
CNR2	0,214719022
MRPS36	0,215108778
JTB	0,215238748
GPCPD1	0,215468414
HSPB1	0,215574265
WDR83OS	0,215895948
BZRAP1-AS1	0,216821755
SEMA4D	0,217725207
HLA-DMB	0,218150865
EDRF1	0,219529819
ZFAND4	0,22109401
SERPINB9P1	0,221387056
GIMAP2	0,221787869
LY9	0,223053447
LOC101927027	0,223294094
PTP4A3	0,22492656
FBXO41	0,226336917
ENOSF1	0,226450605
PSMB10	0,228936161
GALNT7	0,230134726
CHAC1	0,230524723
FGR	0,231913869
TAF6L	0,232597883
PXMP2	0,233452064
SLC25A53	0,234020878
CD84	0,2343549
KIF21B	0,235314051
TRAF3IP3	0,235377191
MRPL54	0,235604186
PRDM15	0,237847702
MAP2K6	0,237860539

SLC15A4	0,237885684
PSAT1	0,239097381
TRIP6	0,239283469
GINS3	0,239805916
CCDC109B	0,240238683
TMEM208	0,240601077
MZB1	0,241495001
FAH	0,241660492
IL3RA	0,241853296
ADAMTS7	0,242253087
ITGB8	0,243369649
APOBEC3B	0,243979299
TMEM140	0,243993973
SPATA13	0,245649188
TMEM160	0,246887555
LRRC61	0,247689187
MYRIP	0,248740957
DGKD	0,248852765
C14orf159	0,24904761
RASSF6	0,250332512
UGGT2	0,250596905
FAM64A	0,250931375
ZNF611	0,25130264
SETD4	0,252243772
C3orf58	0,253205455
DDX60L	0,254073722
IL15	0,256070144
CSRNP1	0,256070578
PP7080	0,257156596
TMC8	0,260073068
MACROD2	0,261771706
TMEM62	0,262832812
SLC38A5	0,262946387
SPARC	0,263967546
IL32	0,266563657
TNFSF11	0,268626821
UGT2B17	0,268741287
C19orf52	0,268882758
ACSM3	0,269052811
FCMR	0,269348318
ZNF273	0,270210224
TNFRSF11A	0,270336321
ITGAL	0,271965247
C10orf128	0,273318261
ABHD11	0,274309835
SLC12A8	0,275390493

ZNF75D	0,276243541
CACNB1	0,278097165
GHDC	0,280163045
EIF5AL1	0,281160875
FAM83D	0,28155372
KMO	0,281838366
D2HGDH	0,282401017
NCF1B	0,28268132
AICDA	0,282941023
TNFRSF17	0,283094031
ALPK2	0,283108527
S1PR4	0,285335051
DDR2	0,28549671
LRIG3	0,288176787
MED18	0,295930405
VDR	0,29636843
CD27	0,296710568
ARHGAP9	0,297333555
CCR10	0,302633356
LIPH	0,302796142
MPZL3	0,302859715
ADCK5	0,305473252
RHOB	0,306612999
HS3ST1	0,306825959
C1orf106	0,308011125
KCNA3	0,309234571
SLC39A10	0,310032858
TREML2	0,311098454
YDJC	0,313629132
H3F3AP4	0,314293402
TLR9	0,314325928
KLK1	0,315779948
CFAP57	0,320009131
CACNA1E	0,323559991
FUOM	0,326551908
CALCRL	0,328546766
FJX1	0,333398616
NCKAP5	0,33393549
SLITRK6	0,334516131
MS4A7	0,338258476
ENPP2	0,340092592
HLA-DOB	0,343846182
ASS1	0,347798422
TMEM86B	0,34853837
ITGA11	0,349451482
CACNA1D	0,350477148

CD24	0,350495029
CCR6	0,35193935
TFAP2B	0,353202518
NCAM2	0,357308415
CD200R1	0,363858682
SLCO4A1	0,364552851
APELA	0,369120344
CXCL10	0,369868324
NOD2	0,373751133
TNFSF15	0,377972921
LINC01055	0,384425515
LOC100507195	0,38551382
CREB3L1	0,38624142
RRN3P3	0,39128435
B3GLCT	0,391994796
EPHA4	0,393988743
CSPG4	0,398646647
DPYD	0,404107075
ASB9	0,415098026
SAMSN1	0,41619098
S100A4	0,416194743
BTNL9	0,418723728
LINC00996	0,423670352
CD101	0,428875128
FGFR4	0,440268017
LINC00426	0,442358831
BZW2	0,444424392
RNASE6	0,445068764
KCNIP2	0,447014816
LINC01551	0,448804259
GAS2	0,464225615
SFN	0,465652579
GPR174	0,469021863
CORO2B	0,469791654
FRMD4A	0,480824747
EVI2A	0,48906891
INHBE	0,491059985
TPRG1	0,491222641
OTOGL	0,491853806
CLNK	0,493473034
TIAM2	0,494388312
RFX3-AS1	0,500890338
SGMS1-AS1	0,503150776
CD28	0,507427629
TGM2	0,511527564
FCGBP	0,513548078

MYO5C	0,519026454
CMKLR1	0,526639812
GRAP2	0,52723991
FGL2	0,52809182
PRLR	0,531522108
DOK2	0,532473927
SMG1P3	0,539625388
VWA1	0,542395418
PCDHGC3	0,545010851
MYH11	0,54615443
ADGRD1	0,546476592
SIX4	0,54675682
NEURL3	0,552418326
CTTNBP2	0,55554532
TDO2	0,555770761
CLDN1	0,561501384
HES2	0,573002198
PTPN13	0,576357624
LOXL3	0,576695127
GPR18	0,581032819
LOC101929450	0,581462748
RASGRP2	0,583749777
CEACAM1	0,584147889
PKP2	0,585944279
CFAP54	0,587077975
AMZ1	0,591580884
MYOF	0,592861327
PVRIG	0,593284511
MIR1282	0,598491019
GNAZ	0,599097131
LINC01226	0,610621644
ZBED2	0,621561272
LOC100128164	0,634511027
IL21R-AS1	0,634688354
PADI2	0,637779764
UGT2A3	0,645345442
CXCL8	0,663747359
EBLN2	0,682903004
LGALS14	0,687187143
LOC100130093	0,704783347
CHST9	0,713731434
CCL25	0,732991288
NINJ2	0,769009986
DOK7	0,770174857
FSD2	0,787083787
F2RL3	0,792281859

NEUROD2	0,800873819
SLFNL1-AS1	0,80847723
TMEM119	0,832893717
LOC728989	0,872768812
IGF1	0,92550886
CDKN1C	0,940395985
NFATC4	0,969091963
LOC100505530	0,996094612
SEPP1	1,01104E+14
PRC1-AS1	1,03715E+14
MIR1268A	1,04096E+14
PDZRN3	1,04536E+14
GPRC5C	1,07297E+14
TCL6	1,08758E+14
NCR2	1,16967E+14
C8orf89	1,42992E+14
GYLTL1B	1,57438E+14
FAM69B	1,71583E+14
HK3	1,72777E+14
GTF2H2C	1,82611E+14
SNORA72	1,96424E+14
THBS1	2,41631E+14
MIR378J	3,52522E+14
C18orf61	5,40073E+14